Integrated Reservoir Simulation and Machine Learning for Enhanced Reservoir Characterization and Performance Prediction

By

© Mohammed Otmane

A thesis submitted to the School of Graduate Studies in
partial fulfillment of the requirements
for the degree of

Master of Engineering

Department of Process Engineering
Memorial University of Newfoundland

October 2024

St. John’s, Newfoundland and Labrador

Abstract

This thesis presents a comprehensive study on reservoir simulation and machine learning techniques for improved understanding and prediction of reservoir behavior. The research focuses on the Sarir C-Main field and utilizes various data sources including seismic cubes, well logs, base maps, check shot data, and production history. The methodology involves the development of static and dynamic models through processes such as data quality control, log interpretation, seismic interpretation, horizon and surface interpretation, fault interpretation, gridding, domain conversion, property and petrophysical modeling. Additionally, well completion, fluid model definition, and rock physics functions are established. History matching and prediction are performed using simulation cases, and machine learning techniques including data gathering, cleaning, dynamic time warping (DTW), long short-term memory (LSTM), and transfer learning are applied. The results obtained through Petrel simulation demonstrate the effectiveness of depletion strategy, history matching, and completion in capturing reservoir behavior. Furthermore, machine learning techniques, specifically DTW and LSTM, exhibit promising results in predicting oil production. The study concluded that machine learning approaches, such as the LSTM model, offer distinct advantages. They require significantly less time and can yield reliable predictions. By leveraging the power of transfer learning, accurate predictions can be achieved efficiently when limited data are available, offering a more streamlined and practical alternative to traditional reservoir simulation methods.

Acknowledgements

I would like to express my deepest gratitude to all those who have contributed to the successful completion of this thesis.

First and foremost, I would like to thank my supervisors Dr. Amer Aborig and Dr. Syed Imtiaz for their guidance, support, and invaluable insights throughout the research process. Their expertise and encouragement have been instrumental in shaping the direction of this study.

I would also like to extend my sincere appreciation to the faculty members of the Engineering and Applied Science department at Memorial University of Newfoundland for their knowledge, expertise, and encouragement. Their commitment to academic excellence has been a constant source of motivation.

I am grateful to Mr. Ashraf Elferjani and Dr. Adel Elzwai from Arabian Gulf Oil Company for providing access to the necessary data and resources. Their cooperation and assistance have been invaluable in conducting this research.

I would like to thank my family and friends for their unwavering support and understanding during this journey. Their encouragement and belief in me have been a constant source of strength.

Finally, I would like to express my heartfelt gratitude to all the participants who generously shared their time and expertise without their contributions, this research would not have been possible.

Table of Contents

List of Tables

List of Figures

List of Abbreviations and Symbols

Abbreviations

AGOCO	Arabian Gulf Oil Company
AI	Artificial Intelligence
ANN	Artificial Neural Network
API	American Petroleum Institute Gravity
ARIMA	Autoregressive Integrated Moving Average
BHP	Bottom Hole Pressure
BOPD	Barrel of Oil Per Day
BWPD	Barrel of Water Per Day
CAL	Caliper Log
DAL	Domain Adaptation Learning
DCA	Decline Curve Analysis
DT	Sonic Log
DTW	Dynamic Time Warping
EBC	Extended Boundary Constraints
EDA	Exploratory Data Analysis
EOR	Enhanced Oil Recovery
GOR	Gas Oil Ratio
GP	Gaussian Processes
GR	Gamma Ray Log
HOT	Heinemann Oil Technology and Engineering
ILD	Resistivity Log
LSTM	Long Short-Term Memory
MBE	Material Balance Equation
MCMC	Markov Chain Monte Carlo
MD	Measured Depth
MSCF	Million Standard Cubic Feet
NPHI	Neutron logs
NPV	Net Present Value

PCDTW	Physics-Constrained Dynamic Time Warping
PDEs	Partial Differential Equations
QA-QC	Quality Assurance-Quality Control
RD	Deep Resistivity
RHOB	Density Log
RMSD	Root Mean Square Deviation
RNN	Recurrent Neural Network
RSMD	Root Mean Square Deviation Error
SEDM	Stretched Exponential Decline Model
SP	Spontaneous Potential
STB	Stock Tank Barrel
TCA	Transfer Component Analysis
TDR	Time Domain Reflectometer
TGS	Transgressive Sand
TMs	Transmissibility Multipliers
TWT	Two Way Time

Symbols

b_c	Bias for candidate cell state
b_f	Bias for the forget gate
b_i	Bias for the input gate
b_o	Bias for the output gate
c_t	Update cell state
$\tilde{c}_t$	Candidate cell state
f_t	Forget gate
h_t	Hidden state
i_t	Input gate
k	Permeability
o_t	Output gate
S_h	Hydrocarbon saturation
S_o	Oil saturation

S_w	Water saturation
V_{sh}	Volume of shale
W_c	Weight matrix for candidate cell state
W_f	Weight matrix for forget gate
W_i	Weight matrix for input gate
W_o	Weight matrix for output gate
σ	Sigmoid activation function
Φ	Porosity

1. Introduction

Reservoir simulation is a tool that gives insight into dynamic rock and fluid properties for evaluation of past reservoir performance, reserve estimation that can be used to understand past reservoir behavior for future prediction including prediction of future reservoir performance. The basic role for reservoir simulation is to generate a reservoir geological model, which is a 3D software representation of an actual reservoir layers that exists beneath the earth's surface. It's derived by extending localized core and log measurements to the full reservoir using many technologies such as geophysics, mineralogy, and depositional environment. In addition, one of the most important reservoir simulation activities during the development and management of petroleum reservoirs is History Matching. History matching is the process of adjusting the reservoir geological model to match the field production data. Matched models are necessary to ensure reliable production forecasts and to increase confidence in understanding the geological and reservoir models. Reservoir production performance greatly determines the economic feasibility of oil and gas recovery and also the future sustenance of production operations. Thus, for efficient reservoir management, a thorough analysis of past, present and future reservoir performance is required, and history matching is a very handy tool for this.

The main objective of this work is to establish complete reservoir engineering study by building a 3D reservoir geological model and then simulate different parameters in order to end up with a dynamic model. This model will illustrate the production, history matching and forecasting of the target formation along with predicting the behavior of the reservoir at different production scenarios. This will be an important tool in planning the future production and development strategy, the geological model incorporates and integrates all geological information, interpretations and defines the most important data necessary for reservoir engineering and simulation.

Another important tool that will be used in this study is machine learning. Machine learning is a rapidly evolving field at the intersection of computer science, mathematics, and artificial intelligence (AI). It is revolutionizing the way we approach complex problems and enabling systems to learn from data, improve performance, and make predictions or decisions without being explicitly programmed. The fundamental principle of machine learning is to create mathematical models or algorithms that can generalize from known examples to make accurate predictions or

decisions on new, unseen data. This process involves training the machine learning model with labeled examples, known as training data, and optimizing its parameters to minimize errors and maximize performance.

Machine learning and reservoir simulation are complementary approaches in reservoir engineering. Machine learning is data-driven, focuses on discovering patterns and making predictions, and can handle complex relationships. Reservoir simulation, on the other hand, relies on mathematical models and physics-based principles to simulate fluid flow and predict reservoir behavior. Both techniques have their strengths and are used in different contexts, depending on the specific objectives, data availability, and computational resources. However, with machine learning it's less time consuming and requires less reservoir characterization data to predict the production of a reservoir, therefore it is more cost effective rather than using expensive resources and reservoir simulation software and tools. Nonetheless, machine learning can be pursued with various objectives, these objectives include prediction, classification, clustering, anomaly detection, optimization, recommendation, pattern recognition, and generative modeling. These objectives offer researchers and students a wide array of possibilities to explore in their machine learning studies, depending on the specific research context and problem domain. The focus of present study is prediction of reservoir production. Prediction involves developing models to accurately forecast outcomes based on input data.

1.1 Objectives

The main objectives of this work is illustrated as shown below:

- To develop a comprehensive reservoir characterization and simulation model for the candidate reservoir using various software tools like Petrel and data-driven techniques . The first step involves creating a Static model by integrating log correlation, seismic interpretation, fault analysis, and domain conversion based on the available data. Log correlation will be employed to define well tops and determine the water-oil contact within the reservoir. Seismic interpretation will track and extract surfaces in a 3D environment, aiding in defining the reservoir's structural features. Fault interpretation will be conducted to outline the boundaries of the study area and identify distinct segments. Additionally, domain conversion will transform the interpreted project from the time domain to the depth

domain, facilitating a more accurate representation of the reservoir. Subsequently, a Reservoir simulation model (Dynamic model) will be constructed by incorporating field and well data. This dynamic model will allow for the simulation of fluid flow and reservoir behavior, enabling a comprehensive analysis of reservoir performance and supporting decision-making for effective reservoir management.

- Develop a complete reservoir management strategy for the candidate reservoir through history matching, production scenario creation, and time series forecasting. The first objective is history matching, where historical reservoir performance will be replicated by adjusting various properties in the model. Next, a production scenario will be designed, considering different well completion options, to optimize hydrocarbon recovery and well productivity. Time series forecasting techniques will be applied to handle missing production data, enabling a more accurate representation of reservoir performance. By integrating these approaches, the study seeks to enhance reservoir management decision-making, offering valuable insights into reservoir behavior and supporting the development of effective strategies.
- The focus of this study is to leverage cutting-edge machine learning techniques, specifically long short-term memory (LSTM) time series analysis and Dynamic Time Warping (DTW). The first aim is to utilize LSTM for training and predicting future production data. By employing LSTM, the study will leverage its capability to capture temporal dependencies and patterns within time series data, leading to more accurate predictions of reservoir production behavior. Furthermore, Dynamic Time Warping (DTW) will be integrated into the LSTM model to enhance its performance and effectively handle missing production data. DTW is well-suited for aligning and comparing time series data with varying temporal scales, making it valuable in filling gaps and improving the completeness of production records. Through the integration of LSTM and DTW techniques, the study aims to offer a robust and reliable approach to predict future production behavior and address data gaps effectively.
- Lastly, the implementation of transfer learning stands out as a novel approach to predict future reservoir production and performance in case of limited data availability. By leveraging knowledge gained from existing well data, this technique empowers the model to adapt and generalize effectively to new well conditions, resulting in more accurate and

reliable predictions. The final contribution centers on the comparison of all results and scenarios obtained through the integration of LSTM and DTW, the implementation of transfer learning, and the comprehensive history matching. The meticulous evaluation and comparison of these different approaches will provide valuable insights into their respective strengths and limitations, ultimately guiding the selection of the most effective strategies for reservoir management.

Flowchart shown in (Figure 1.1) outlines the thesis chapters and the construction of the research work:

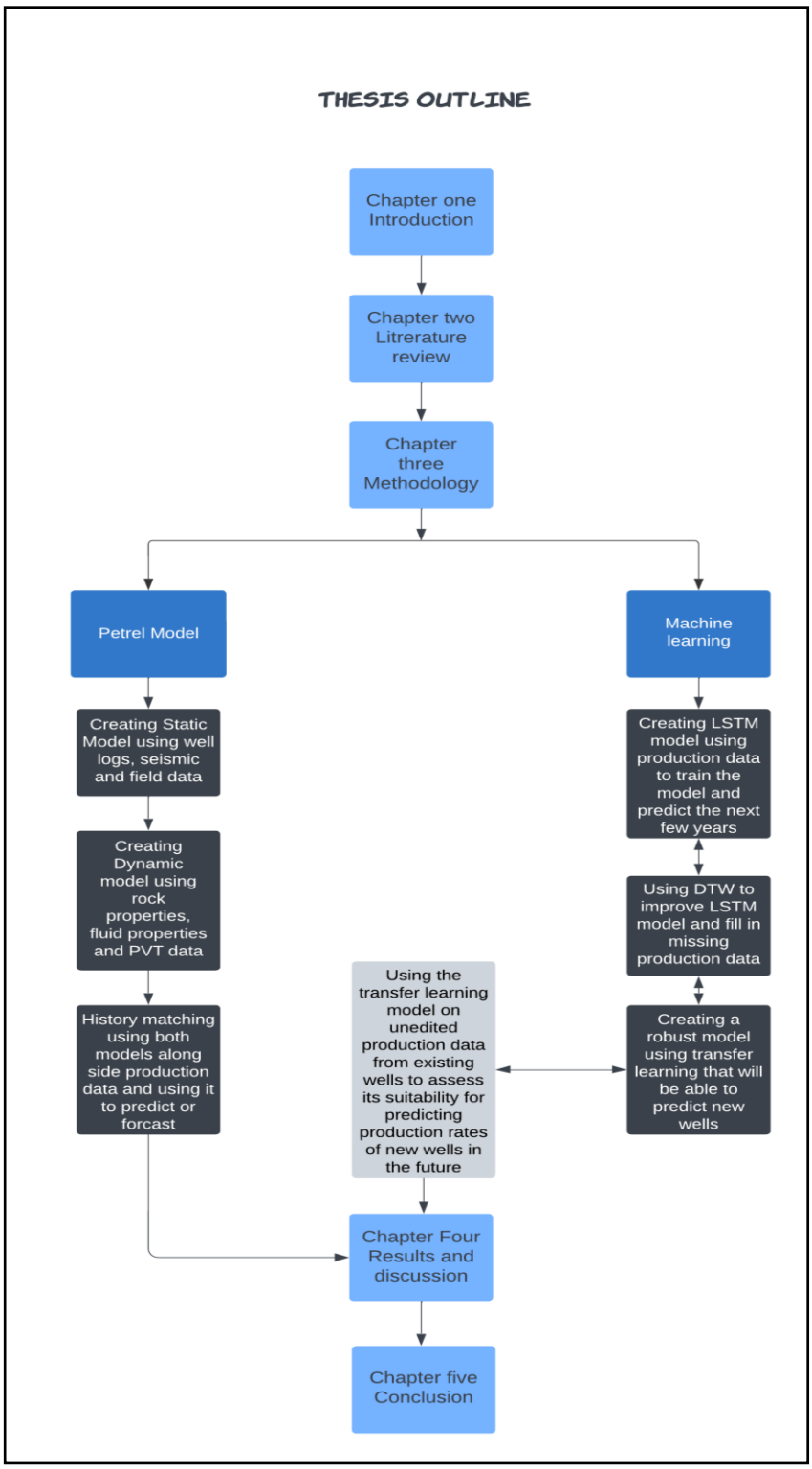

Figure 1.1: Flowchart of the thesis outline

2. Literature Review

In this literature review, we explore into the evolution of reservoir simulation as the predominant method utilized in the oil and gas industry for predicting hydrocarbon production. Initially, reservoir simulation heavily relied on techniques such as history matching, which aimed to improve the fidelity of predictions by calibrating simulation models with observed field data. Over time, significant advancements have occurred both within the industry and the field of computer science, leading to notable improvements in processing time and cost-efficiency. As a result, reservoir simulation methods have become less complicated, allowing for more widespread adoption and utilization. Recently, the emergence of artificial intelligence (AI) has steered in a new era of possibilities. AI technologies, such as machine learning, have made substantial progress and offer promising tool to enhance the traditional reservoir simulation approaches. These advancements have paved the way for more efficient and accurate prediction models. In this study we aim to highlight the differences between reservoir simulation and machine learning through a comprehensive comparison. By examining the strengths and limitations of both approaches, we can assess the potential benefits that machine learning brings to the table. Notably, machine learning techniques often require significantly less time and data to produce high-quality predictions, thus reducing the reliance on resource-intensive and expensive simulators. Additionally, a robust transfer learning model will be developed to allow the model to retain knowledge from prior training, making it capable of generating accurate predictions even when new data is introduced. By showcasing the efficiency, cost-effectiveness, and improved prediction quality offered by machine learning techniques, this research contributes to the ongoing efforts to optimize reservoir management and decision-making processes in the oil and gas industry.

2.1 Reservoir Simulation

Odeh in 1969 began by highlighting the historical context of reservoir simulation, emphasizing its roots in well-established reservoir engineering equations and techniques. The author asserted that reservoir simulation builds upon these existing foundations and expands its capabilities through the use of digital computers. The paper acknowledged that while reservoir simulation itself is not a new concept, advancements in computer technology have enabled engineers to develop more

detailed and accurate simulations. This advancement has led to a revolution in the petroleum industry, with reservoir simulators becoming increasingly prevalent and essential tools for reservoir characterization and performance evaluation. Odeh explained that reservoir simulation involves the representation of fluid behavior within cells, with interactions between cells governed by the material balance equation (MBE) and Darcy's law. Different models, ranging from zero-dimensional tank models to one-, two-, and three-dimensional representations, are discussed, highlighting their applicability in capturing the variations in reservoir properties and pressure. He also touched on the challenges associated with reservoir simulation, particularly the complexity of the mathematical expressions involved and the potential for misuse of simulators. Furthermore, the author emphasized the need for engineers to gain competence in setting up simulation problems, selecting appropriate input data, and accurately evaluating simulation results. Throughout the study he underlined the significance of data preparation and discussed the importance of dividing the reservoir into cells by assigning rock properties, fluid properties, and initial fluid distribution for each cell. The concept of history matching involves comparing simulated results with actual field data to improve the accuracy and reliability of the simulator. Odeh's insights contribute to the broader body of knowledge in reservoir engineering and provide a foundation for further research and development in the field of reservoir simulation.

The multicell reservoir simulation models have reached a stage of development where they are being transferred from scientists and mathematicians to reservoir engineers for practical implementation. Stags & Herbeck (1971) discussed the development, applications, and considerations associated with multicell reservoir simulation models from an engineer's perspective. These models are regarded as powerful tools for comprehending reservoir behavior, as they allow for the division of a reservoir into cells, enabling engineers to analyze various field operations and assess fluid properties' sensitivity. These considerations include assigning specific properties to each cell, such as elevation, pressure, size, porosity, permeability, and fluid saturations. Additionally, well data, including location, production/injection rates, and limiting conditions, must be incorporated into the model. The selection of representative rock and fluid properties, as well as determining relative permeability and cell size are critical for accurate model results. Multicell models employ mathematical equations derived from the continuity equation, Darcy's law, porous media principles, and the fluid distribution within the reservoir. The Finite-difference method is commonly used to solve these equations, although it introduces inherent

errors. The authors acknowledged the wide range of valid applications for multicell models in reservoir engineering, (Figure 2.1).

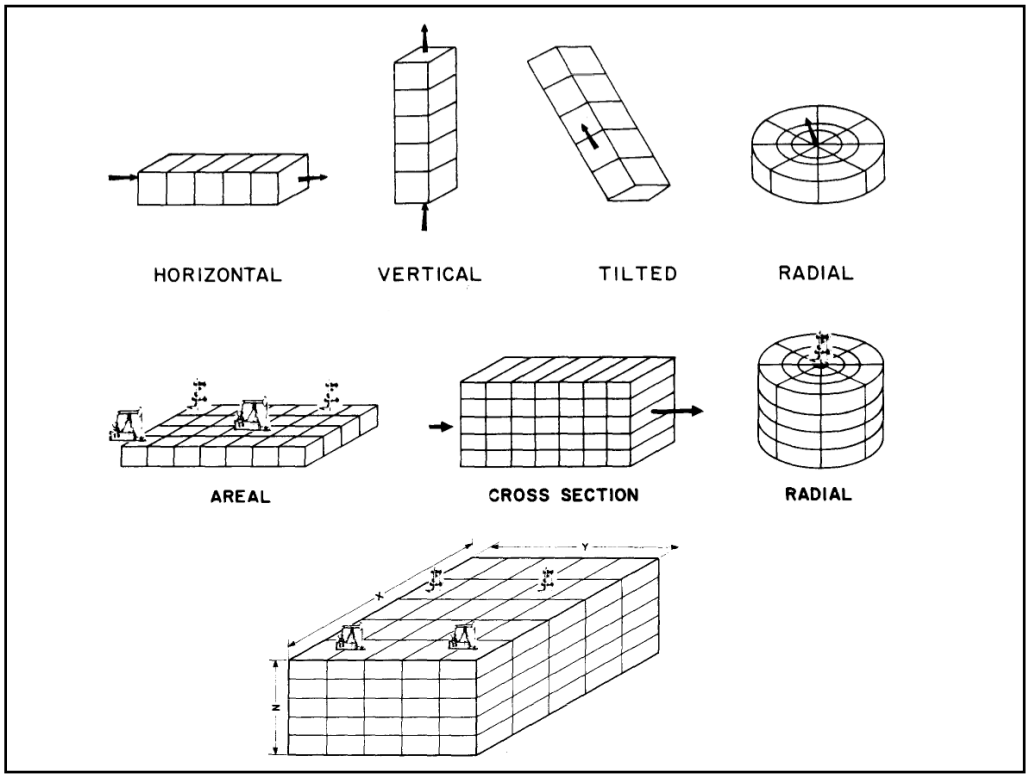

Figure 2.1: Multicell in one-, two-, and three-dimensional models, (Stags & Herbeck, 1971)

Harris (1975) described reservoir simulation models, including their dimensions, fluid phases, and the technological advancements that have enabled the development of more detailed and complex computer programs for simulating fluid flow. It highlights the ability of these models to handle vertical variations in porosity, permeability, and capillary properties for a certain area. The heterogeneity of the rock framework in most reservoirs must be recognized and quantitatively expressed to incorporate it into the simulation models accurately. Geologists are responsible for conducting various geological activities throughout the reservoir description phase which includes rock studies, framework studies, reservoir-quality studies, and integration studies. Rock studies involve establishing lithology, determining the depositional environment, and distinguishing reservoir rock from non-reservoir rock. Framework studies focus on determining the structural style, continuity, and gross thickness trends of the reservoir rock. Reservoir-quality studies aim to understand the variability of reservoir rock in terms of porosity, permeability, and capillary properties. Integration studies involve developing three-dimensional patterns of hydrocarbon pore

volume and fluid transmissibility. Geologists collaborate with engineers who provide assistance and guidance for core analysis measurements, well testing, and pressure-production history matching to validate the physical model against real-world performance. To illustrate the application of geological methods in a simulation study, Harris presented a case study conducted in the Loudon field in central Illinois which involved a pilot-test site that included core data, well logs, and rock description information. The author also highlighted the importance of recognizing the depositional environment to understand the quality and distribution of the reservoir rock.

Odeh (1982) reported an overview of the research and advancements in mathematical modeling techniques used to describe the behavior of hydrocarbon reservoirs. The focus was on understanding the flow equations, nonlinearity, solution methods, and modeling of complex processes. Additionally, he highlighted the existing numerical challenges that require further investigation and outlined the functional relations among variables that give rise to the nonlinearity of these equations. Odeh highlighted the importance of selecting appropriate solution methods based on the complexity of the reservoir system and the desired level of accuracy. In addition to the basic flow equations, he briefly described the mathematical modeling of more intricate processes such as chemical injection and heat injection. These processes have a significant impact on reservoir behavior and require specialized modeling techniques. Despite the progress made in mathematical modeling, several numerical challenges remain unsolved. Identifying and resolving these issues are crucial for developing robust and reliable reservoir models, and hence the need for further research and innovation to overcome these numerical challenges.

Geologic models and flow simulation studies play a crucial role in understanding and predicting the behavior of reservoirs in the oil and gas industry. Larue et al. (2005) reported valuable insights into the impact of stratigraphy on flow simulation and history matching studies. Three main steps in the simulation have been conducted. Firstly, the geology of the reservoir was carefully interpreted, leading to the generation of various cross-section correlations and maps that yield a geostatistical characteristic such as variogram type and range. Secondly, a suite of 50 geologic models were constructed, representing both simple and complex interpretations by employing various modeling techniques which resulted in visually distinct models from each other. Lastly, flow simulation studies were performed in three stages. Initially, all models were simulated under unconstrained flow conditions, followed by simulating fixed flow rates based on observed data.

Finally, a subset of models was modified to match historical data using adjusted rock properties. Some key findings were:

- Simple and complex geologic models can provide similar predictions of flow performance. This suggests that overly complex models may not necessarily lead to more accurate predictions.
- Geologic models that appear visually different can still perform in a similar manner. This highlights the importance of considering performance measures rather than relying solely on visual interpretations.
- Reservoir volume is the most uncertain characteristic in the reservoir. Accurate estimation of reservoir volume remains a challenge, impacting predictions of reservoir behavior and performance.
- Unconstrained flow simulations which do not rely on historical data, can be useful predictors of future reservoir behavior. These simulations can be particularly valuable in development studies where historical data may not be available.

By understanding the impact of stratigraphy on flow simulation and history matching, reservoir engineers and geoscientists can make more accurate predictions of oil and gas production.

Petroleum reservoir simulations face the challenge of lacking real-time data verification due to the inaccessibility of the reservoir. As a result, significant research efforts have been dedicated to developing sophisticated mathematical models and simulators to overcome this limitation (Mustafiz & Islam, 2008). The development of a reservoir simulator involves several major steps. The formulation step establishes the fundamental assumptions and translates them into mathematical terms, which are then applied to control volumes within the reservoir. Nonlinear partial differential equations (PDEs) describing fluid flow through porous media are derived and discretized using numerical methods. The most common approach is the finite-difference method, which converts the PDEs into a set of nonlinear algebraic equations. Linearization techniques are employed to solve these equations, incorporating fluid production and injection. The validation step ensures the accuracy and reliability of the simulator before its practical application in field studies (Figure 2.2). Advancements in reservoir simulation has been reported by Mustafiz & Islam as shown below:

- Integration of 3-D Imaging and Reservoir Models: The coupling of 3-D imaging technologies with comprehensive reservoir models have the potential to create real-time

reservoir monitoring systems. By using drilling data as input information, this integration enables accurate reservoir characterization and performance prediction.

- Virtual Reservoir and Production Schemes: The integration of virtual reservoirs, advanced data acquisition systems, and digital/analog converters introduces exciting opportunities for diverse production schemes. By leveraging virtual reality techniques within reservoir models, engineers can visualize and analyze reservoir behavior, providing valuable insights to inform decision-making processes.
- Intelligent Reservoir Simulators: Reservoir simulators are evolving to incorporate intelligent features that integrate environmental impacts of EOR processes into the technical and economic feasibility analysis. This broader perspective ensures sustainable petroleum production by considering both short-term and long-term impacts.
- Advanced Modeling Techniques: Advancements in geomechanical modeling, thermal modeling, and fluid flow equations have contributed to enhanced accuracy and reliability in reservoir simulation. These techniques enable the simulation of complex reservoirs with varying formation and fluid properties.

The future of petroleum reservoir simulation holds tremendous promise. The ongoing integration of cutting-edge technologies, such as remote sensing and sonic-while-drilling, has the potential to revolutionize reservoir monitoring and data acquisition.

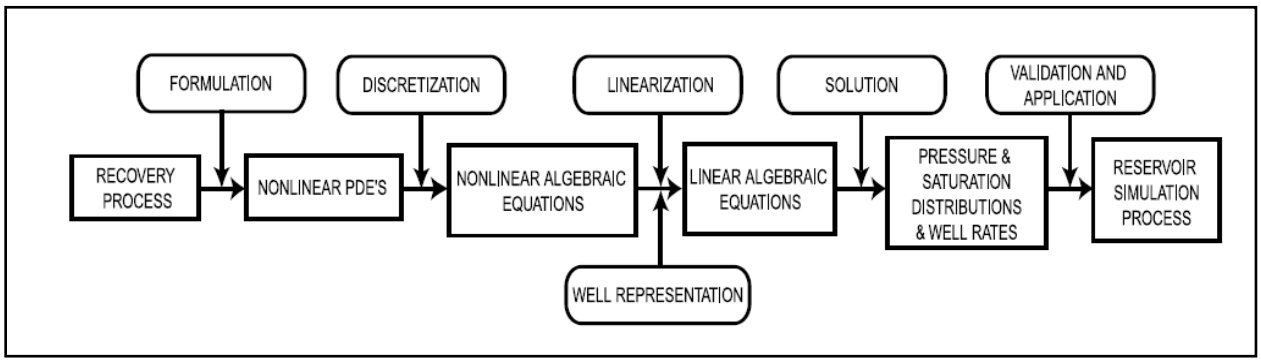

Figure 2.2: Development of a reservoir simulator, (Odeh, 1982. Mustafiz & Islam, 2008)

Hossain et al. (2009) revealed the challenges and complexities inherent in reservoir simulation within the petroleum industry. They underlined the significance of grasping the concepts of mystery and uncertainty and their profound impact on decision-making in reservoir management. In addition, highlighted the intricate nature of petroleum field development, which is fraught with

various sources of mysteries and uncertainties. These uncertainties arise from factors such as limited data availability, inherent subsurface complexities, and the need to make approximations and assumptions when characterizing the reservoir. The study presented a comparative analysis between a newly developed model and an existing risk analysis model, demonstrating how the former eliminates false assumptions. However, the accuracy and efficacy of reservoir simulation are heavily contingent upon the quality and precision of input and output data through the history matching process, (Figure 2.3). The complexity arising from variations in formation and fluid properties across time and space is also underscored. Advanced technologies and further research are deemed crucial in tackling the challenges posed by reservoir complexity. As a result, (Hossain, 2010) reported the importance of properly addressing these challenges to enhance the accuracy a nd reliability of simulation results. One of the key factors contributing to uncertainties in reservoir simulation is the geologic and fluid models. Proper understanding and modeling of these uncertainties are essential for accurate predictions. Additionally, the development of theories and laws related to reservoir behavior is critical for reaching a closer representation of real phenomena, also eliminate false assumptions and incorporate new models to improve the accuracy of reservoir simulations. The conventional approach to reservoir simulation often relies on linearization of mathematical models and inherent assumptions, which can lead to inaccurate solutions. Hossain emphasized the challenges associated with capturing the nonlinear and chaotic behavior of reservoirs. Many researchers have attempted to address these challenges through modifications and advancements in mathematical and computational tools. He provided a comprehensive overview of the existing challenges and the need for a pattern shift in the approach of reservoir simulation. Hossain & Islam (2010) introduced a new perspective by incorporating the knowledge dimension into reservoir simulation, and they argued that reservoir simulation equations have embedded variability and multiple solutions that align with physics rather than spurious mathematical solutions. It offers solutions and demonstrates that proper reservoir simulation should be transparent and empower decision-makers rather than creating a black box. The authors developed a new governing equation based on an in-depth understanding of the factors influencing fluid flow in porous media under different flow conditions. In addition, they introduced the concept of the fluid memory factor and presents mathematical developments of new governing equations without linearization. Then they compared their approach to currently available reservoir

simulators, and provided examples of how the knowledge-based approach extends the range of solutions and offers a useful tool for prediction models.

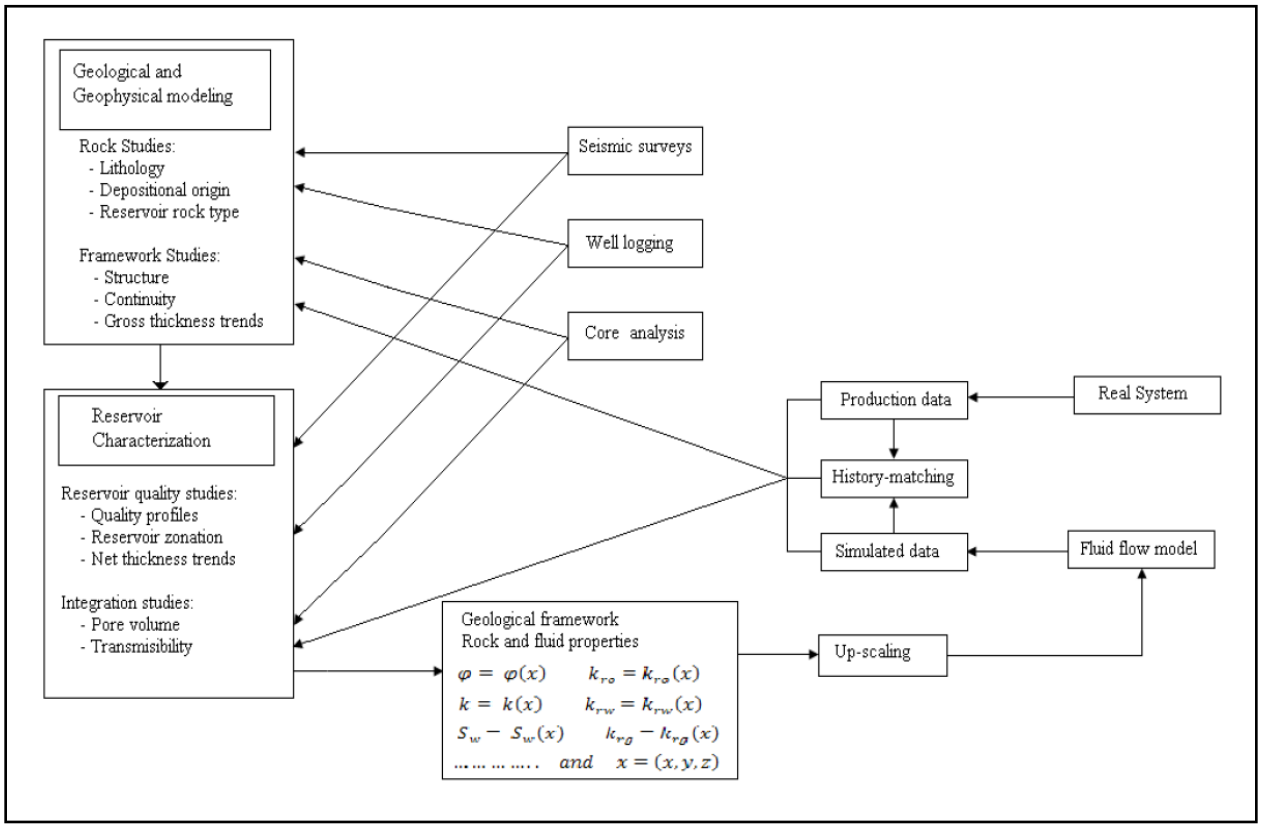

Figure 2.3: A schematic description of history matching and geological activities regarding to a reservoir, (Islam et al., 2008. Hossain et al., 2009)

Reservoir history matching is an essential process in the field of reservoir engineering, where observed reservoir behavior is used to estimate the variables of a mathematical model that accurately represents the reservoir. This process enables the prediction of future reservoir performance and the optimization of reservoir management strategies. Oliver & Chen (2011) provided an overview of the advancements made in reservoir history matching over the past decade. The authors highlighted several key developments in history matching that have contributed to significant progress in the oil field. One important factor is the increase in computational power, which has allowed for the generation of reservoir simulation models that can match large amounts of production data. Additionally, the widespread adoption of geostatistics and Monte Carlo methods has played a crucial role in improving history matching techniques. The

paper discussed the advancements in reparameterization techniques for model variables, which involves transforming these variables to more suitable forms that facilitate accurate history matching. Various approaches have been developed to address the challenge of nonlinearity and improve the efficiency of the history matching process. Methods for computing sensitivity coefficients, which quantify the relationship between model variables and reservoir behavior, have also seen significant progress. These coefficients are essential for adjusting the model variables to match observed data. An important aspect of history matching is the quantification of uncertainty in reservoir properties and predictions. The authors discussed the advancements in uncertainty quantification methods, such as the combination of Kalman filter and Bayesian approaches. These methods provide a means to assess the range of possible outcomes and estimate the associated risks. They also compared representative procedures in history matching and identify their limitations. This comparative analysis helps researchers understand the strengths and weaknesses of different techniques and choose the most appropriate approach for their specific reservoir modeling and history matching needs. However, challenges remain, and further research is needed to address the complexities of nonlinearity, high-dimensional inverse problems, and the incorporation of various types of data in the history matching process.

Singh et al. (2013) provided valuable insights into the challenges and solutions associated with achieving accurate production forecasts in reservoir engineering, by emphasizing the integration of data, improved understanding of geostatistics, and comprehensive evaluation of uncertainties. The authors proposed practical approaches to enhance the accuracy and reliability of 3D reservoir modeling. key findings and contributions of the study:

- Three-dimensional reservoir interpretation, modeling, and flow-simulation studies are essential for accurate production forecasts and supporting value-based exploration and production decisions.
- Advances in computing power and software have significantly improved the efficiency and accuracy of 3D reservoir modeling. Improved parallel networking algorithms and reduced CPU run times enable the creation of more detailed and larger-scale reservoir models.
- Several factors contribute to production forecast uncertainty, including sparse and unrepresentative data, biased estimates of original hydrocarbon in place volume, inadequate static and dynamic models, poor use of seismic data, and improper utilization of uncertainty workflows and tools.

- Conventional modeling workflows have limitations, such as misused geostatistical techniques, insufficient integration between static and dynamic models, and a lack of focus on delivering uncertainty at each step of the modeling process. These limitations hinder the investigation of how static model uncertainty impacts dynamic outcomes.

The study proposed several practical solutions to address the limitations of conventional modeling workflows and enhance production forecasts. Firstly, improved integration of diverse data sets, technologies, and tools from various disciplines. Closed-loop modeling workflows are recommended to consider the impact of modeling parameters and uncertainties on decision outcomes. Secondly, the importance of a better understanding and application of geostatistical techniques, particularly in complex reservoirs. It suggests considering multiple seismic attributes and cautioning against relying solely on porosity as a modeling constraint in such settings. Lastly, the significance of conducting a comprehensive evaluation of reservoir uncertainties at each step of the modeling process is essential. Integrated quality assurance-quality control (QA-QC) procedures are deemed necessary to identify and address issues related to static and dynamic reservoir modeling. The findings presented in this paper contribute to the ongoing efforts in the industry to improve production forecast accuracy and support effective decision-making in exploration and production operations.

Despite significant advancements in reservoir simulation, numerous challenges and uncertainties persist. Traditionally, reservoir simulations have heavily relied on the expertise of geologists to construct models and the judgment of engineers to validate them. However, the appeal of predictive models lies in their speed and cost-effectiveness. With the continuous advancements in computer technology and computational power, machine learning has emerged as a promising tool that requires less data, thereby reducing uncertainty and generating more accurate predictions in less time. This introduces a new dimension to the field, presenting the potential to enhance or serve as a substitute in situations where field data is limited.

2.2 Machine Learning

In recent years, machine learning has experienced significant growth and adoption within the oil and gas industry, primarily due to its diverse range of tools and capabilities. Shirangi (2012) proposed the use of fast proxy models and net present value calculations as an alternative to full physics simulators, offering a simpler and faster approach. By employing artificial neural networks

or support vector regression, a proxy model is generated and optimized by repeating the process with using the most recent optimal point. The main objective is to determine the optimal well control point that maximizes production, using well bottom hole pressure, oil rate, or total liquid rate as the controlling factor. The study focuses on using well bottom hole pressure (BHP) with simple boundary considerations. The utilization of support vector regression and artificial neural network models presented significant time and cost savings compared to water flood optimization without the use of proxy models. Foroud et al. (2014) reported that history matching is a technique employed to minimize discrepancies between field production data and simulated results, but it can be time-consuming and costly. To address this challenge, an artificial neural network (ANN) is utilized in the context of an Iranian fractured oil reservoir. A comparison between the manual history matching results and the ANN data reveals that the manual data provides superior matching quality. However, the ANN results demonstrate the ability to achieve multiple matches while requiring less simulation time (Figure 2.4). Therefore, this study provides evidence that ANN can serve as a viable alternative to computational reservoir simulation, offering a satisfactory level of accuracy and significantly faster execution times.

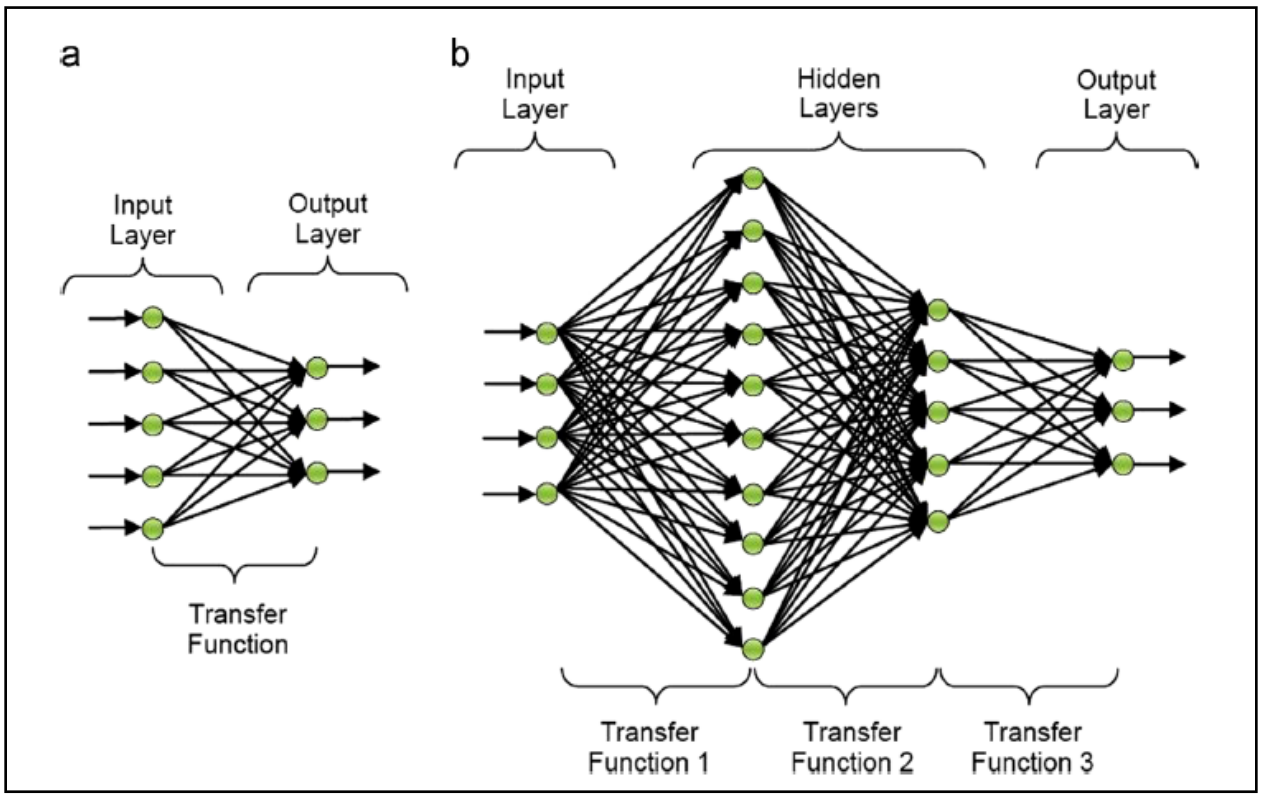

Figure 2.4: Classification of network architecture. (a) Singlelayer network and (b) multilayer network, (Foroud et al., 2014)

Maschio & Schiozer (2014) presented a novel approach that utilizes a proxy model, in the form of an artificial neural network (ANN), to replace the flow simulator for the purpose of history matching. The proposed methodology combines Markov Chain Monte Carlo (MCMC) and ANN training, and it demonstrates promising results when applied to a realistic reservoir model with 16 unknown features. The research methodology involved the iterative application of MCMC sampling and ANN training for Bayesian history matching. Each iteration consists of two stages: the sampling stage using MCMC and the training stage for the ANN. These stages are performed sequentially, with the sampling stage preceding the ANN training and vice versa. The authors concluded that this method offers a simple yet effective solution that reduces computational efforts. Additionally, they suggested exploring alternative types of artificial neural networks in future research. Furthermore, alternative approaches to applying MCMC methods, such as parallel tempered Markov chains, should be investigated to leverage distributed computing and improve the exploration of complex subsequent distributions with multiple modes. These enhancements would improve the method's capability to handle more challenging scenarios. In the other hand (Q. Cao et al., 2016) developed artificial neural networks (ANN) to forecast production in unconventional reservoirs, utilizing inputs such as pressure, production history, and geological maps. The neural network approach in machine learning excels at learning from large datasets and adapting to new data as it becomes available. Consequently, the ANN model is employed to forecast production for existing wells and leverage their historical data to predict production for new wells by analyzing nearby historical well data. This method requires a greater amount of data inputs compared to decline curve analysis, but it offers increased consistency and accuracy in production forecasting. It is important to note that the ANN method does not replace conventional reservoir simulation methods; rather, it complements them by providing additional insights and confidence in the forecasting techniques.

J. Cao & Roy (2017) reported that time-lapse seismic analysis is a crucial tool in well planning, reservoir management, and reservoir model updating. While it works effectively in simple 4D cases, it becomes less reliable when estimating complex reservoir dynamics and 4D reservoir property changes. To overcome this limitation, data-driven quantitative methods are utilized, leveraging the inherent physics between seismic attributes and time-lapse reservoir property changes. These methods utilize machine learning techniques and can incorporate multiple seismic

attributes simultaneously. The study was conducted on a complex North Sea reservoir with extensive injection and production history. This data-driven approach demonstrates remarkable accuracy in predicting saturation, compaction, and pressure changes. The estimation maps of all reservoir property changes closely match the simulation model in the synthetic study. Consequently, the authors established that integrating a substantial amount of 4D seismic data with machine learning prediction models significantly improves the capabilities and opportunities for reservoir management. This integration enables informed decision-making by harnessing geophysical data in various types of reservoir settings. Nonetheless, (Vyas et al., 2017) introduced a novel approach for predicting decline curves at new well locations by establishing a connection between decline curve model parameters and well completion data. By avoiding the need for expensive and time-consuming reservoir simulators, the study utilizes production data to rapidly generate decline curve models, which can then be employed to predict decline curves for new wells. The authors demonstrated that this methodology enables the estimation of ultimate recovery for new wells based on data from previous wells. Various types of decline curve models, including Arp's, Stretched Exponential Decline Model (SEDM), Doug's model, and Weibull growth curve, were employed in the study. Among these models, SEDM combined with support vector machine learning exhibited the highest success rate in predicting flow rates. Furthermore, the study highlighted additional factors that influence production prediction, such as the initial flow rate, the total amount of support, and the total vertical depth. These factors contribute significantly to the accuracy of production predictions.

The study by (Dong et al., 2021), a deep learning model based on stacked Long Short-Term Memory networks (LSTM) is proposed for the prediction of reservoir production, (Figure 2.5). Transfer learning is utilized to extend the model's applicability to well patterns with limited production data and short production times within the same oilfield block (Figure 2.6). The model successfully incorporates the actual reservoir production process and leverages the knowledge gained from existing well patterns, along with sufficient historical data, to develop a well pattern model with minimal data requirements. As a result, this approach enables more accurate prediction outcomes while reducing the time required for model training, thus delivering more effective application results compared to compositional simulation. Furthermore, (Han & Kwon, 2021) focused on the application of machine learning techniques to predict production rates in a shale reservoir. A data-driven deep learning model, along with an alternative proxy model, is employed

in the study. Gas production is predicted using a deep neural network, where cumulative gas serves as the independent variable, while other production data, well information, and completion parameters act as the dependent variables. The research aims to extend the application of this approach to other shale formations. Furthermore, the article highlighted the widespread use of decline curve analysis (DCA) in recent years, as proposed by Arps, for predicting reserves in unconventional and conventional wells. DCA has proven to be a valuable technique for predicting future production with limited data, despite the challenges it presents in the pre-drilling stage of prediction.

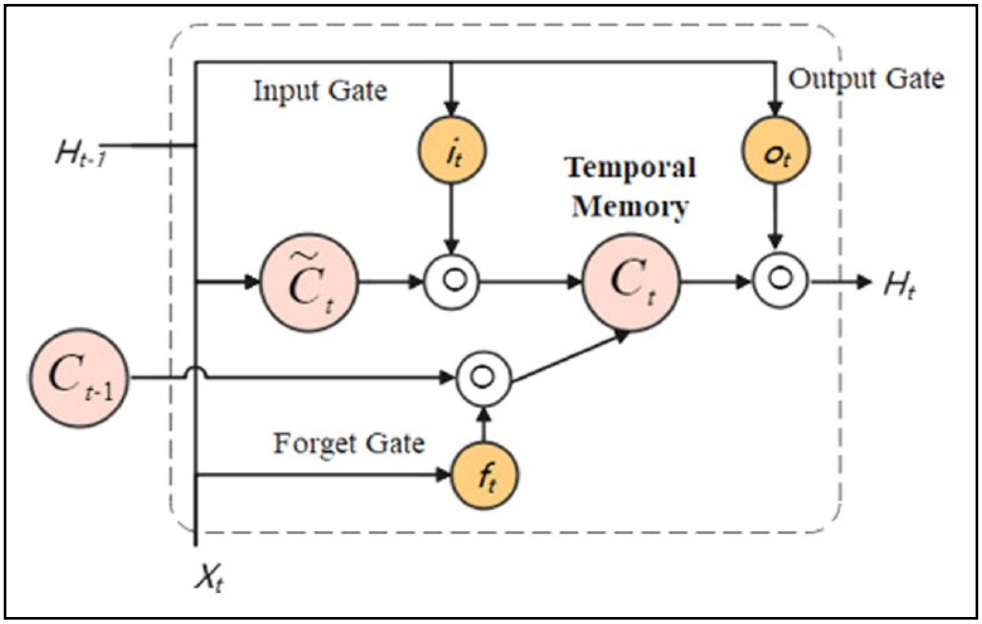

Figure 2.5: Schematic diagram of the LSTM unit structure (Dong et al., 2021)

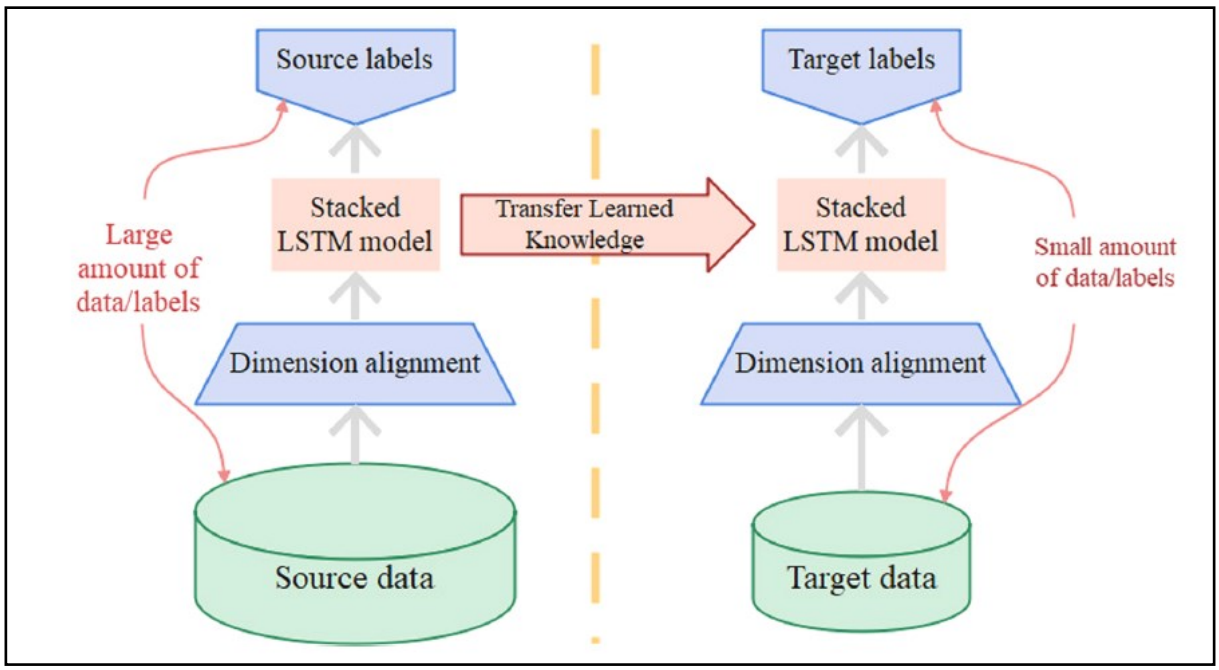

Figure 2.6: Flow chart of production prediction based on transfer learning (Dong et al., 2021)

Desbordes et al. (2022) introduced a novel technique for maximizing the net present value (NPV) of production over the estimated life of a reservoir. Traditional methods for reevaluating prediction models are computationally expensive and fail to consider inter-cycle correlation in changing production controls. The utilization of transfer learning algorithms in the oil and gas industry has been challenging due to their high processing costs and the randomness or unavailability of learning samples. In response, the research presented a new optimization framework based on transfer learning for dynamic production optimization challenges. The method entails the following steps: domain adaptation learning (DAL) is employed to reduce differences between data from two inter-cycles, using extended boundary constraints (EBC) to embed the optimization issue within the learning samples during the DAL stage. This makes the algorithm feasible for production optimization while reducing the computational burden. Additionally, a transfer component analysis (TCA) method is applied to reduce data format and extract data correlations. The developed framework is incorporated into three well-known evolutionary algorithms (non-dominated sorting genetic algorithm II, multi-objective particle swarm optimization, and multi-objective evolutionary algorithm based on decomposition) as well as a single-objective optimizer (particle swarm optimization) for NPV maximization and comprehensive optimization. The proposed method is tested on dynamic benchmark scenarios and an actual situation using a three-

channel reservoir model. The results indicate that the proposed strategy reduces the number of simulation calls required to reach optimal control options when applied with population-based evolutionary algorithms. Furthermore, the proposed technique demonstrates higher NPV and faster computational time compared to their original evolutionary algorithms.

Hernandez-Mejia et al. (2023) presented a method for evaluating the connectivity between water injection and oil production wells in reservoirs. The authors highlighted the importance of determining well interference to enhance oil recovery through waterflooding. The existing techniques for assessing connectivity between injectors and producer wells, such as correlation coefficients, linear regression models, and capacitance resistance models are discussed. However, these methods have limitations as they rely on simplified flow physics and make various assumptions about the data and subsurface conditions. To address these limitations, the authors proposed a new approach called the physics-constrained dynamic time warping algorithm (PCDTW). The PCDTW method is based on the dynamic time warping (DTW) algorithm, which is commonly used for detecting similarities between temporal sequences. The authors adapt DTW to map the water injection signal onto the oil production signal, effectively determining the lag time between injection and production responses. This mapping allows for the characterization of reservoir formation connectivity and heterogeneity between paired injection and production wells. The proposed method is grounded in an enhanced physics-based model that incorporates constraints for subsurface flow through porous media. By considering the physics of the system, the method improves accuracy, avoids incorrect signal matches or non-physical results, and reduces uncertainty. Furthermore, the PCDTW method is robust in the presence of data measurement noise and relies on fewer assumptions about the data. The paper emphasized that the proposed method is a data-driven approach that combines domain knowledge and physics-based modeling. It offers a valuable tool for subsurface engineering data science by providing insights into reservoir characterization and facilitating the development of effective waterflood plans.

Based on the literature review conducted, several key findings and insights can be drawn regarding reservoir simulation and its evolution in the oil and gas industry. Initially, reservoir simulation heavily relied on techniques such as history matching to improve prediction accuracy by calibrating simulation models with field data. Over time, advancements in both industry practices and computer science have led to significant improvements in processing time and cost-efficiency,

making reservoir simulation methods more accessible. The literature review also highlighted the importance of data preparation, including the division of the reservoir into cells and assigning rock and fluid properties to each cell. Geological studies play a crucial role in reservoir characterization, including understanding the variability of reservoir rock in terms of porosity, permeability, and capillary properties. Stratigraphy was identified as a significant factor influencing flow simulation and history matching studies. The findings suggest that both simple and complex geologic models can provide similar predictions of flow performance, emphasizing the importance of performance measures over visual interpretations. Despite the advancements made in mathematical modeling and simulation techniques, challenges such as numerical issues and the uncertainty of reservoir volume remain. Further research and innovation are needed to address these challenges and develop robust and reliable reservoir models. The emergence of artificial intelligence (AI), particularly machine learning, has introduced new possibilities for enhancing traditional reservoir simulation approaches. Machine learning techniques offer advantages such as faster processing and the ability to generate high-quality predictions with less reliance on resource-intensive simulators. Additionally, machine learning models can retain knowledge from prior training through transfer learning, enabling accurate predictions even when new data is introduced.

In this research, we will leverage the power of machine learning tools to address key challenges in reservoir management. Specifically, we will employ dynamic time warping (DTW) to align well production data and fill in missing values, thereby enhancing the completeness and accuracy of the dataset. Furthermore, we will utilize long short-term memory (LSTM) networks to improve the prediction of oil production, taking advantage of their ability to capture temporal dependencies and patterns in the data. To extend the applicability of our models, we will incorporate transfer learning techniques. By using prior knowledge and pre-trained models, we can enhance the predictive capabilities for new wells or wells with missing data. This approach not only saves computational resources and time but also ensures accurate predictions even when faced with limited or incomplete information. By combining the strengths of DTW, LSTM, and transfer learning, our research aims to provide more robust and reliable predictions for oil production. These advanced machine learning techniques offer the potential to optimize reservoir management strategies and decision-making processes in the oil and gas industry, ultimately leading to improved operational efficiency and resource utilization.

3. Methodology

This study explores into the systematic and comprehensive approach to analyze and model the candidate reservoir using a combination of industry-leading software tools and advanced machine learning techniques. In this chapter, we present the step-by-step process adopted to achieve the study's objectives, encompassing the use of Petrel, Eclipse, and machine learning as primary tools. Petrel, a widely utilized software platform in the oil and gas industry, forms the foundation of our reservoir characterization efforts. Leveraging Petrel's robust capabilities in geological modeling and reservoir simulation, we gained valuable insights into the subsurface geology, fluid properties, and reservoir behavior. This enabled us to construct a static reservoir model that serves as a reliable representation of the candidate reservoir's geological and petrophysical properties. In addition to Petrel, Eclipse, a reservoir simulation software, that was used in the backend of Petrel and played a crucial role in the dynamic characterization of the reservoir. Eclipse facilitated the simulation of fluid flow, reservoir performance, and recovery mechanisms, enabling us to predict production behavior under various scenarios and operational conditions.

To further augment our analysis and optimize reservoir management strategies, we incorporated machine learning as a powerful technique. Machine learning allowed us to unlock valuable patterns and relationships hidden within large volumes of data, providing insights into reservoir behavior and aiding in predictive modeling. In particular, long short-term memory (LSTM) time series analysis and dynamic time warping (DTW) alongside with transfer learning were employed as cutting-edge machine learning techniques, promising to deliver enhanced accuracy in predicting future production and effectively handling missing data.

By amalgamating the capabilities of Petrel, Eclipse, and machine learning, we aim to provide a comprehensive reservoir management framework that optimizes production strategies, enhances hydrocarbon recovery, and facilitates informed decision-making. This work will detail the implementation of these techniques and their integration, ultimately setting the stage for the subsequent analysis and results presented in the following section 4.

3.1 Case Study

For this study, we have selected a specific oil reservoir as our candidate for analysis. The Sarir or, more specifically, the Sarir "C" field lies on the western edge of the Calanscio Sand Sea in southern Cyrenaica and is the largest oil field in Libya. It occurs at the southeastern margin of the Upper Cretaceous-Tertiary Sirte basin or embayment that contains all the major oil fields of Libya and is the most prolific oil-producing basin in North Africa which is Sirt basin (Figure 3.1). The understanding of the studied area's geology relies on acknowledging significant geological events that impacted the Sirt basin and its surroundings. (Abadi et al., 2008) offers a concise overview of these events, which are detailed as follows: The Late Jurassic - Early Cretaceous period initiated rifting, creating a complex system of northwest-southeast horst-grabens due to extension. Subsequently, during the Late Cretaceous, further extension and fault reactivation led to major subsidence. This allowed Late Cretaceous seas to invade and fill the basin, characterized by shale and shallow water carbonates. The conclusion of the Cretaceous marked widespread Kalash carbonate deposition. Carbonates were present along the shelf margin, their characteristics influenced by water depth, topography, and currents. (Figure 3.2) demonstrates Horst-Graben system in Sirt basin. The chosen reservoir possesses unique geological characteristics, complex fluid properties, and a history of production data. A thorough examination of this reservoir presents an ideal opportunity to showcase the efficacy and applicability of the methodologies adopted in this study. The reservoir is also known as Nubian sandstone formation and the basal sandstones are the main reservoir of the field. They are far from homogeneous and have been subdivided into five members, three of shaly or tight sandstone separated by two clean sandstone units. The (Figure 3.3) shows the stratigraphic column of Sarir trough.

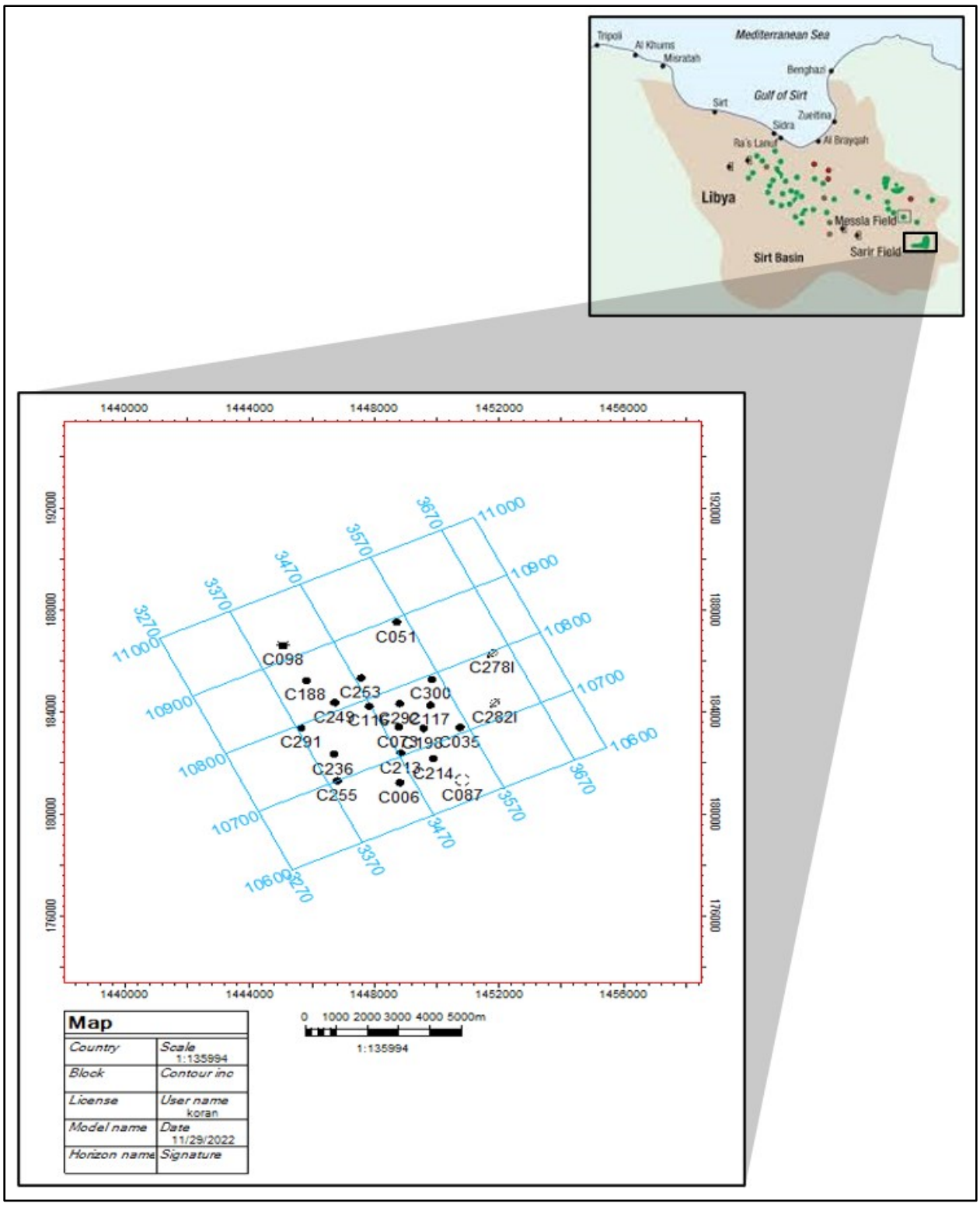

Figure 3.1: The location of the study area of the Sarir C field

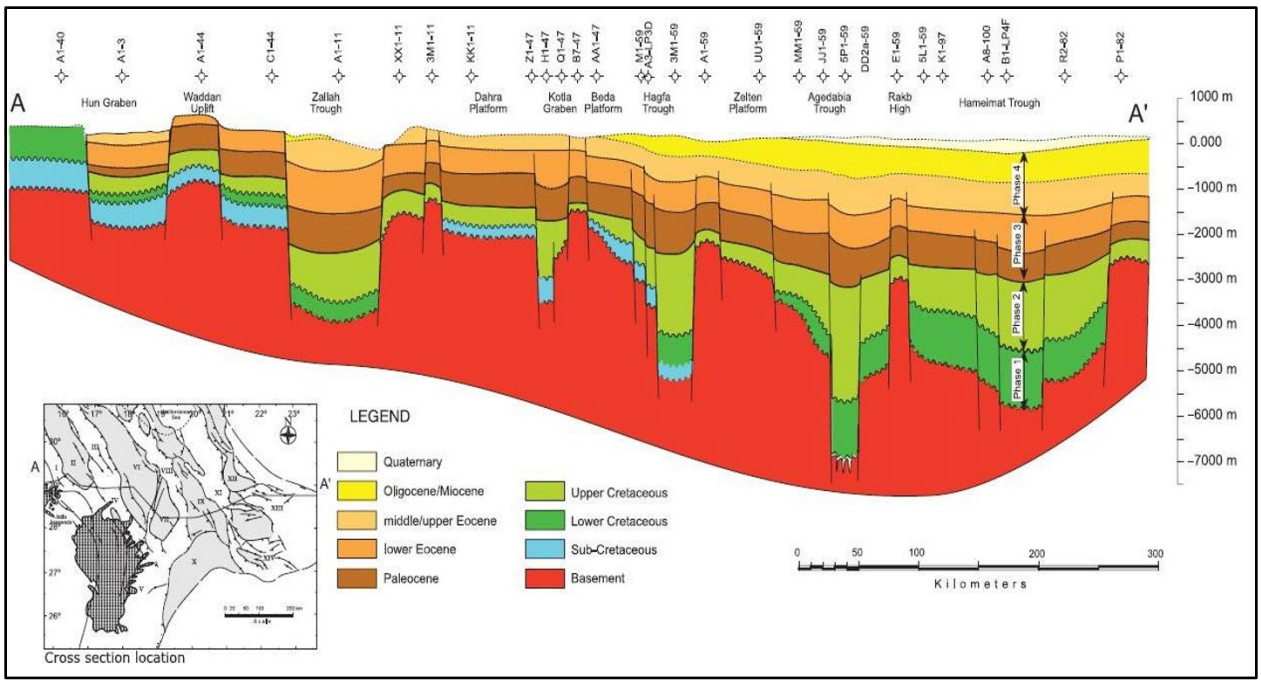

Figure 3.2: Horst-Graben system in Sirt basin, (Abadi et al. 2008)

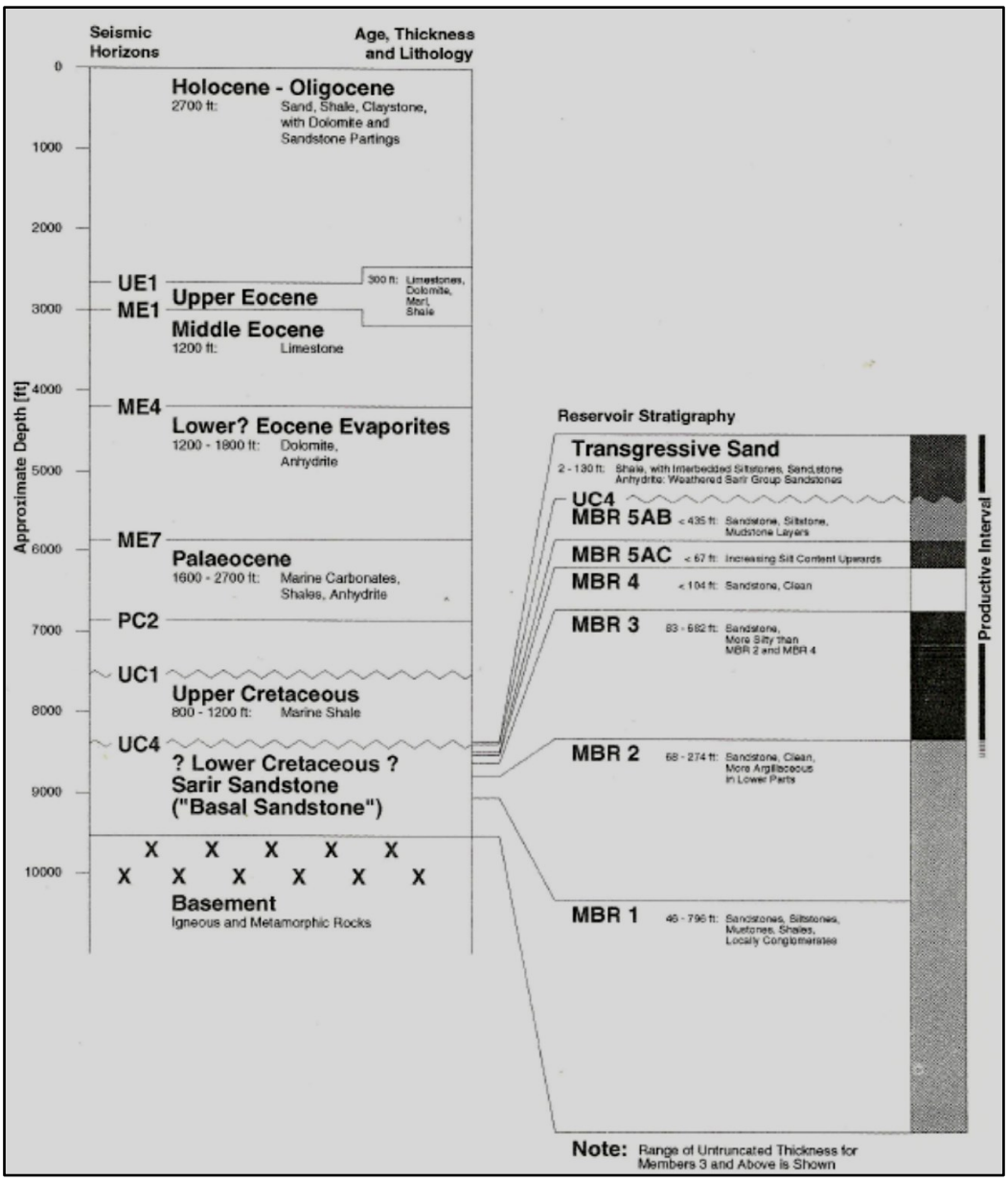

Figure 3.3: Stratigraphic column of Sarir trough, (Heinemann oil technology and engineering (HOT), 1993)

3.2 Sarir C-Main Petrophysics Data

The data utilized in this study was generously provided by the Arabian Gulf Oil Company (AGOCO). In order to enhance the dynamic modeling process, certain improvements were made to the original dataset. This study relies on comprehensive information gathered from 21 boreholes and geophysical data obtained through a 3D seismic survey, which covers a substantial portion of the study area. Data preparation and formatting are vital for accurate research. Despite being time-

consuming, particularly when dealing with data from diverse software packages with varying formats it ensures data integrity and minimizes errors. Organized data forms a strong foundation for meaningful analysis, enabling researchers to identify and rectify incomplete, inaccurate, or missing data and enhancing overall quality. Informed decisions and valuable insights stem from reliable data. In short, data preparation is essential for credible and impactful research.

To facilitate the current study, a comprehensive set of data is indispensable. The following essential datasets must be available for effective analysis:

- Seismic data: High-quality seismic data provides crucial insights into the subsurface structures and geological features of the reservoir. It aids in mapping potential hydrocarbon-bearing zones and understanding the reservoir's spatial characteristics.
- Well logs data: Well logs offer valuable information on rock properties, fluid content, and reservoir behavior. They serve as a key source for characterizing the reservoir's petrophysical properties and its potential productivity.
- Base map: The base map provides the foundational spatial context for the study area. It includes geographical features, well locations, and other essential details necessary for precise reservoir characterization.
- Check Shots data: Check shots data is vital for accurate seismic velocity modeling. It aids in calibrating seismic data, ensuring more precise interpretation and modeling of the subsurface.
- Production data: Production data offers crucial insights into the reservoir's performance over time. It includes oil and gas production rates, water production, and other relevant parameters that enable the assessment of reservoir productivity and depletion.
- Petrophysical data: Petrophysical data encompasses core analysis and well log interpretations. It is instrumental in understanding rock properties, fluid saturation, and permeability, which are essential for reservoir modeling and simulation.
- Geological reports & papers: Existing geological reports and research papers provide valuable knowledge about the reservoir's geology, depositional environment, and structural characteristics. They offer a solid foundation for building the reservoir model and validating the study's findings.

The availability and thorough analysis of these diverse datasets are pivotal to the success of the current study. They form the backbone of the research, enabling a comprehensive understanding of the reservoir and supporting informed decision-making for reservoir management strategies.

3.2.1 Seismic Cube

The seismic cube plays a crucial role in identifying the specific area of interest for the study and determining its precise coordinates. In this study, the seismic cube is centered within the C-main Field, encompassing the region between the points 1441106.24 to 1455432.17 on the X coordinate and 18275.55 to 186891.64 on the Y coordinate. This spatial coverage is further detailed by 445 X-Line and 400 In-line time slices, providing a comprehensive description of the structural layers within the seismic cube's area (Figure 3.4 & 3.5). By leveraging this seismic cube, the study gains valuable insights into the subsurface structure, which is vital for conducting an accurate and comprehensive analysis of the field.

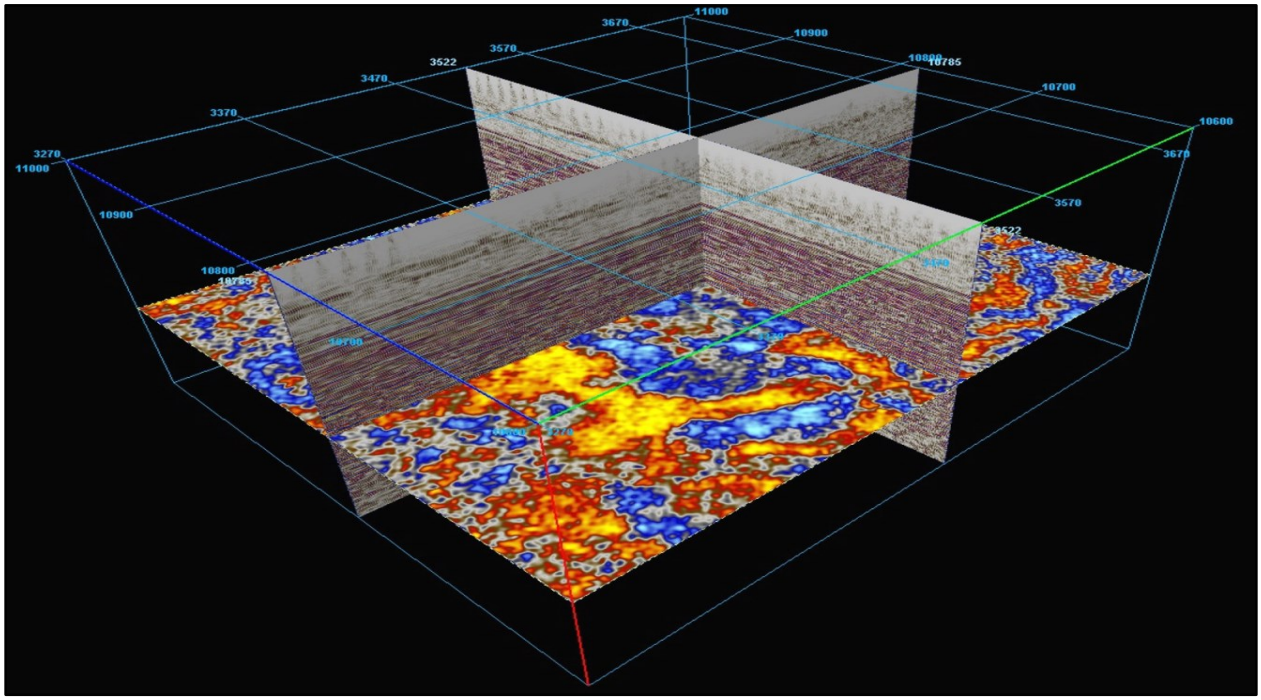

Figure 3.4: Seismic cube of the study are illustrate the In-line, Cross-line and time slice

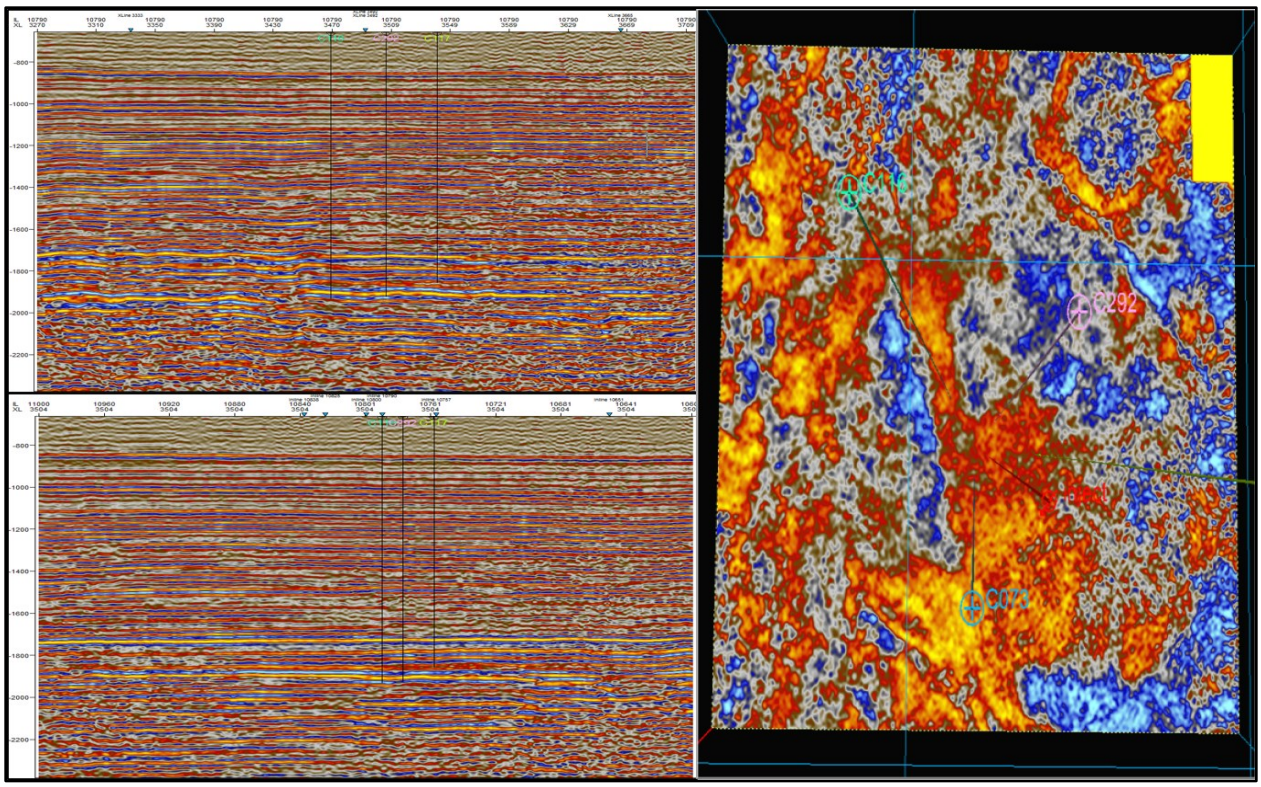

Figure 3.5: Shows the reservoir part throughout In-line, Cross-line and time slice with wells location

3.2.2 Well Logs Data

A wide range of logs is essential to determine the Well-Tops, sequence of layers, and rock properties. These logs include Caliper log (CAL), Gamma ray logs (GR), Spontaneous potential (SP), Density logs (RHOB), resistivity logs (ILD), Neutron logs (NPHI), water saturation (S_w), and sonic logs (DT), all of which will be thoroughly explained in this study (Tables 3.1 & 3.2). Moreover, the study relies on data from 21 wells, each contributing significant parameters and information. The following table summarizes the key details of these 21 wells.

Table 3.1: Main surface and subsurface information of well logs data

Well name	X coordinate	Y coordinate	Kelly bushing elevation	Measured depth	Well Symbol
C051	1448721.00	187564.80	331.8	9040.0	Oil
C073	1448784.00	183442.50	420.8	9030.0	Oil

C087	1450826.00	181372.80	466.2	10.0	Undefined
C116	1447836.00	184259.90	442.2	8890.0	Oil
C098	1445067.00	186646.40	405.9	10.0	Abandoned oil and gas
C006	1448821.00	181269.00	431.9	9670.0	Oil
C035	1450751.00	183434.80	474.3	9050.0	Oil
C198	1449580.00	183392.90	453.0	9000.0	Oil
C213	1448858.00	182428.60	467.5	8938.0	Oil
C236	1446694.00	182394.00	394.0	8940.0	Oil
C249	1446730.00	184407.80	426.9	9162.0	Oil
C253	1447573.00	185374.50	440.6	9060.0	Oil
C255	1446816.00	181346.20	435.2	8920.0	Oil
C117	1449802.00	184309.00	460.0	8880.0	Oil
C188	1445813.00	185274.10	429.8	9040.0	Oil
C214	1449895.00	182213.80	474.4	8980.0	Oil
C278I	1451810.00	186357.10	479.8	9600.0	Injection water
C282I	1451872.00	184401.20	428.1	9640.0	Injection water
C291	1445650.00	183415.00	409.8	9010.0	Oil
C292	1448818.00	184369.50	440.0	9310.0	Oil
C300	1449841.90	185318.70	420.8	9310.0	Oil

Table 3.2: Shows different type of log data availability for each well

Well \ Log	**Caliper [Cali]**	**Gamma Ray [GR]**	**Spontaneous Potential [SP]**	**Density [RHOB]**	**Neutron [NPHI]**	**Sonic [DT]**	**Deep Resistivity [RD]**
C051	√	√	√			√	√
C073	√	√	√				√
C087	√	√	√	√	√		√
C116	√		√			√	√
C098							
C006							

C035							
C198	√	√	√	√	√	√	√
C213							
C236	√	√	√	√	√	√	√
C249							
C253							
C255							
C117	√	√	√	√	√	√	√
C188	√	√	√	√	√	√	√
C214	√	√	√	√	√	√	√
C278I	√	√	√	√	√	√	√
C282I	√	√	√	√	√	√	√
C291	√	√	√	√	√	√	√
C292	√	√	√	√	√	√	√

For wells that lack raw well data in the table, interpreted data will be provided, including essential parameters such as Porosity (Φ), Permeability (k), Vshale (V_{sh}), Oil saturation (S_o), Water saturation (S_w), and Facies. These interpreted data points will be further utilized in the procedure section, outlining their significance in the study. The interpretation process plays a crucial role in characterizing the reservoir and facilitating a comprehensive understanding of the well's properties and behavior. (Figures 3.6 & 3.7) provides well log data for some of the candidate wells in this study.

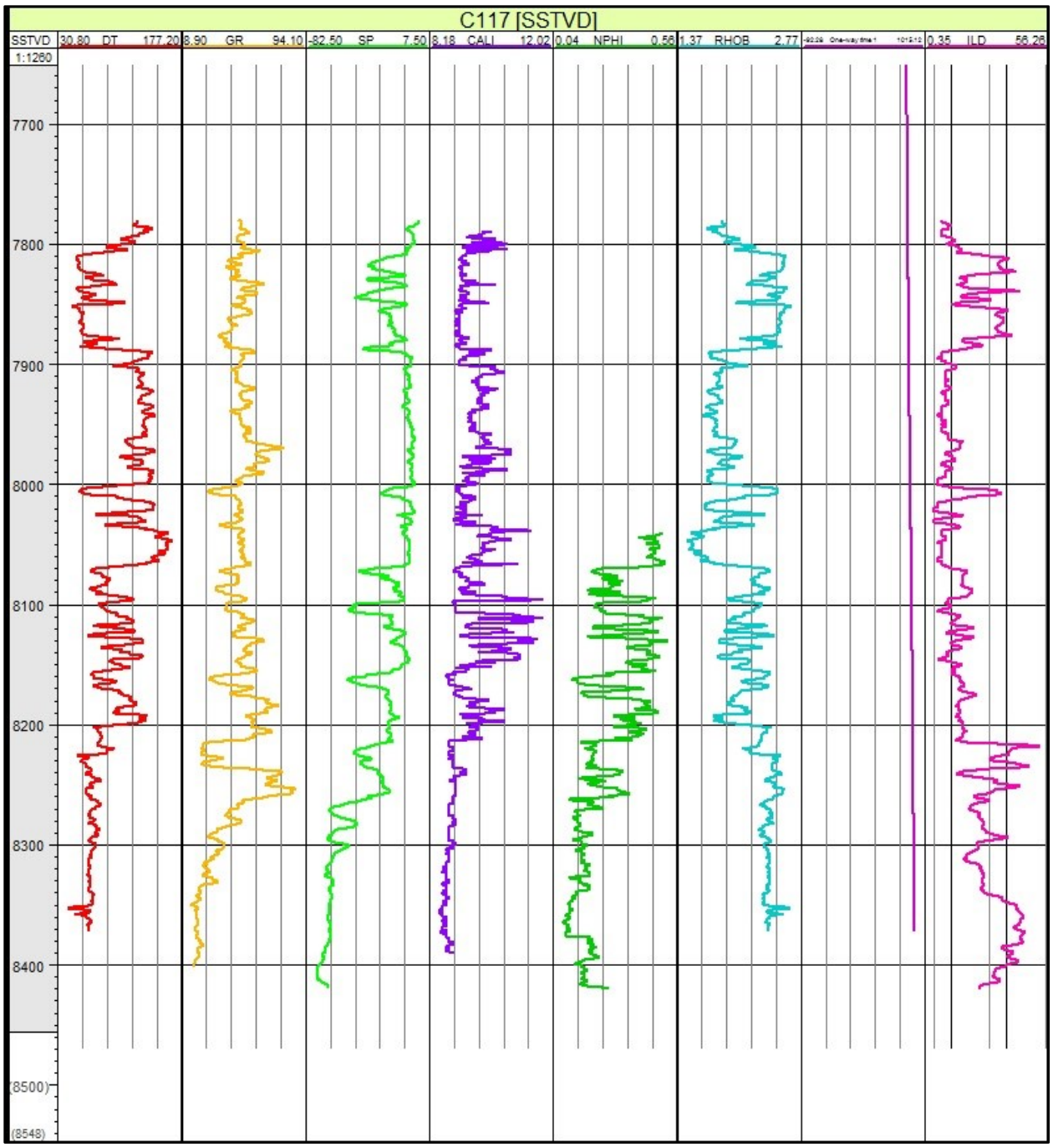

Figure 3.6: A set of Log responses from well C117

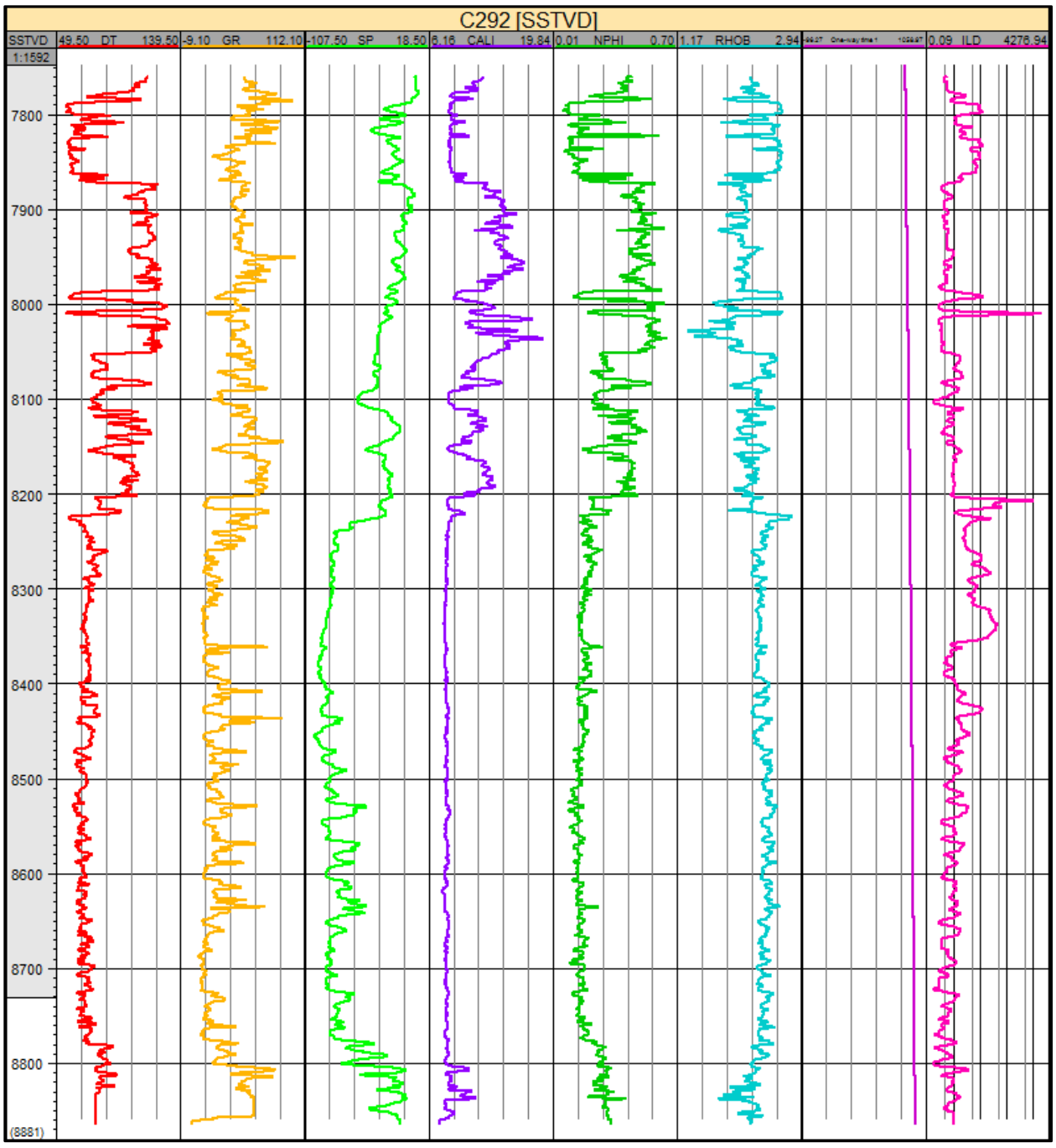

Figure 3.7: A set of Log responses from well C292

3.2.3 Base Map

A base map serves as a comprehensive reference map encompassing various geographic features (Figure 3.8). It acts as a foundation that brings together geological and geophysical data within a single mapping canvas. This integration incorporates a wide range of information, including

seismic 3D or 2D surveys, well locations, markers, surfaces, faults, cross sections, production data, and down-hole well data such as logs and litho-facies. By consolidating diverse datasets, the base map facilitates regional evaluation and interpretation, enabling a holistic understanding of the study area's geological and geophysical characteristics.

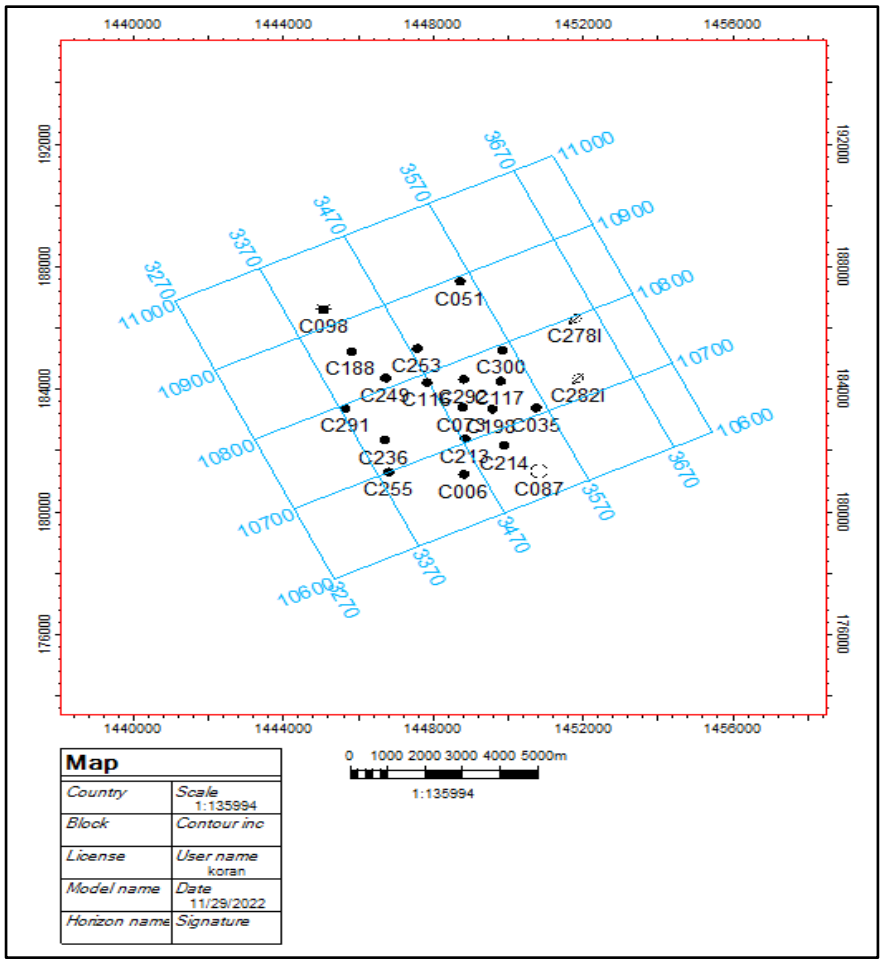

Figure 3.8: Base map of the project area (seismic survey & wells location)

3.2.4 Check Shot Data

Check Shot Data is a specialized type of borehole seismic data used to precisely measure the seismic travel time from the surface to a known depth. This method enables the direct measurement of P-wave velocity for formations encountered in a wellbore. The process involves lowering a geophone to each formation of interest, emitting a source of energy from the Earth's surface, and recording the resulting signal. Subsequently, the data is correlated with surface seismic data,

allowing for the correction of the sonic log and the generation of a synthetic seismogram. This invaluable procedure serves to validate or adjust seismic interpretations, providing a robust tool for enhancing subsurface imaging and refining our understanding of geological structures (Table 3.3). Check Shot Data plays a significant role in improving the accuracy and precision of subsurface exploration and reservoir characterization.

Table 3.3: Check Shot Data for wells (C117 & C292)

Well No.	Tops	Measured Depth [MD]	Two Way Time [TWT]
C117	5AB	8251.56	1824.32
	Member 3	8331.85	1843.37
C292	5AB	8230.61	1832.43
	Member 3	8323.73	1849.4

3.2.5 Production History

The data used in this study was collected from wells located within the study area. Production data was available for a subset of wells, including C006, C035, C198, C213, C236, C249, C253, and C255. As an illustration, we present an example of the production data available for the well C035 and C006. The production records for well C035 in (Figure 3.9) commence from 8/1/1984 and extend until 1/1/2019. As for well C006 in (Figure 3.10) commence from 10/1/2000 and extend until 1/1/2019. (BOPD) being barrel of oil per day, (BWPD) barrel of water per day, and (GOR) is gas oil ratio. This comprehensive dataset provides valuable insights into the reservoir's production history, enabling a detailed analysis of the well's performance over the specified period.

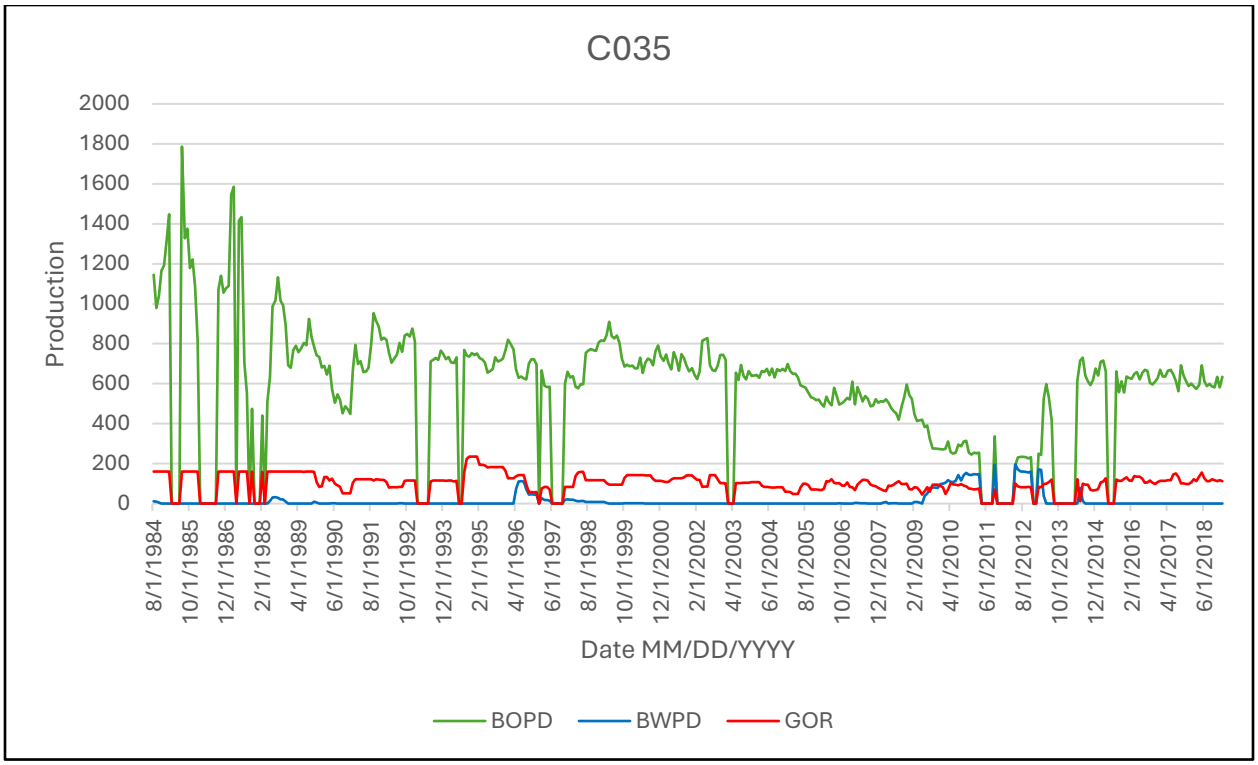

Figure 3.9: Production data for C035 from 1984 to 2019

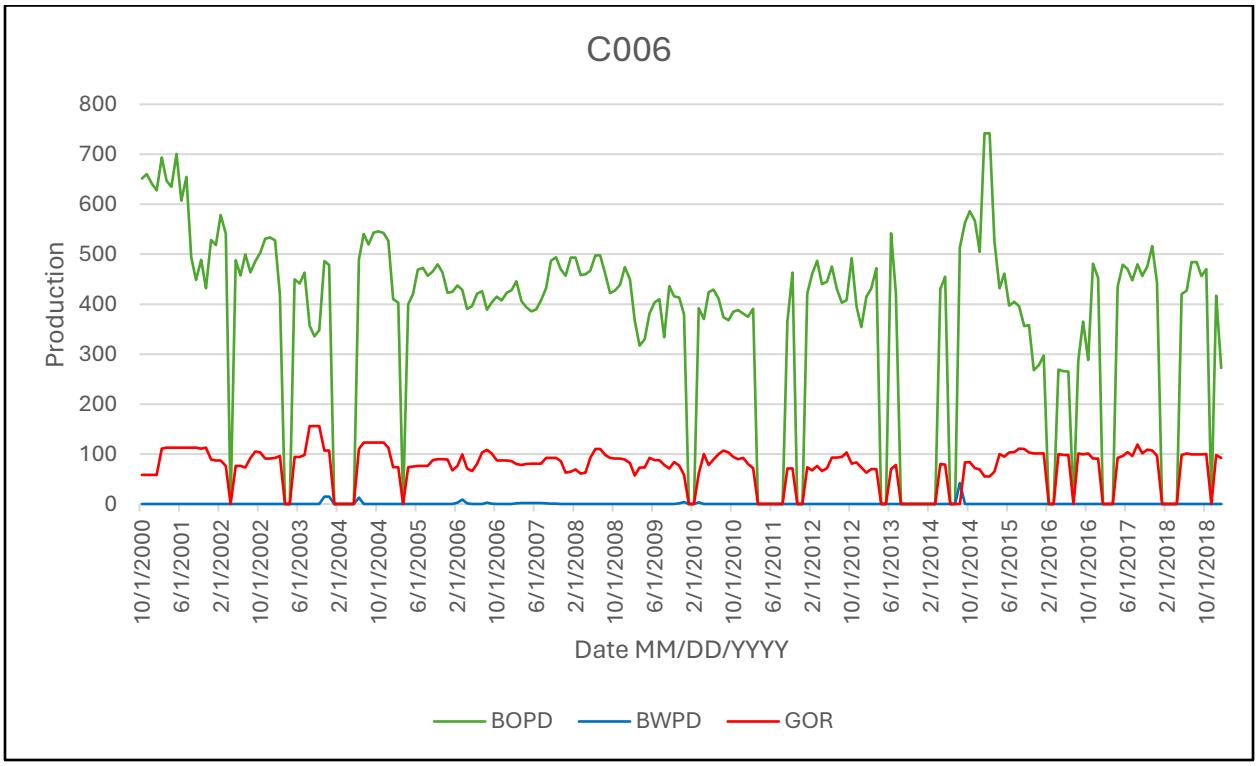

Figure 3.10: Production data for C006 from 2000 to 2019

3.3 Procedure

The procedure begins by establishing a static model, which is then transformed into a dynamic model. Subsequently, the prediction phase involves history matching and depletion strategies will be conducted. In addition, the study explores various machine learning methods, including DTW, LSTM, and transfer learning, to enhance prediction strategies.

3.3.1 Static and Dynamic Model

One of the objectives of this study is to construct a 3D reservoir model for the Nubian Sandstone Formation. Subsequently, the aim is to simulate various parameters to develop a dynamic model that portrays the production history matching and forecasting of the targeted formation. Additionally, this endeavor seeks to anticipate the reservoir's response to diverse production scenarios. Below is a flowchart that demonstrates the steps of building a static and dynamic model (Figure 3.11).

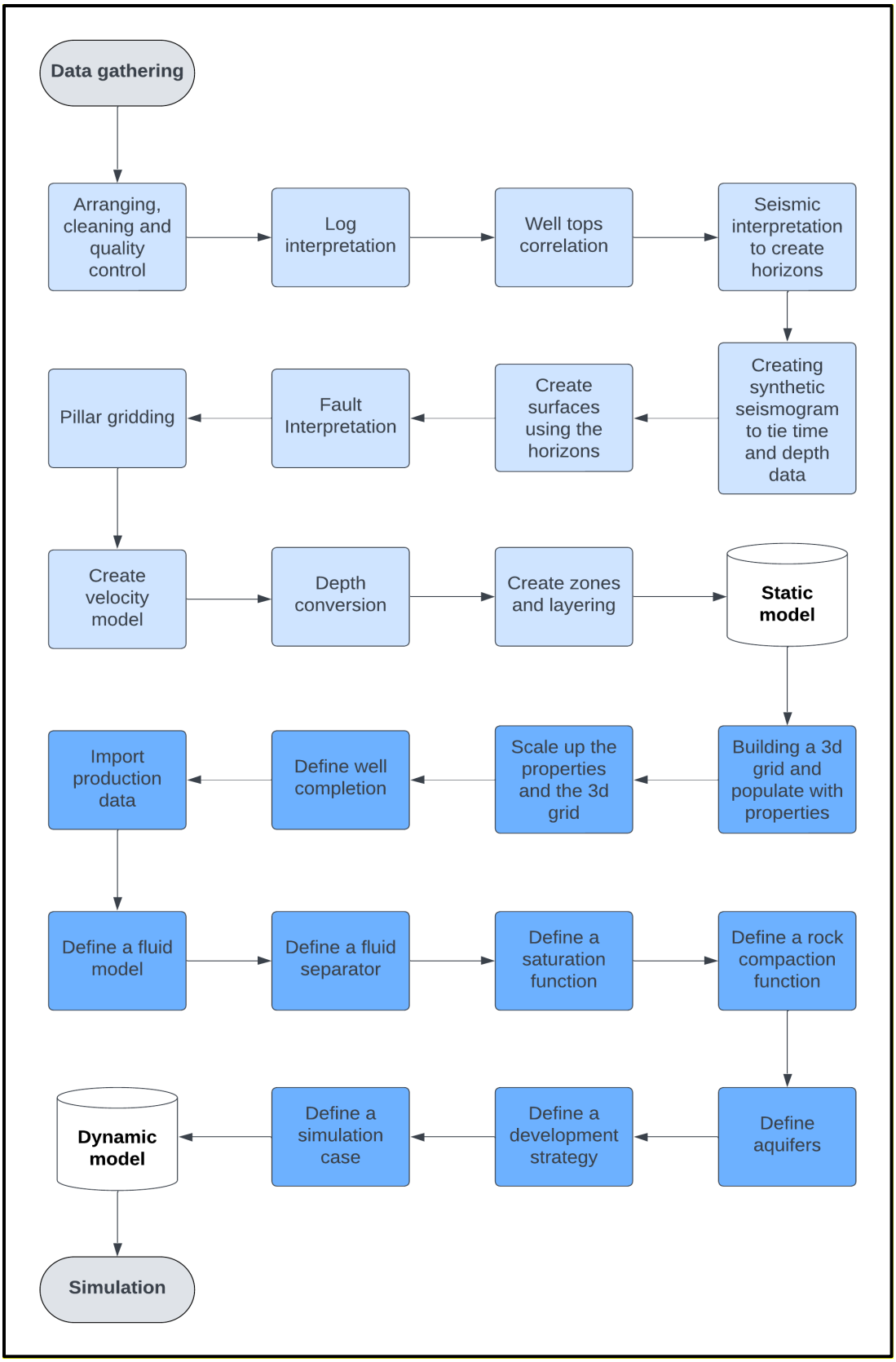

Figure 3.11: Flowchart for the steps of building a static and a dynamic model

3.3.1.1 Quality Control

The raw data when it was collected was in a (.ELG) format and had to be arranged and changed specially for well logs data into (.las) file and adjust the header so Petrel can read it and identify the logs. Also, the lab data that was taking from reports, tables and figures by (Heinemann oil technology and engineering (HOT), 1993) had to be organized and filtered. Lastly the production data was reviewed and allocated the missing data and sections of certain wells and will be explained later how these missing data were filled with machine learning techniques.

3.3.1.2 Log Interpretation

The purpose of well logging is to ascertain the characteristics of rock formations with potential hydrocarbon reserves. Specifically, these logs provide essential information on the Lithology of the Formation, Porosity, Permeability, and Saturation. To assess a reservoir's potential for production, understanding the ease with which fluids can move through the pore system becomes crucial. Furthermore, factors such as reservoir geometry, formation temperature, pressure, thickness area and lithology also play pivotal roles in assessing, completing, and producing from a reservoir.

Porosity refers to the volume of pores or voids within a formation per unit of total volume; essentially, it represents the portion of a sample's volume occupied by these spaces. For instance, materials like glass, which possess uniform density, exhibit zero porosity, while highly porous materials like sponges display significant porosity. Determining porosity offers insights into the subsurface properties. There exist diverse methods for calculating porosity, including in-situ techniques employing logs like Neutron and density logs, as well as laboratory measurements. (Figure 3.12) which provide insights into the porosity as an example of some wells that was calculated within the study area.

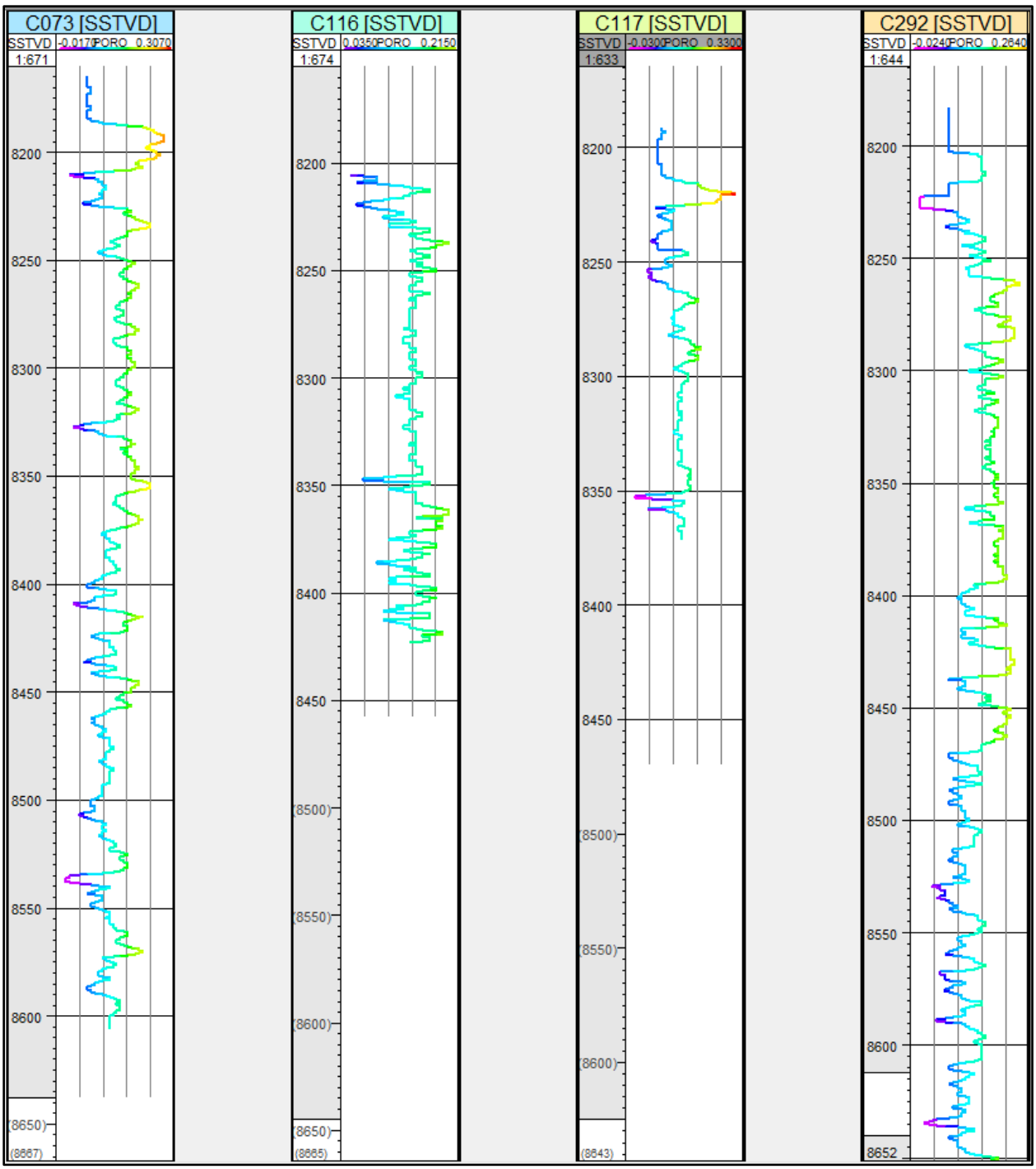

Figure 3.12: Porosity (Density) logs for the wells (C073, C116, C117, C292)

Saturation refers to how much of a formation's pore space is occupied by a particular fluid. Specifically, water saturation tells us how much of the pores contain water. If a formation's pores are filled only with water, its water saturation is 100%. We use the symbol 'S' to represent

saturation, with different subscripts like 'S_w' for water saturation, 'S_o' for oil saturation, and 'S_h' for hydrocarbon saturation. To calculate water saturation, we use Archie's equation within Petrel's software. (Figure 3.13) shows the results of certain wells.

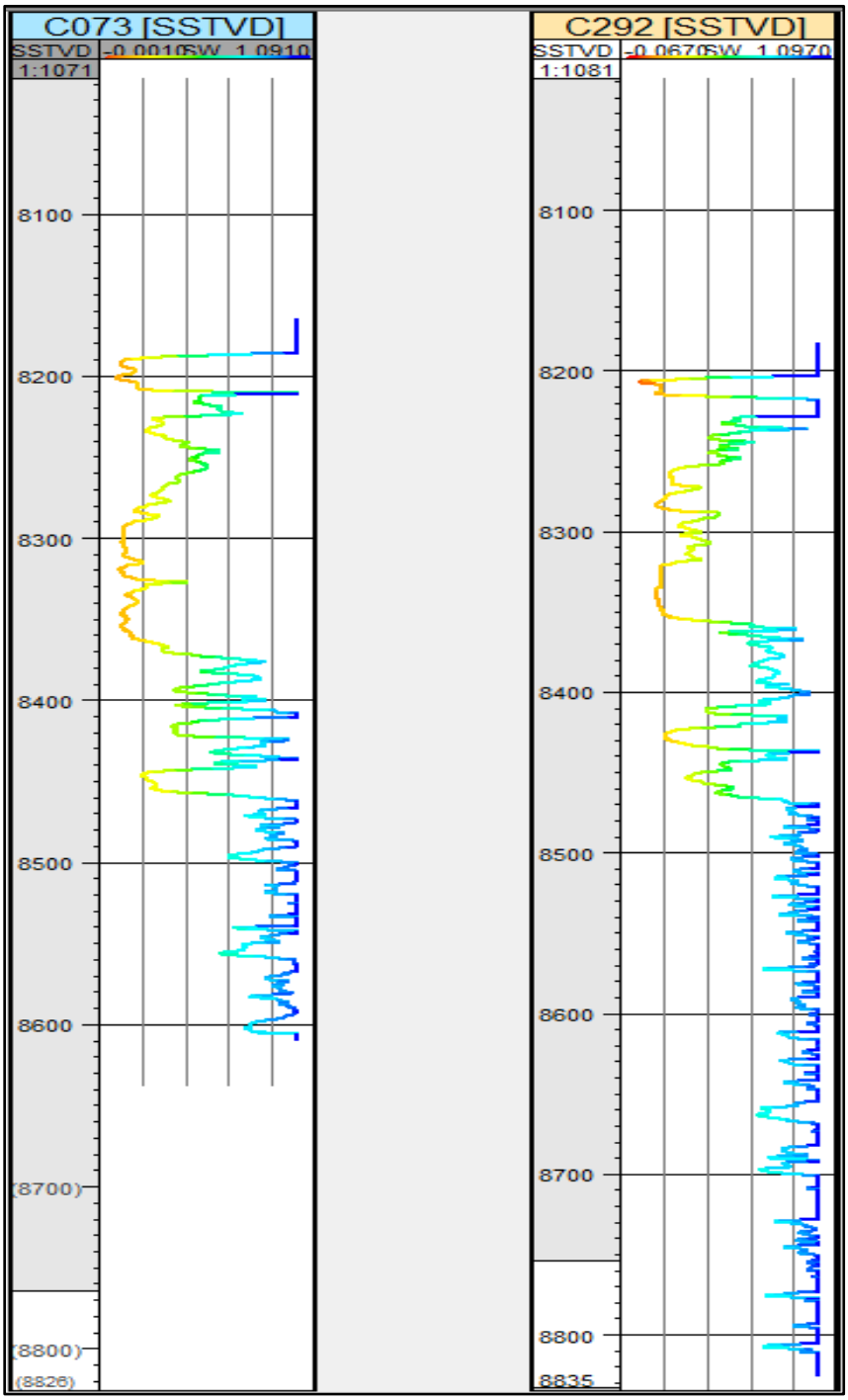

Figure 3.13: Water Saturation log for the wells C073 and C292

The neutron log is a porosity log that measures the hydrogen ion concentration in a formation while the density log is a porosity log that measures the electron density of a formation. Both neutron and density logs are used for fluid bearing identification and porosity calculation, now we will use the neutron density logs to determine the main and secondary reservoir. (Figure 3.14) shows there are 3 or 4 possible reservoirs marked in yellow, including the Nubian Sandstone Formation.

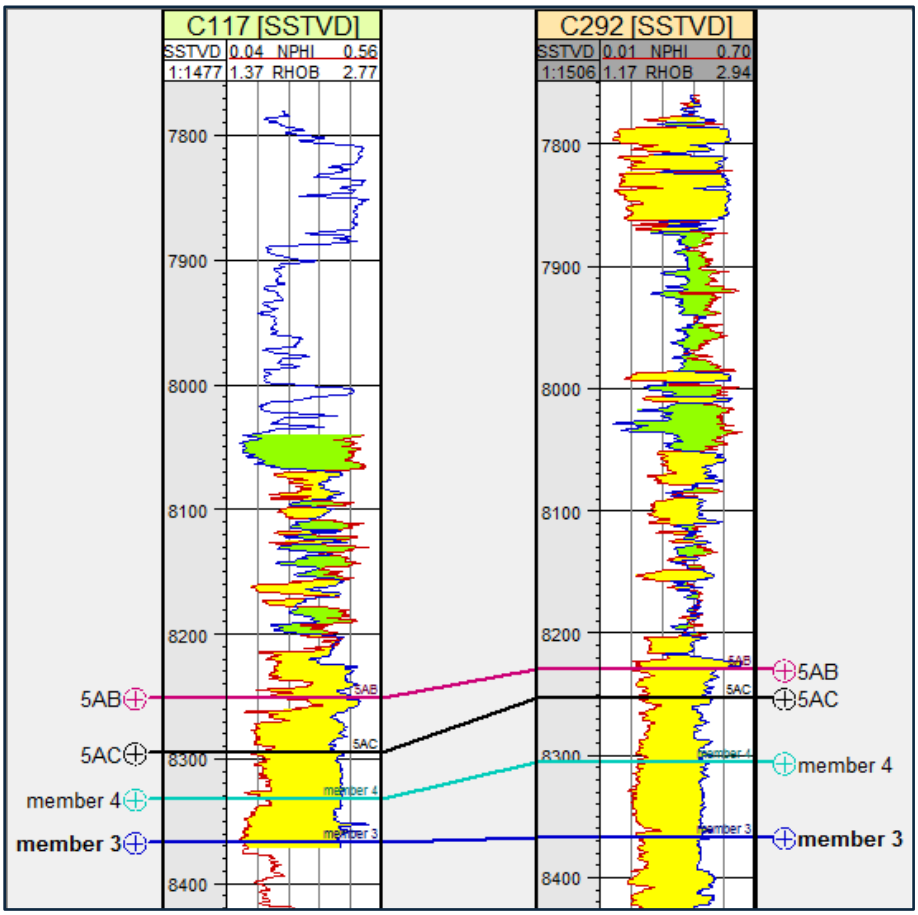

Figure 3.14: Neutron – density correlation with well tops

Resistivity logs are used to measure the resistivity of the formation rock and the fluid contained within the rock pores to an applied electrical current. (Figure 3.15) presents the coloration of shallow and deep resistivity logs.

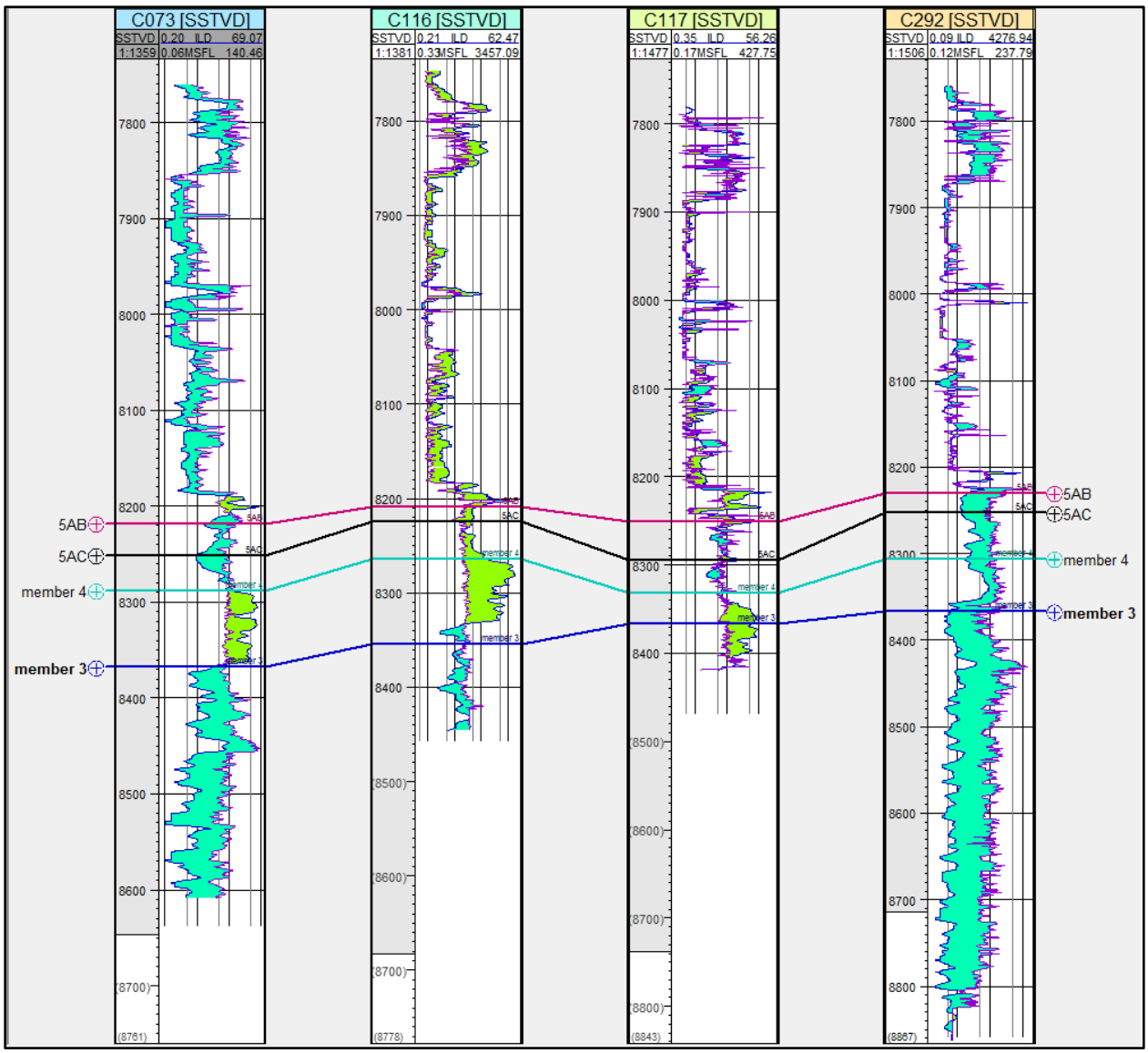

Figure 3.15: Correlation based on Shallow and Deep resistivity logs

The Gamma ray-SP logs are used to correlate the well tops according to their lithologies and the top and the bottom for each layer in the formation. (Table 3.4) shows the results of well tops for each well.

Table 3.4: Well tops of the study area

Well identifier	Surface	X	Y	Z	MD
C006	TGS	1448821.00	181269.00	-8278.32	8710.22
C006	Member 5AB	1448821.00	181269.00	-8318.54	8750.44
C006	Member 5 AC	1448821.00	181269.00	-8418.95	8850.85
C006	Member 4	1448821.00	181269.00	-8462.64	8894.54
C006	Member 3	1448821.00	181269.00	-8556.97	8988.87
C006	Member 2	1448821.00	181269.00	-8929.94	9361.84
C035	TGS	1450751.00	183434.80	-8235.99	8710.29
C035	Member 5AB	1450751.00	183434.80	-8286.27	8760.57
C035	Member 5 AC	1450751.00	183434.80	-8353.54	8827.84
C035	Member 4	1450751.00	183434.80	-8394.41	8868.71
C073	TGS	1448784.00	183442.50	-8185.44	8606.24
C073	Member 5AB	1448784.00	183442.50	-8218.23	8639.03
C073	Member 5 AC	1448784.00	183442.50	-8245.14	8665.94
C073	Member 4	1448784.00	183442.50	-8288.97	8709.77
C073	Member 3	1448784.00	183442.50	-8368.83	8789.63
C116	TGS	1447836.00	184259.90	-8181.26	8623.46
C116	Member 5AB	1447836.00	184259.90	-8208.46	8650.66
C116	Member 5 AC	1447836.00	184259.90	-8224.08	8666.28
C116	Member 4	1447836.00	184259.90	-8264.01	8706.21
C116	Member 3	1447836.00	184259.90	-8340.98	8783.18
C117	TGS	1449802.00	184309.00	-8211.55	8671.55
C117	Member 5AB	1449802.00	184309.00	-8251.34	8711.34
C117	Member 5 AC	1449802.00	184309.00	-8295.82	8755.82
C117	Member 4	1449802.00	184309.00	-8331.63	8791.63
C188	TGS	1445813.00	185274.10	-8247.55	8677.35
C188	Member 5AB	1445813.00	185274.10	-8261.13	8690.93
C188	Member 5 AC	1445813.00	185274.10	-8320.06	8749.86
C188	Member 4	1445813.00	185274.10	-8353.02	8782.82
C188	Member 3	1445813.00	185274.10	-8442.98	8872.78
C198	TGS	1449580.00	183392.90	-8208.72	8661.72
C198	Member 5AB	1449580.00	183392.90	-8241.18	8694.18
C198	Member 5 AC	1449580.00	183392.90	-8296.25	8749.25
C198	Member 4	1449580.00	183392.90	-8327.97	8780.97
C198	Member 3	1449580.00	183392.90	-8408.36	8861.36
C213	TGS	1448858.00	182428.60	-8212.56	8680.06
C213	Member 5AB	1448858.00	182428.60	-8243.66	8711.16
C213	Member 5 AC	1448858.00	182428.60	-8358.32	8825.82
C213	Member 4	1448858.00	182428.60	-8387.61	8855.11
C214	TGS	1449895.00	182213.80	-8234.22	8708.62
C214	Member 5AB	1449895.00	182213.80	-8272.12	8746.52
C214	Member 5 AC	1449895.00	182213.80	-8390.01	8864.41
C214	Member 4	1449895.00	182213.80	-8424.12	8898.52
C236	TGS	1446694.00	182394.00	-8261.84	8655.84
C236	Member 5AB	1446694.00	182394.00	-8283.07	8677.07
C236	Member 5 AC	1446694.00	182394.00	-8362.03	8756.03
C236	Member 4	1446694.00	182394.00	-8389.29	8783.29
C236	Member 3	1446694.00	182394.00	-8482.04	8876.04
C249	TGS	1446730.00	184407.80	-8256.60	8683.50
C249	Member 5AB	1446730.00	184407.80	-8295.66	8722.56
C249	Member 5 AC	1446730.00	184407.80	-8398.52	8825.42
C249	Member 4	1446730.00	184407.80	-8433.25	8860.15
C249	Member 3	1446730.00	184407.80	-8515.28	8942.18

C253	TGS	1447573.00	185374.50	-8188.73	8629.33
C253	Member 5AB	1447573.00	185374.50	-8201.39	8641.99
C253	Member 5 AC	1447573.00	185374.50	-8214.05	8654.65
C253	Member 4	1447573.00	185374.50	-8254.56	8695.16
C253	Member 3	1447573.00	185374.50	-8341.37	8781.97
C253	Member 2	1447573.00	185374.50	-8595.27	9035.87
C255	TGS	1446816.00	181346.20	-8212.26	8647.46
C255	Member 5AB	1446816.00	181346.20	-8235.04	8670.24
C255	Member 5 AC	1446816.00	181346.20	-8286.77	8721.97
C255	Member 4	1446816.00	181346.20	-8324.38	8759.58
C255	Member 3	1446816.00	181346.20	-8397.80	8833.00
C278I	TGS	1451810.00	186357.10	-8275.56	8755.36
C278I	Member 5AB	1451810.00	186357.10	-8330.68	8810.48
C278I	Member 5 AC	1451810.00	186357.10	-8420.96	8900.76
C278I	Member 4	1451810.00	186357.10	-8450.04	8929.84
C278I	Member 3	1451810.00	186357.10	-8531.63	9011.43
C278I	Member 2	1451810.00	186357.10	-8778.16	9257.96
C282I	TGS	1451872.00	184401.20	-8295.59	8723.69
C282I	Member 5AB	1451872.00	184401.20	-8355.05	8783.15
C282I	Member 5 AC	1451872.00	184401.20	-8510.43	8938.53
C282I	Member 4	1451872.00	184401.20	-8548.19	8976.29
C282I	Member 3	1451872.00	184401.20	-8628.05	9056.15
C282I	Member 2	1451872.00	184401.20	-8977.88	9405.98
C291	TGS	1445650.00	183415.00	-8235.31	8645.11
C291	Member 5AB	1445650.00	183415.00	-8271.64	8681.44
C291	Member 5 AC	1445650.00	183415.00	-8324.16	8733.96
C291	Member 4	1445650.00	183415.00	-8362.79	8772.59
C291	Member 3	1445650.00	183415.00	-8486.05	8895.85
C292	TGS	1448818.00	184369.50	-8203.08	8643.08
C292	Member 5AB	1448818.00	184369.50	-8229.48	8669.48
C292	Member 5 AC	1448818.00	184369.50	-8238.89	8678.89
C292	Member 4	1448818.00	184369.50	-8273.97	8713.97
C292	Member 3	1448818.00	184369.50	-8360.42	8800.42
C292	Member 2	1448818.00	184369.50	-8641.81	9081.81
C300	TGS	1449841.90	185318.70	-8235.95	8656.75
C300	Member 5AB	1449841.90	185318.70	-8268.06	8688.86
C300	Member 5 AC	1449841.90	185318.70	-8334.47	8755.27
C300	Member 4	1449841.90	185318.70	-8417.80	8838.60
C300	Member 3	1449841.90	185318.70	-8553.59	8974.39
C300	Member 2	1449841.90	185318.70	-8861.42	9282.22

Geologists use the term "facies" to group bodies of rock into mappable units based on their physical traits, chemical composition, formation, or a variety of other characteristics. Facies are primarily utilized to distinguish distinct rock units physically, chemically, or biologically from adjacent rock units within a continuous body of rock. Facies were a significant addition to the stratigraphic system. Lithofacies is a combination of physical rock features, such as mineral composition, grain size, color, and texture, which can be used to define rock facies. To calculate the facies using petrel

calculator, Porosity, Vshale and Net Gross is used. Displayed in (Figure 3.16) is an example of well C117 and C292 facies.

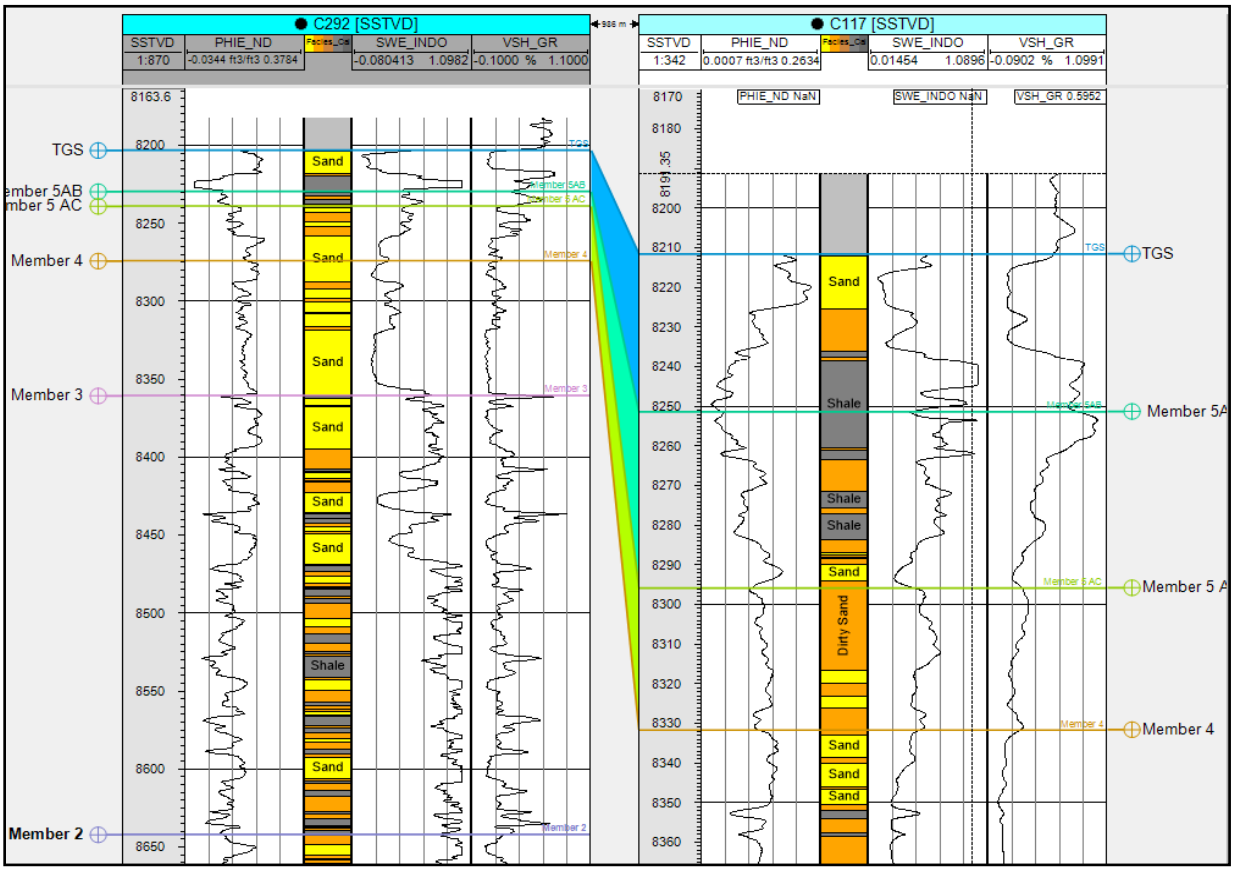

Figure 3.16: Facies of well C117 and C292

3.3.1.3 Seismic Interpretation

In the realm of seismic interpretation, synthetic seismograms serve as crucial links connecting geological information from well data in depth to geophysical data represented in seismic time. This process involves two key steps:

- Time Conversion of Wells: This initial step entails the conversion of well data into seismic time using data like check shot data and sonic logs. Through this, a time-depth relationship is established for each well.
- Generation of Synthetic Seismograms: Using density logs, sonic logs, and a seismic wavelet, synthetic seismograms are generated. This involves calculating acoustic impedance and reflection coefficients, followed by convolving them using a wavelet.

These synthetic seismograms can be adjusted based on modifications to the time-depth relationship. Furthermore, seismic horizons can be correlated with stratigraphic boundaries identified within well logs, facilitating a comprehensive understanding. (Figures 3.17 & 3.18) present the result of synthetic seismogram for well C117 and C292.

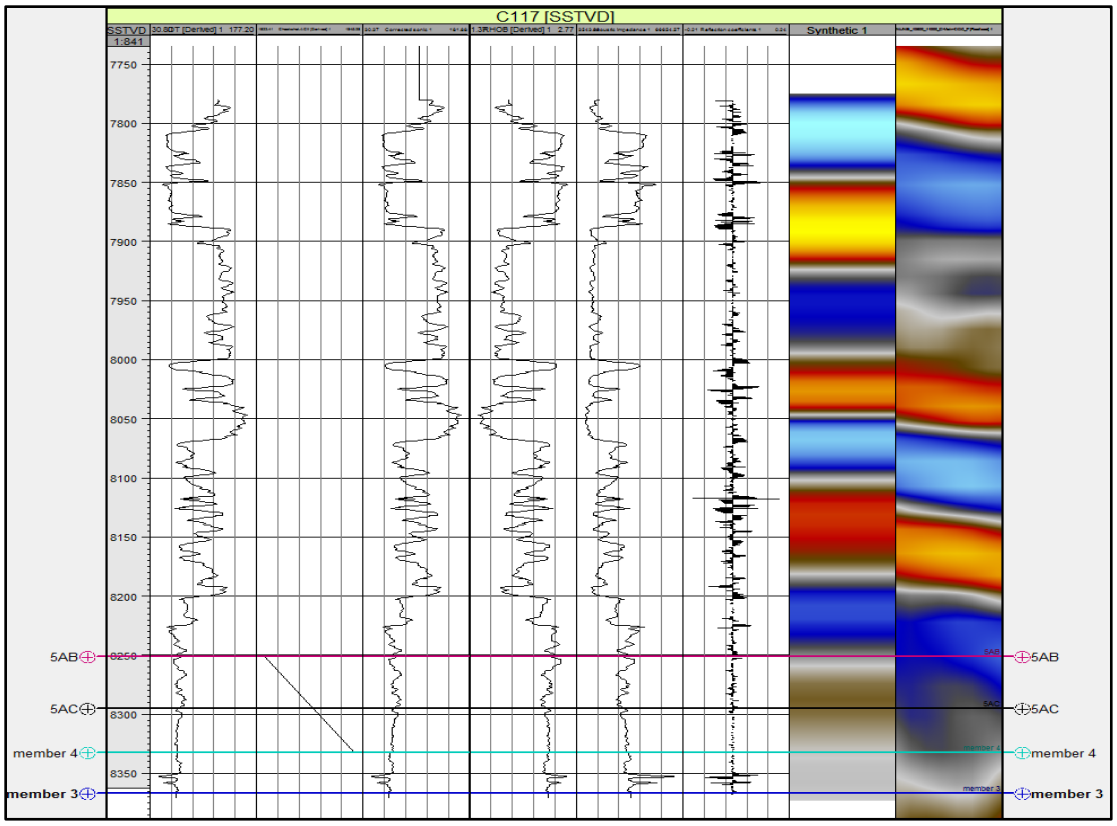

Figure 3.17: Well C117: (1) Original sonic, (2) Checkshot, (3) Corrected sonic, (4) Density, (5) Acoustic impedance, (6) Reflection coefficient, (7) Seismic trace, (8) Synthetic trace

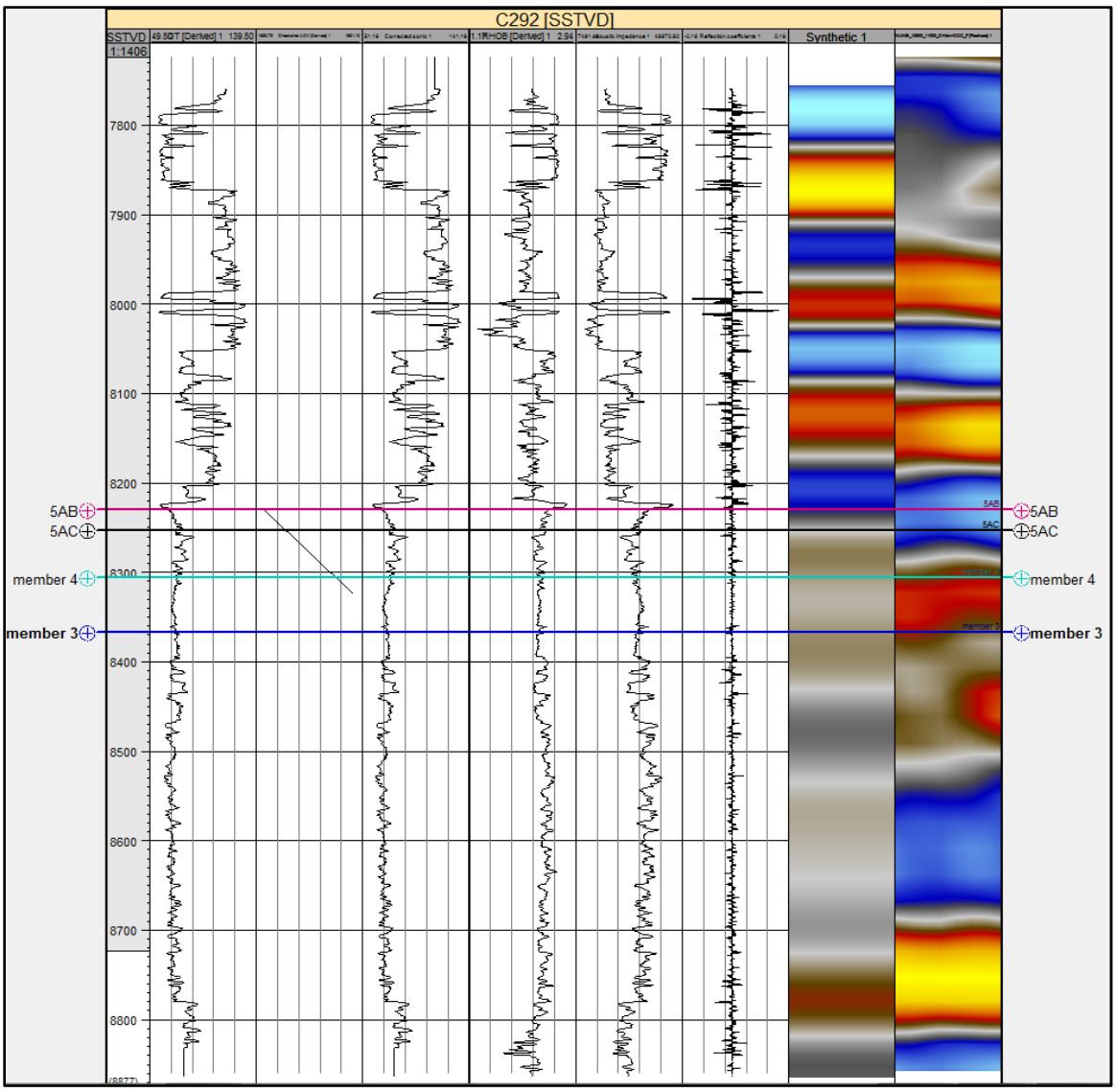

Figure 3.18: Well C292:(1) Original sonic, (2) Checkshot, (3) Corrected sonic, (4) Density, (5) Acoustic impedance, (6) Reflection coefficient, (7) Seismic trace, (8) Synthetic trace

3.3.1.4 Interpreting Horizons and Surfaces

Synthetic seismograms streamline the process of tracking and interpreting horizons, providing clarity even in regions with subpar data quality. However, in situations where data quality is compromised, guided auto-tracking can become challenging to implement. In such instances, manual interpretation stands as the sole viable approach for deciphering the seismic data. The utilization of synthetics facilitated precise horizon location. Employing an auto-tracking technique, horizons such as TGS, Member 5AB/5AC, Member 4/3, and Member 2 were accurately identified

(Figure 3.19). In scenarios where layers or surfaces exhibited minimal thickness, certain members were combined due to challenges in individual mapping.

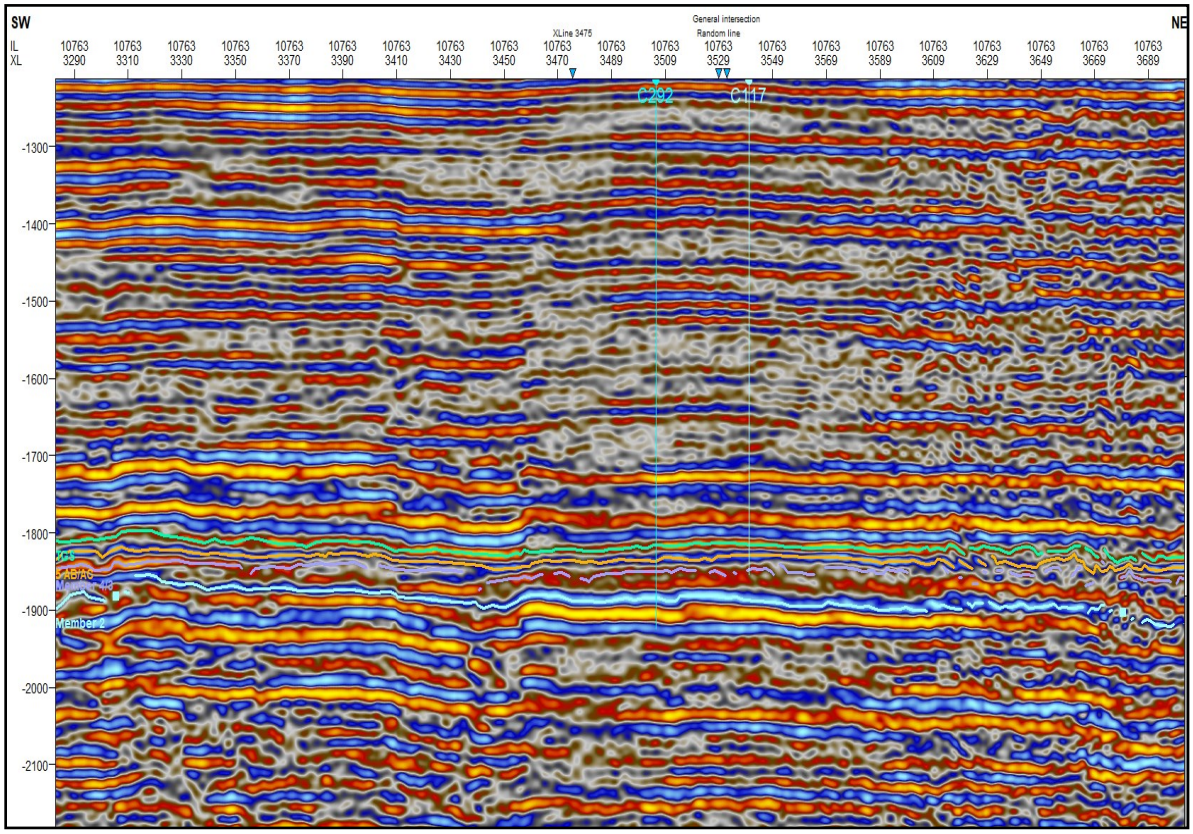

Figure 3.19: Inline 10763 shows the four picked horizon

In Petrel, 2D grids are commonly used, and surfaces are simpler versions of 3D horizons. Surfaces provide a quick indication of developing surface geometry, generated from point data or 3D seismic horizon interpretations. The resulting surface is constrained by input data and can be limited by specified boundaries (Figures 3.20 - 3.23). This aids in interpreting surface construction, the development of interpretations, and quality control checks. Input data can include bitmaps, horizons, points, lines, surfaces, well tops, and properties. The user can define a boundary using a closed polygon or surface to restrict the surface's extent.

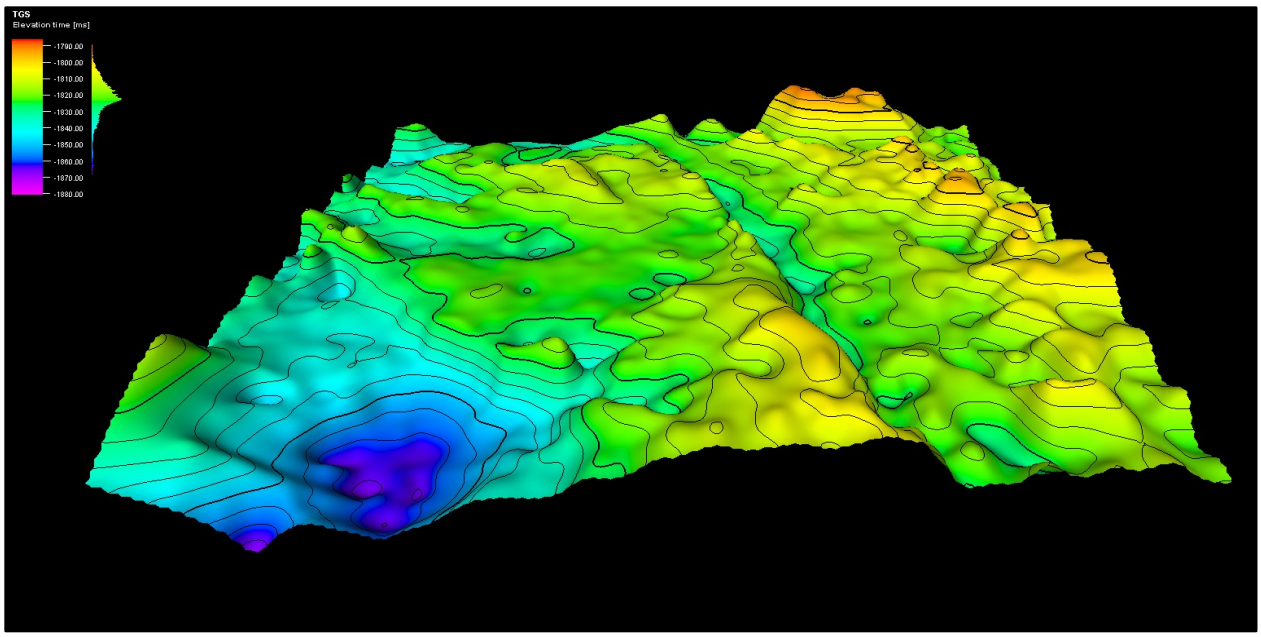

Figure 3.20: Member TGS surface after smoothing in 3D

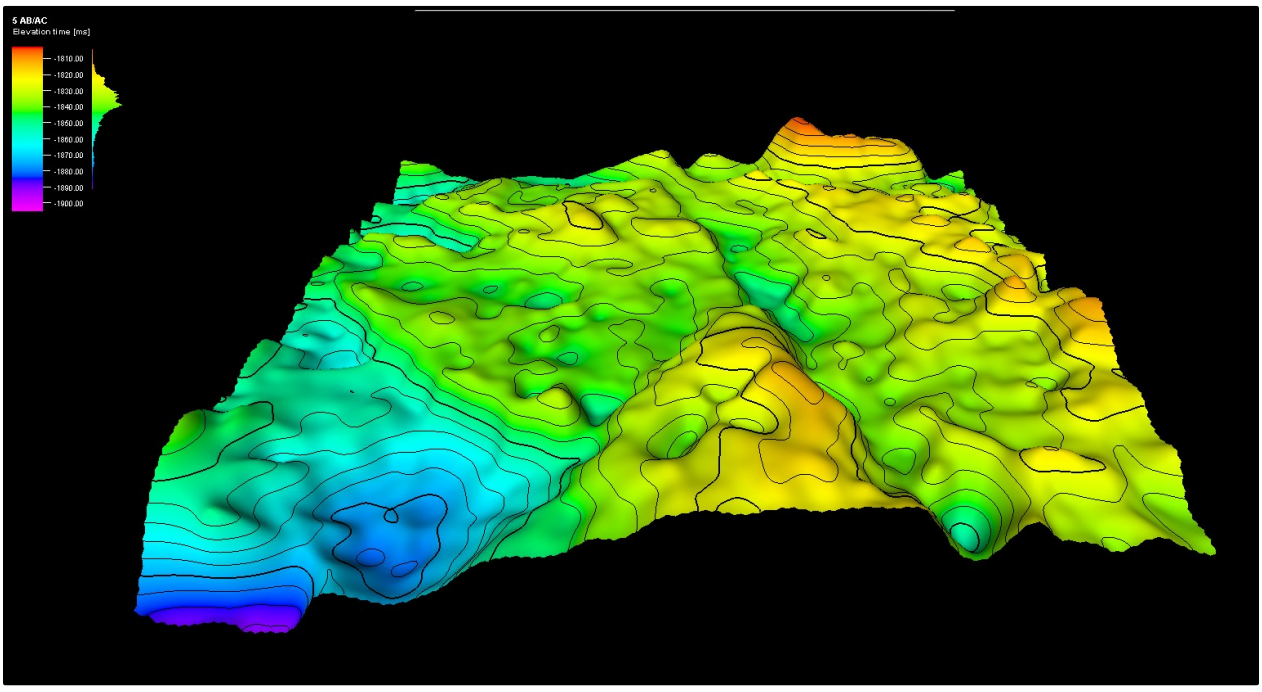

Figure 3.21: Member 5AB/AC surface after smoothing in 3D

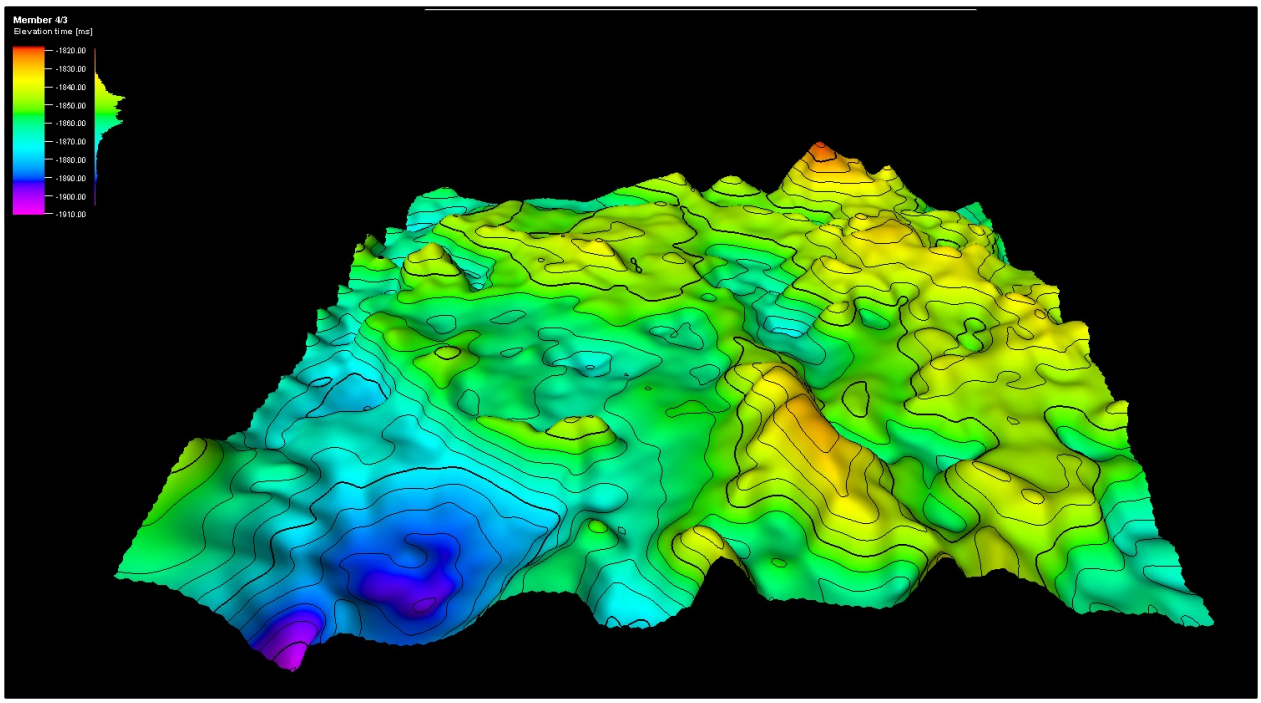

Figure 3.22: Member 4/3 surface after smoothing in 3D

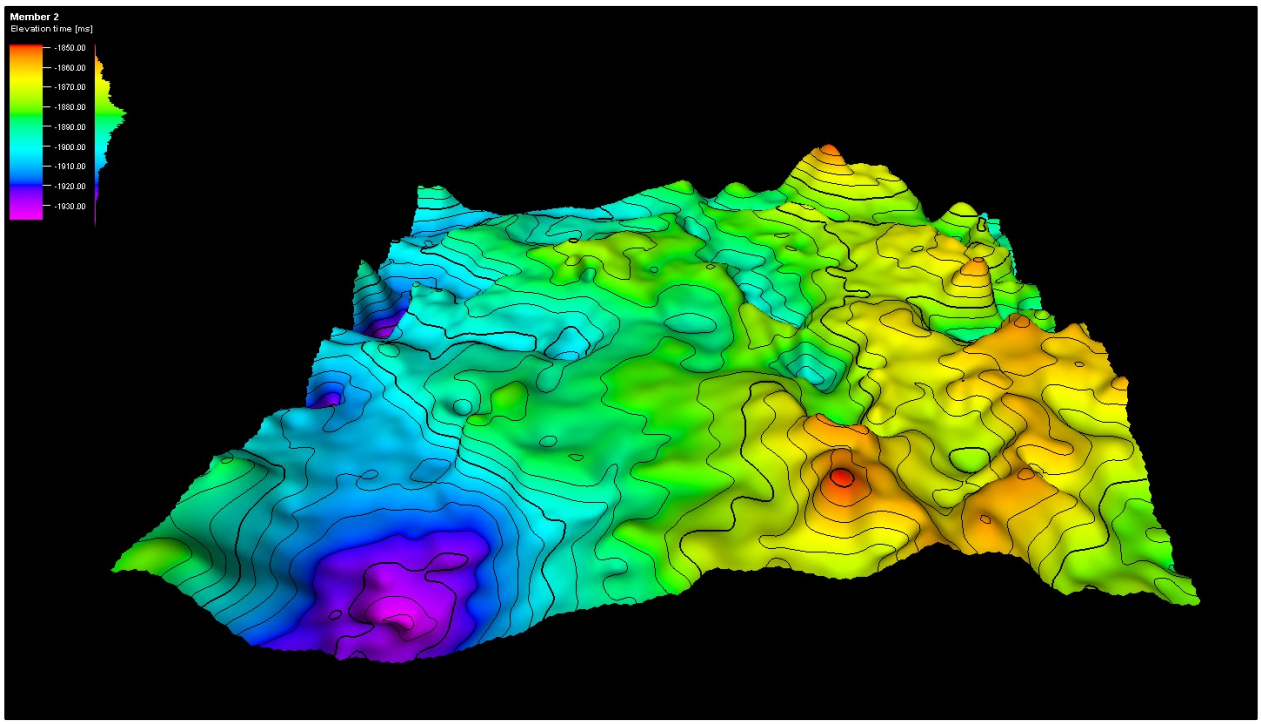

Figure 3.23: Member 2 surface after smoothing in 3D

3.3.1.5 Fault Interpretation

Fault interpretation in Petrel involves two approaches: classic interpretation in seismic slices and direct modeling of faults on seismic data in 3D using the Fault Modeling process. Several processes are employed for fault interpretation, including Structural Smoothing to enhance seismic reflector continuity, Dip and Azimuth computation to determine local structural information, Gaussian smoothing, and Chaos process to assess dip and azimuth estimation reliability, and the Anti-tracking process to detect faults within a designated area. Fault segments, or fault sticks, are interpreted by digitizing seismic intersections using either 3D windows or Interpretation windows. Additionally, faults can be incorporated into a 3D grid for transmissibility calculations, where transmissibility multipliers (TMs) account for potential deformity effects of fault rock material. Due to limited data about the fault nature, transmissibility is often assumed to be zero. Furthermore, fault modeling involves generating Key Pillars, lines that define fault slope and shape, along with Shape Points to adjust fault contours. These Key Pillars are established based on various input data sources, requiring manual adjustment in the 3D window. (Figure 3.24) shows that the faults cover the entire area and divide the model into segments, so the pillar gridding process can be applied.

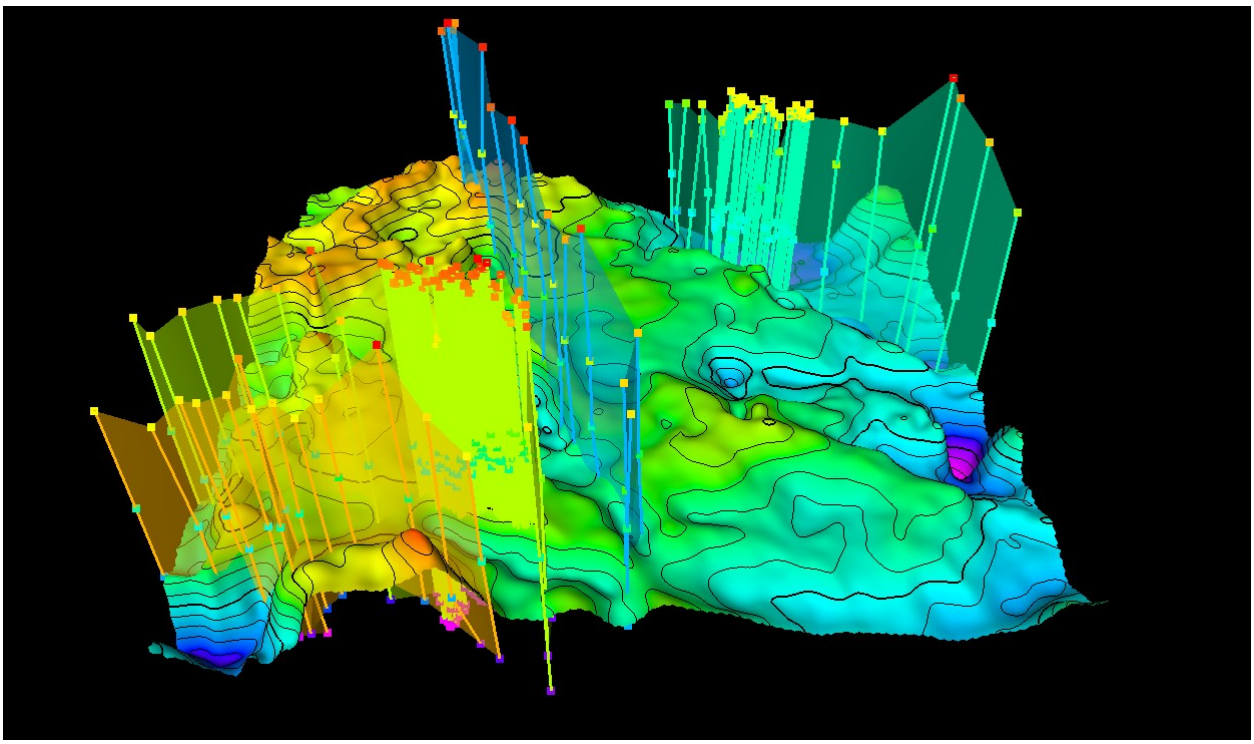

Figure 3.24: Distribution of the faults through the surface of Member 2

3.3.1.6 Gridding

In the process of 3D gridding, the model is divided into cells, each possessing properties like porosity, water saturation, and rock type. The method encompasses several steps, including Pillar Gridding, which establishes the 3D framework using pillars to define potential positions for grid block corners, guided by user-defined directions along faults and borders. Grid resolution is a crucial factor as it influences result accuracy; high-resolution grids offer spatial complexity but longer processing times, while lower resolution grids are quicker and enable rapid testing. Grid structure consideration becomes vital when faults play a role in simulation as flow barriers or conduits, involving decisions on their inclusion and its impact on model creation time. Defining the top and base of the 3D grid can involve constant values or surfaces, including horizons organized in stratigraphic order. The grid boundary aligns with the boundary used for surface creation, contributing to the formation of the Grid Top, Mid, and Base skeleton as show in (Figures 3.25 - 3.27).

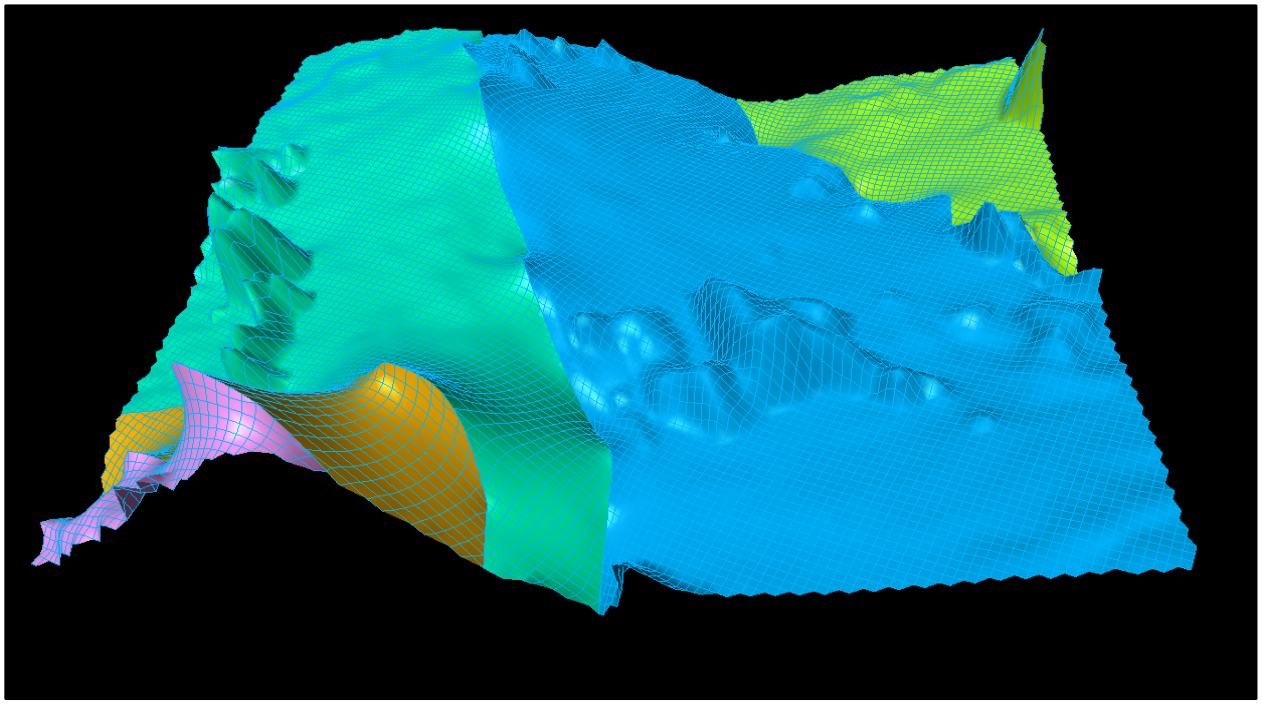

Figure 3.25: Grid Top skeleton

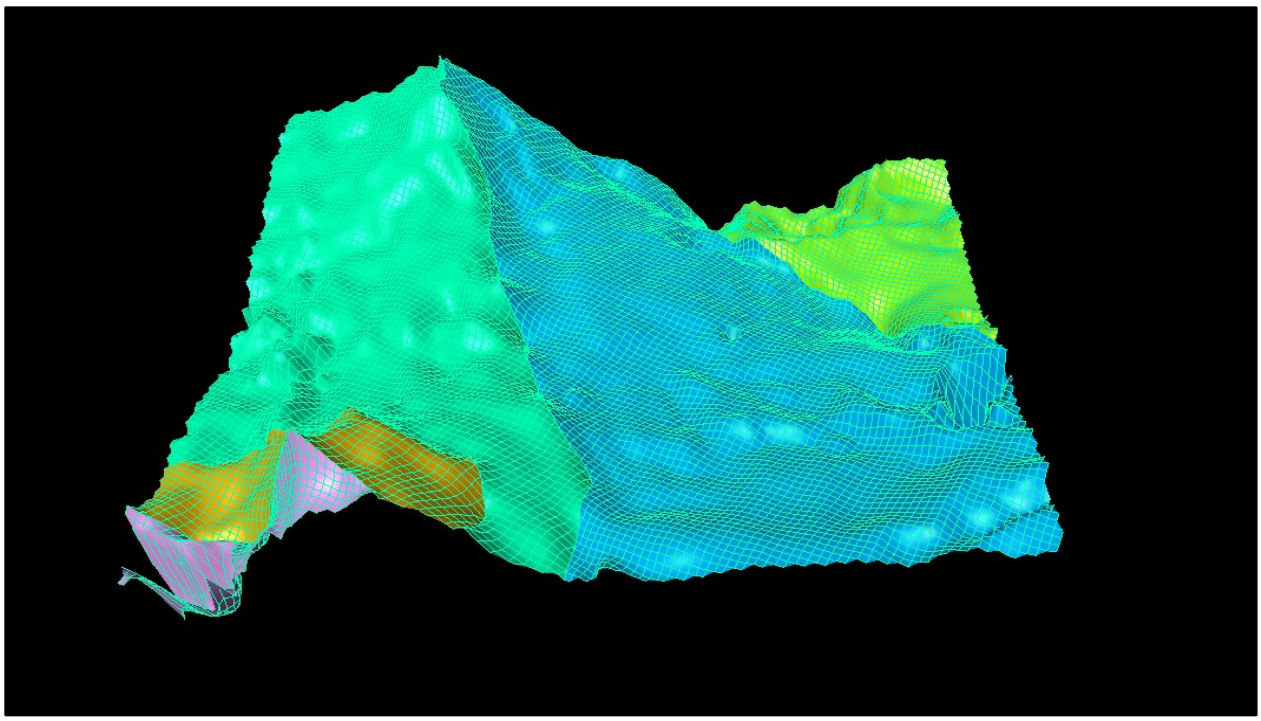

Figure 3.26: Grid Mid skeleton

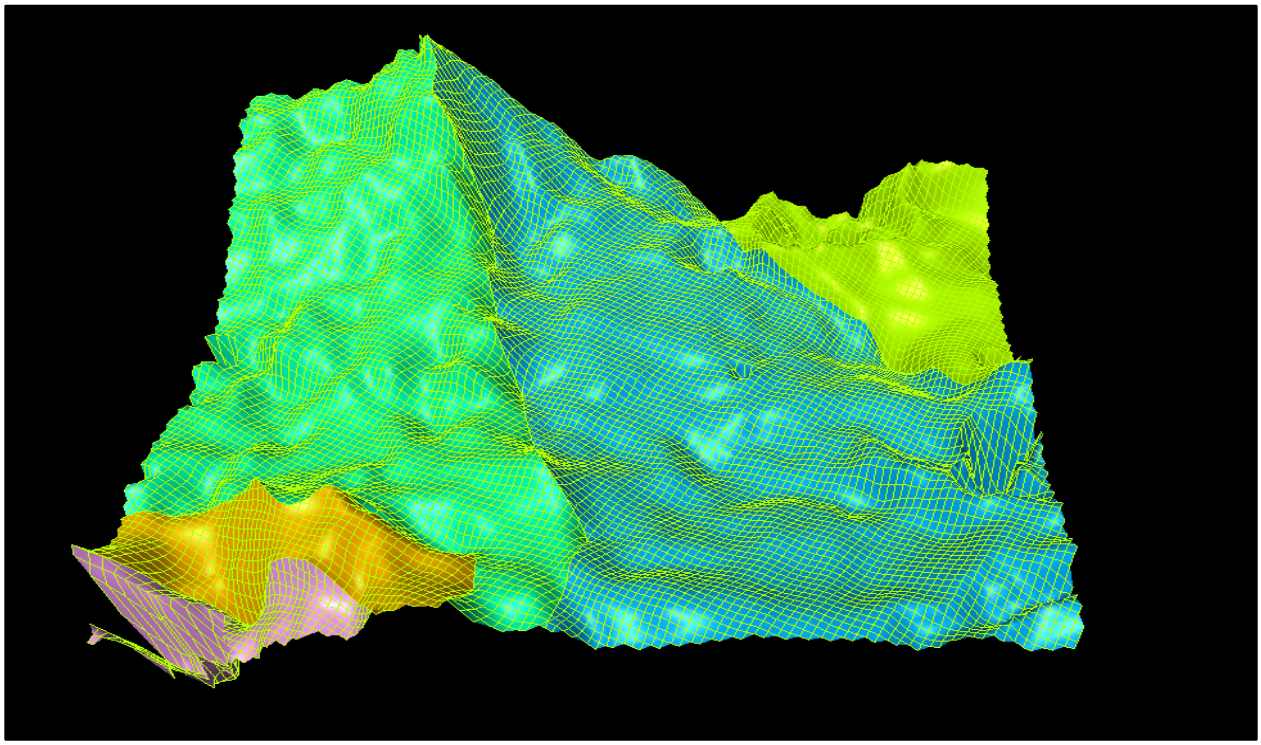

Figure 3.27: Grid Base skeleton

3.3.1.7 Domain Conversion

The Petrel domain conversion process facilitates the transition of data between domains, such as converting seismic data from time to depth for correlation with well data and volume calculations. Geophysicists typically work in the time domain, while geologists deal with depth data. Petrel's Domain Conversion bridges this gap by making depth data more prevailing. The process is simplified into two key stages: first, creating and calibrating a velocity model based on available well markers, and second, selecting the data to be converted between domains, which can include surfaces, horizon and fault interpretations, points, well data, and 2D or 3D data.

Velocity models can be defined through three methods: Velocity Model 1 involves interval modeling by distributing velocity trends based on the established time/depth relationships from wells. Velocity Model 2 utilizes a SEG-Y velocity volume to extract velocities, while Velocity Model 3 relies on stacking velocity points for upscaling and distribution. These models necessitate four sets of input: a zone description (e.g., surfaces in two-way time), a definition of the velocity model per zone (e.g., V=Vint), input parameters for the velocity model (e.g., surface of Vint), and correction data if needed (e.g., well tops for specific zones). The process also allows for generating intermediate data, such as quality control-related well reports or well information representing velocity models, along with settings for data extrapolation. In the absence of available velocity cubes or stacking velocity points, the time/depth relationship is the sole method for extracting a velocity model. Due to insufficient check-shot coverage across the area, a fully extracted TDR velocity model wasn't feasible, resulting in a single averaged velocity value across each surface. (Figure 3.28) presents the data used to create the velocity model alongside the calculated average velocity value for each surface.

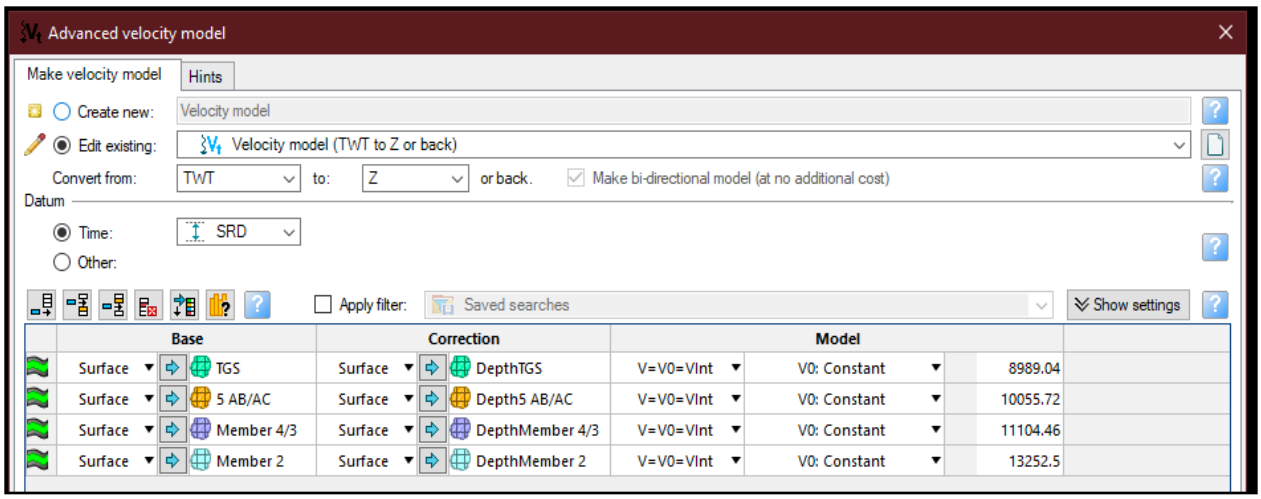

Figure 3.28: Advanced velocity model creating tab in petrel

3.3.1.8 Static or Structural Model

Upon completion of the velocity calculation, the time-based model undergoes a conversion into the depth domain, as illustrated in (Figure 3.29). The resultant 3D structural model presents a comprehensive representation of the reservoir's broader framework, containing two key constituents: the bounding surfaces and the fault network. It's essential to note that, at this stage, the interstitial volume between these bounding surfaces remains unaccounted for. During this phase, seismic surfaces are typically transformed into the depth domain and meticulously aligned with the well tops of the key marker surfaces. This process ensures the accuracy and coherence of the structural model by incorporating well-derived data and seismic interpretations within the depth framework. Lastly zones and layers are defined for each individual member.

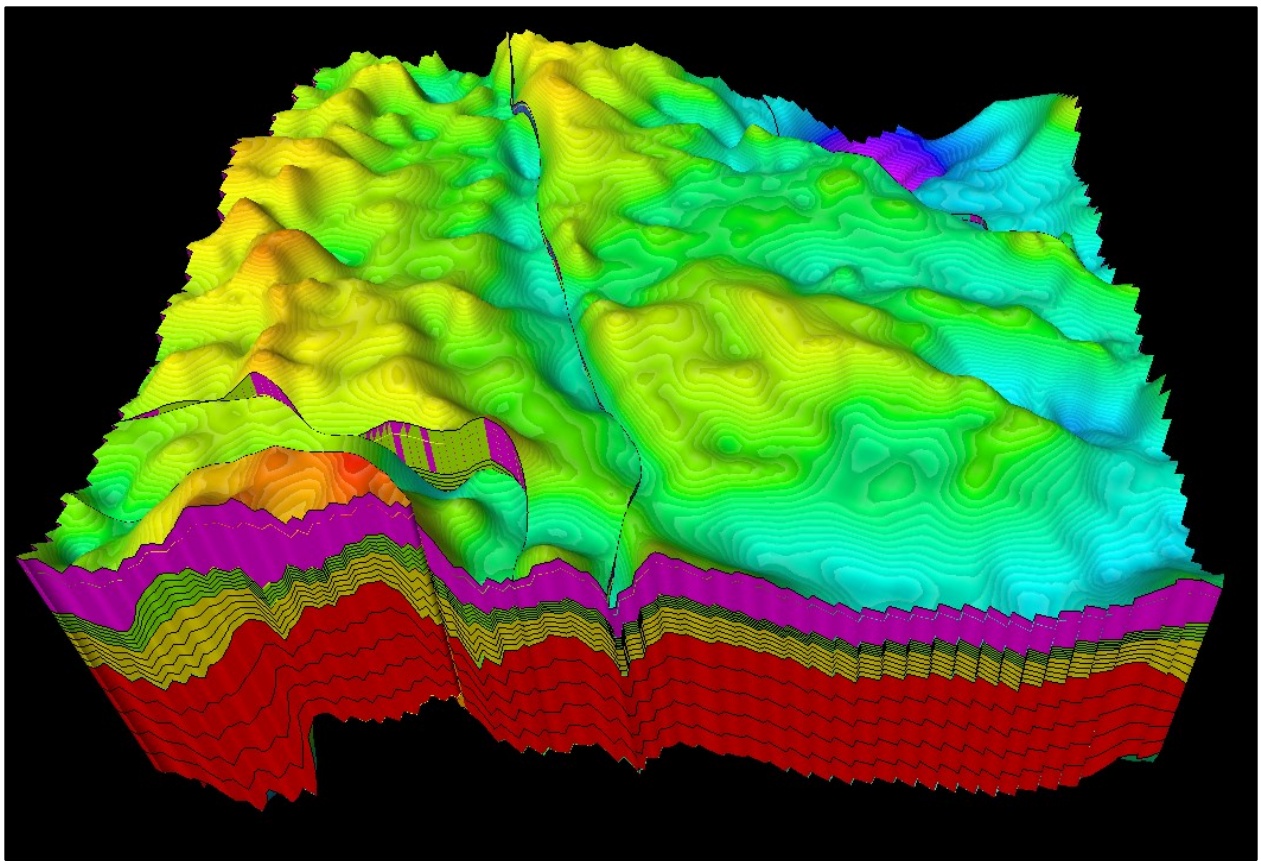

Figure 3.29: The 3D static reservoir model in depth domain

3.3.1.9 Property Modeling

Property modeling is a critical step in the reservoir characterization process, involving the assignment of discrete or continuous properties to the cells of a 3D grid. The primary objective is to leverage all available geological information to construct a realistic property model. This intricate process typically includes the following key steps:

- Scale Up Well Logs: Scaling up involves transferring data from well logs to the grid cells. It's the process of sampling values from the well logs and distributing them appropriately within the grid.
- Data Analysis: Data analysis is a crucial preparatory step that involves working with the input data, often the scaled-up well logs, for property modeling. This step encompasses various tasks, such as applying data transformations, identifying trends in continuous data, assessing vertical proportions, and establishing probability distributions for discrete data.

It also involves defining variograms, which describe the spatial continuity and variability of the input data, for both continuous and discrete cases.

- Trend Modeling: Trend modeling is a technique used to generate a vertical proportion volume. It accomplishes this by performing a block kriging of the probabilities associated with each facies. This step is vital for characterizing the vertical distribution of properties within the reservoir.
- User-Defined Object Creation: In certain cases, reservoir features may have irregular shapes or complex 3D geometries. User-defined object creation allows modelers to define and incorporate such features into the property model. This flexibility is particularly useful when dealing with geological structures that don't conform to standard grid cells.
- Training Image and Pattern Creation: A training image serves as an idealized and simplified representation of the geological characteristics of the reservoir. It's a reference that helps guide the property modeling process, ensuring that the model aligns with expected geological patterns and structures.
- Fault Analysis: Fault analysis involves evaluating the impact of geological faults on reservoir properties. This process can encompass generating fault transmissibility multipliers directly or modeling the properties of faults themselves. These multipliers, along with grid permeabilities, are used to calculate how faults influence fluid flow within the reservoir. Additionally, this analysis can provide insights into the sealing potential of faults, which is critical for understanding reservoir behavior.

These steps collectively contribute to the construction of an accurate and reliable property model, which is essential for reservoir simulation and production forecasting.

3.3.1.10 Petrophysical Modeling

Petrophysical modeling is the interpolation or simulation of continuous data (porosity, permeability), throughout the model grid. The software offers two methods of modeling: deterministic (estimation, interpolation) and stochastic for modeling the distribution of continuous properties in the reservoir model. (Figure 3.30) shows the porosity and permeability histograms extracted from the interpolation of well logs data.

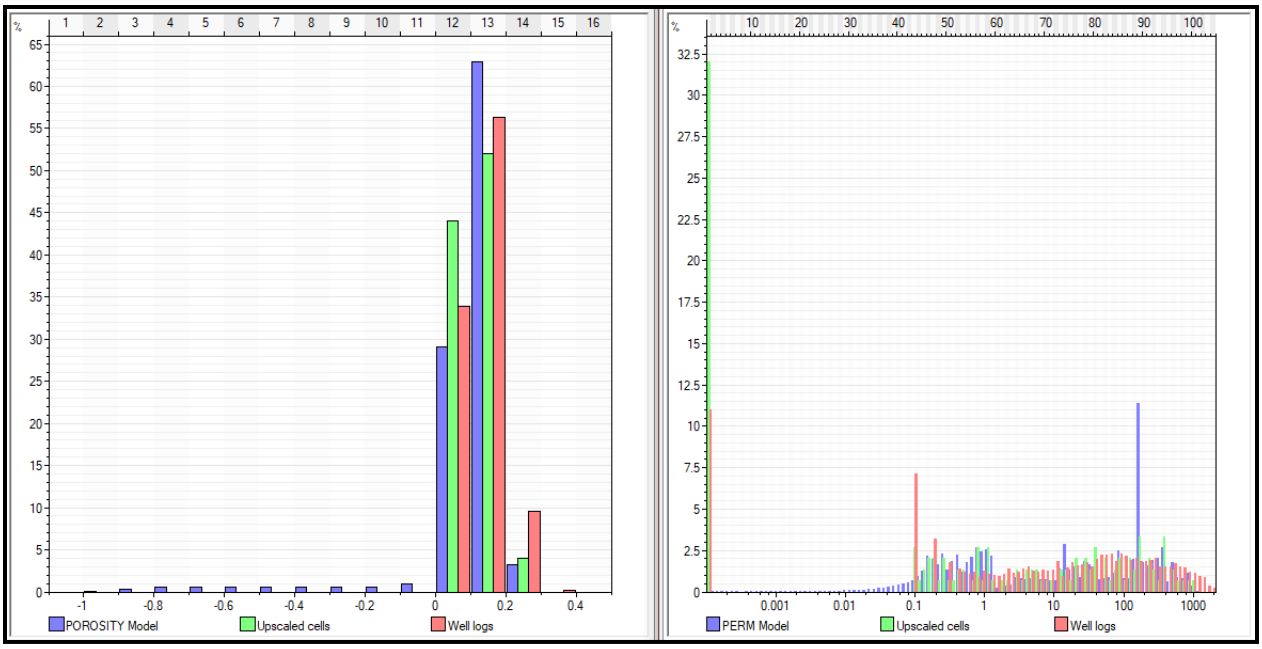

Figure 3.30: Porosity and permeability histogram

The estimation technique used in probabilistic framework is Kriging to produce the best result in terms of local accuracy.

3.3.1.11 Upscaled 3D Dynamic Modeling

Until this point, each successive model has been constructed by incrementally incorporating information from the previous one. The high-resolution petrophysical model typically comprises millions of grid cells, and simulating such a vast number of cells can be a time-consuming and laborious process. Upscaling addresses this challenge by considering the coarsening of the grid dimensions (X and Y) and defining stratigraphic layering sequence by sequence. This geometric upscaling also extends to the petrophysical properties, ensuring a more efficient and manageable modeling process. (Figures 3.31 - 3.33) illustrate the results of the porosity, permeability, and facies model respectively.

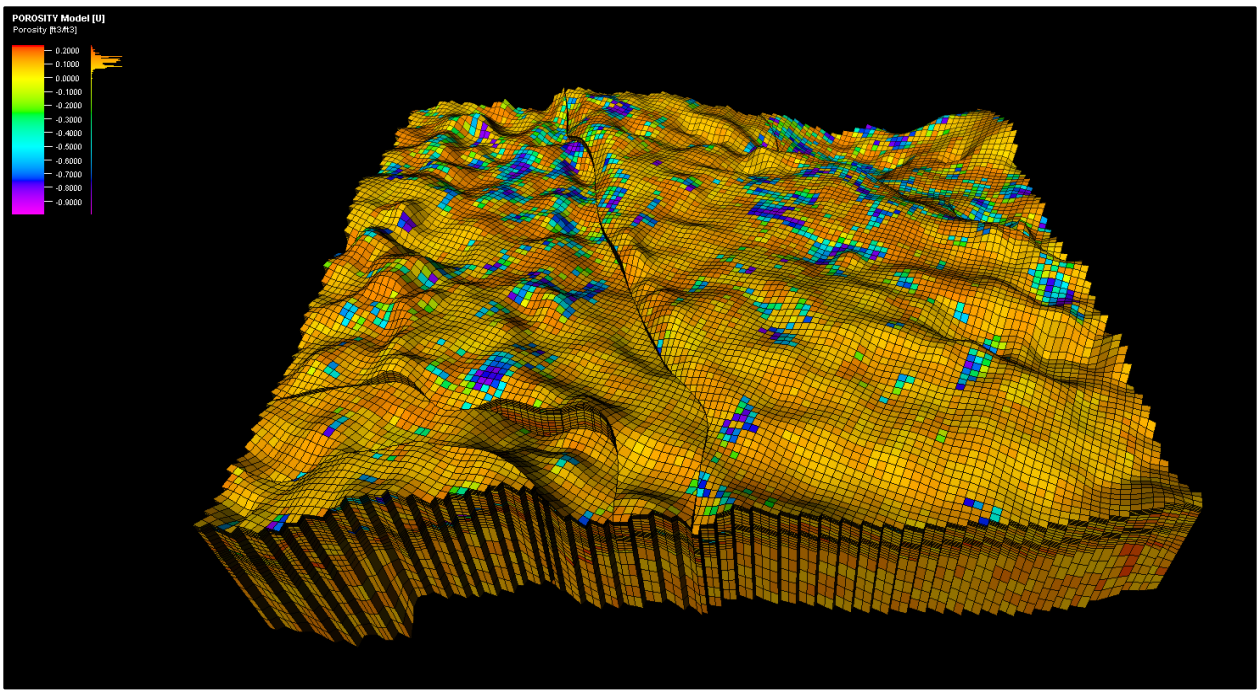

Figure 3.31: Porosity model is 3D distribution of the porosity values throughout the study area

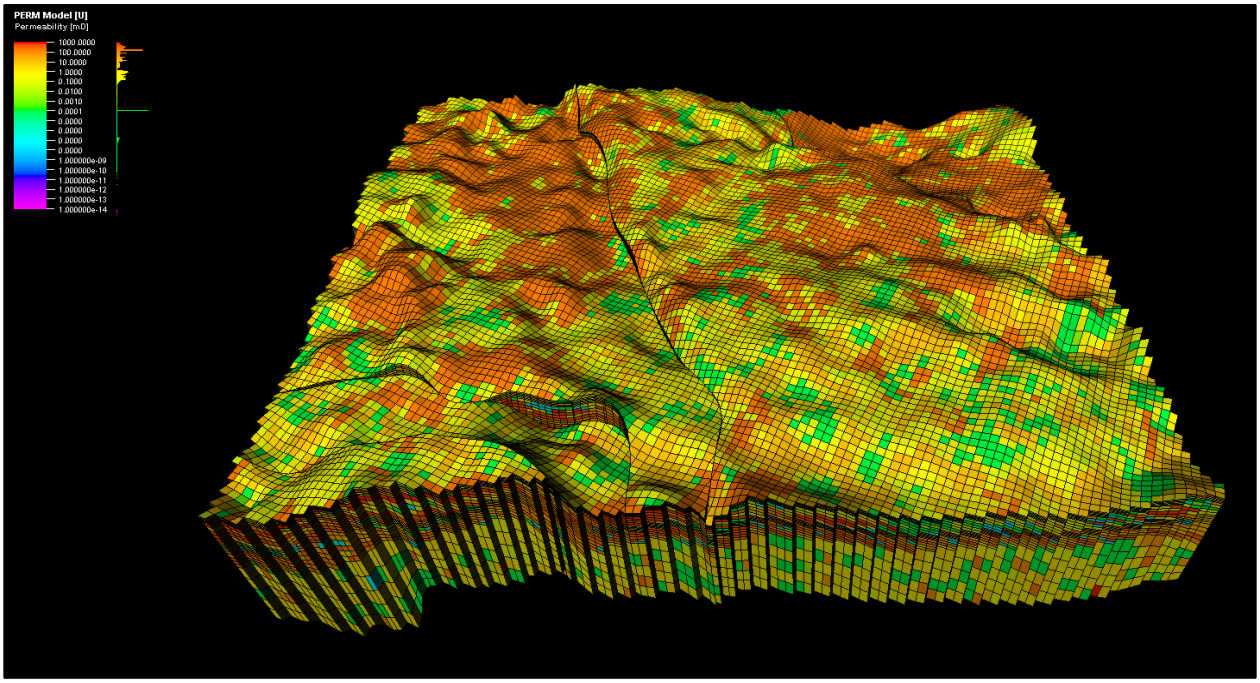

Figure 3.32: Permeability model constructed by using kriging method

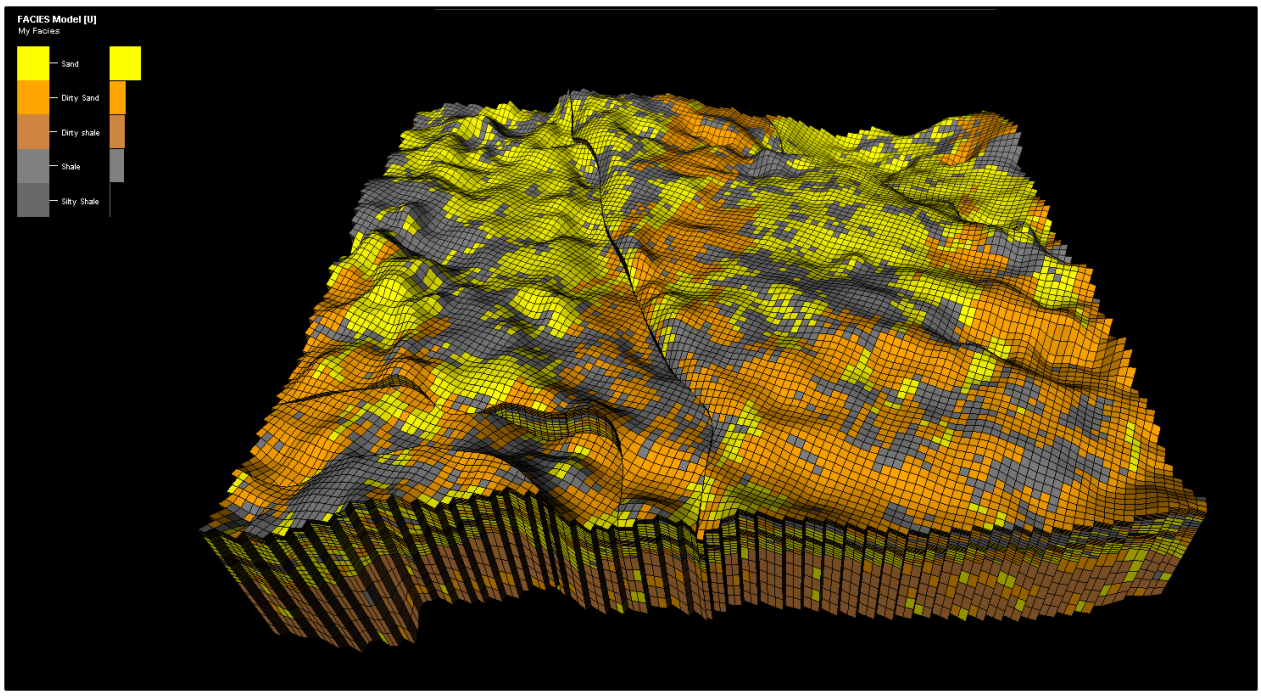

Figure 3.33: Facies model of the study area

3.3.1.12 Well Completion

Well completion is a critical phase in the development of an oil or gas well. It involves a series of processes and technologies aimed at preparing the well for production. During completion, various components are installed downhole to optimize reservoir access and fluid recovery. Key tasks include casing and cementing, perforating the well casing to allow fluid flow, and installing production tubing and safety equipment. Well completion is tailored to the specific reservoir and production requirements, ensuring safe and efficient extraction of hydrocarbons from deep beneath the Earth's surface. Below is a (Figure 3.34) displaying the well completion of the wells (C006, C035, C255), Alongside Porosity and permeability logs; to have a clear view of the production zone. Notice the gas-oil contact is close explaining the high gas production.

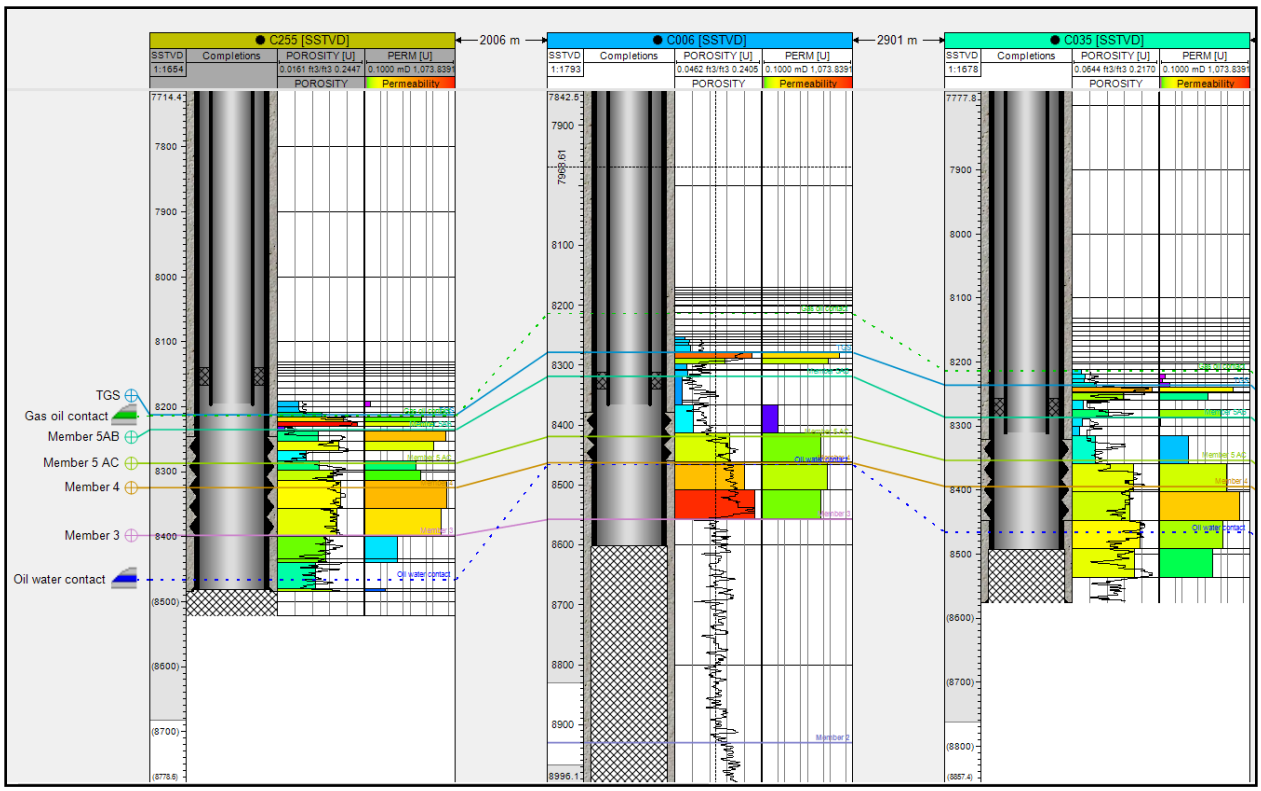

Figure 3.34: Well completion of the wells (C006, C035, C255)

3.3.1.13 Define A Fluid Model

Reservoir fluid models commonly fall into two categories: compositional and black oil models. Black oil models simplify the representation of oil and gas by assuming that their saturated phase properties are solely pressure dependent. In contrast, compositional models incorporate the definition of multiple hydrocarbon components, providing a more detailed representation. The process of creating black oil fluid models, known as the Make fluid model process, involves specifying essential properties like viscosity, density, and volume formation factors for each fluid phase. These properties are typically input as pressure-dependent tables or correlations. Additionally, initial reservoir conditions must be provided as part of this process. This, along with the fluid properties and saturation functions, enables the determination of the initial fluid distribution within the reservoir. Finally, rock compressibility data is incorporated using the Make rock physics functions process. In (Figure 3.35) we input fundamental fluid properties for the model, where we define the temperature and pressure conditions, both within the reservoir and at the separator.

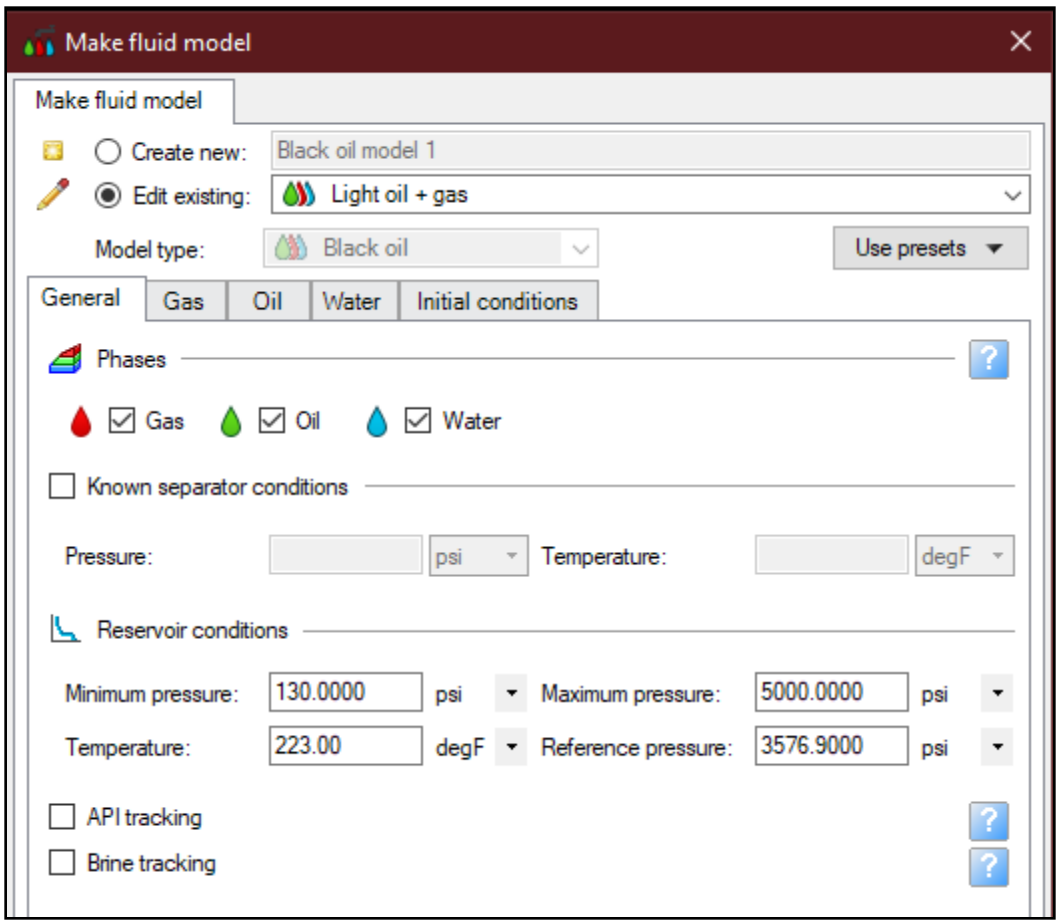

Figure 3.35: Parameters used in Petrel to make Fluid Model

There are two methods to define initial conditions: utilizing a contact set or defining them within a table. When opting for a contact set, you can select the "Define from contact set" option and import the contact set from the Petrel Models pane. For contact sets generated from user-entered contact depths, the Make fluid model process establishes an initial condition region for each distinct set of contacts. If datum depth and pressure aren't defined in the contact set, defaults are applied, and a discrete grid property is created, named after the contact set, to map the initial conditions regions to the grid blocks. When configuring a black oil fluid model, key information includes phases, known separator conditions, pressure range, temperature, reference pressure, gas and oil properties, solution gas/oil ratio, bubble point pressure, and salinity, which are all configured within the "Initial Conditions" tab for black oil models. (Tables 3.5 & 3.6) show these properties.

Table 3.5: Initial conditions of the reservoir

Depth (ft)	Rs (MSCF/STB)	Pb (psi)
-8362	0.7411	3597.2711
-8423.65	0.7131	3464.6737

Table 3.6: Oil & Gas gravity, water salinity & Bubble point pressure

Oil Gravity	Gas Gravity	Water Salinity	Bubble point pressure
37 API	0.6636 sg air	198000 ppm	700 psi

3.3.1.14 Define a Rock Physics Functions

Several saturation or pressure functions are employed in simulation to capture the underlying physics of fluids, rocks, and their interactions. In this context, the Make fluid model process generates functions that represent fluid physics, while the Make rock physics functions process is employed to create functions encapsulating rock behavior and the interplay between rocks and fluids. These functions facilitate the generation of saturation functions and rock compaction functions.

Saturation functions, presented as tables showing relative permeability and capillary pressure versus saturation, serve crucial roles in determining initial phase saturation in each cell, initial transition zone saturation, and fluid mobility for solving flow equations. When creating saturation functions using the Make rock physics functions process, gas-oil and water-oil capillary pressure versus saturation curves are also automatically generated.

Rock compaction functions are tables illustrating pore volume multipliers as functions of pressure, or alternatively, a single rock compressibility value used by the simulator to calculate pore volume changes. The creation of rock compaction functions through the Make rock physics functions process additionally produces transmissibility multiplier versus pressure curves, which are set to zero by default.

It's noteworthy that the outcome of this process, as mentioned earlier, manifests as relative permeability curves and saturation functions, as shown in accompanying (Figures 3.36 - 3.42) and

(Tables 3.7 - 3.9). Some adjustments, particularly to capillary pressure values, may be applied to align the results more closely with observed data.

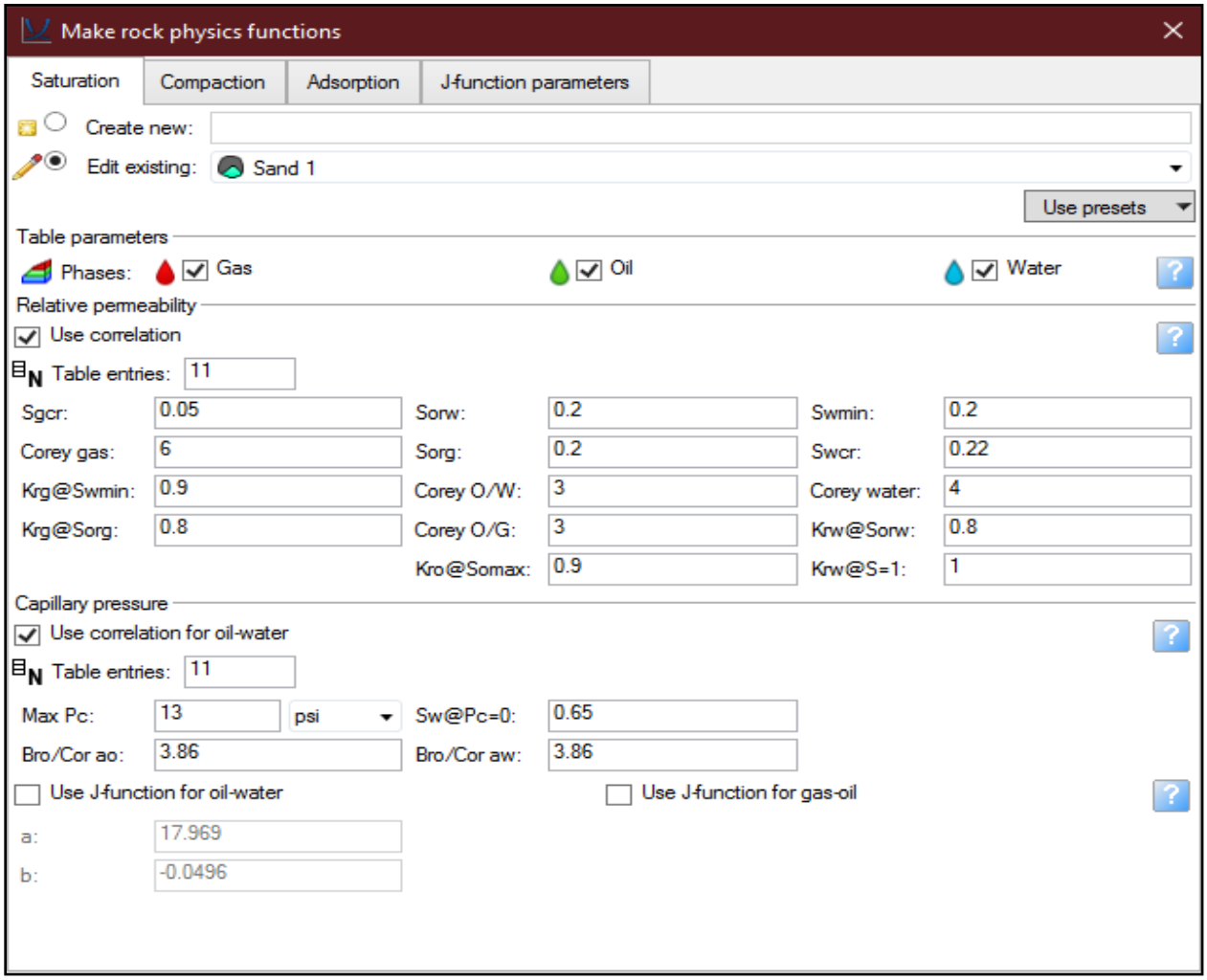

Figure 3.36: Parameters used for sand formation

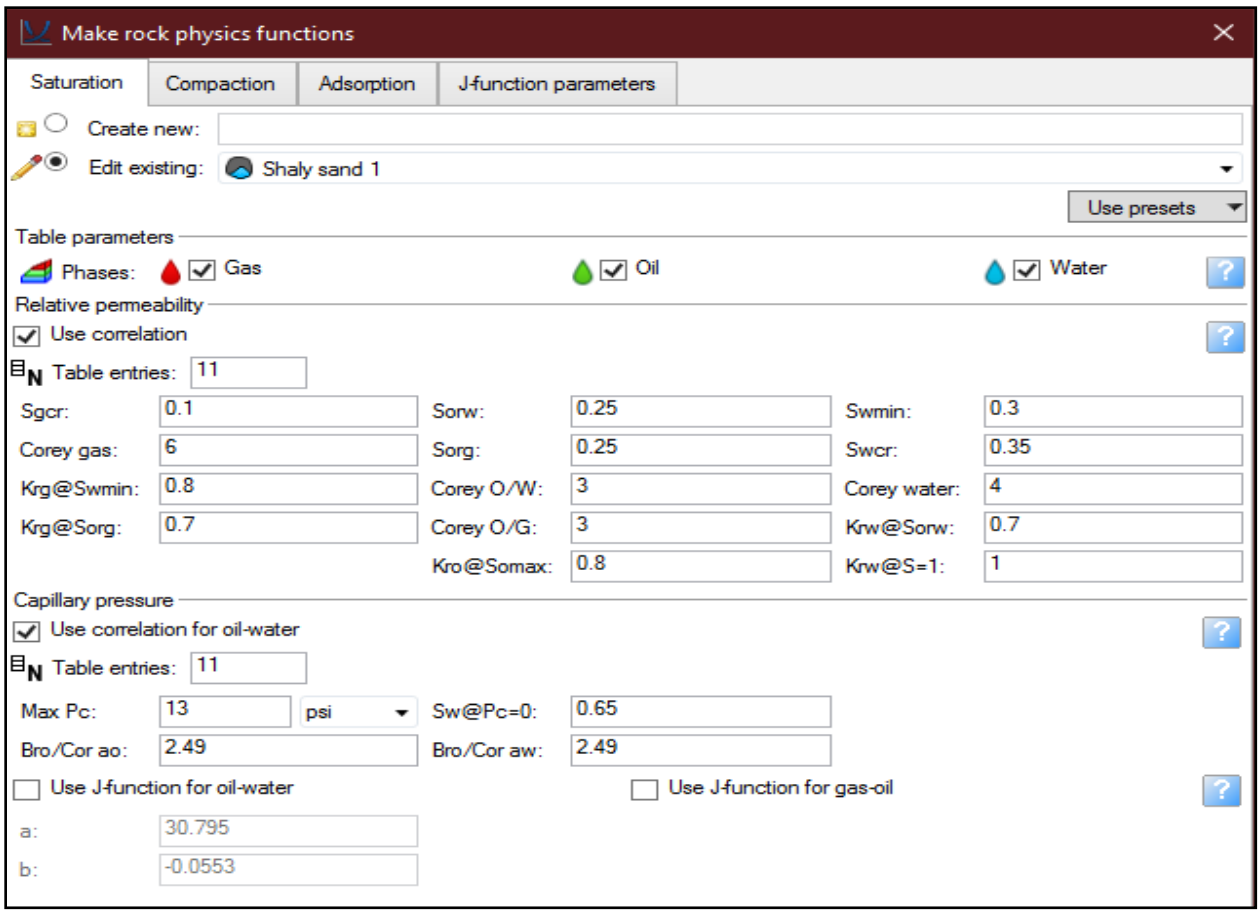

Figure 3.37: Parameters used for shaly sand formation

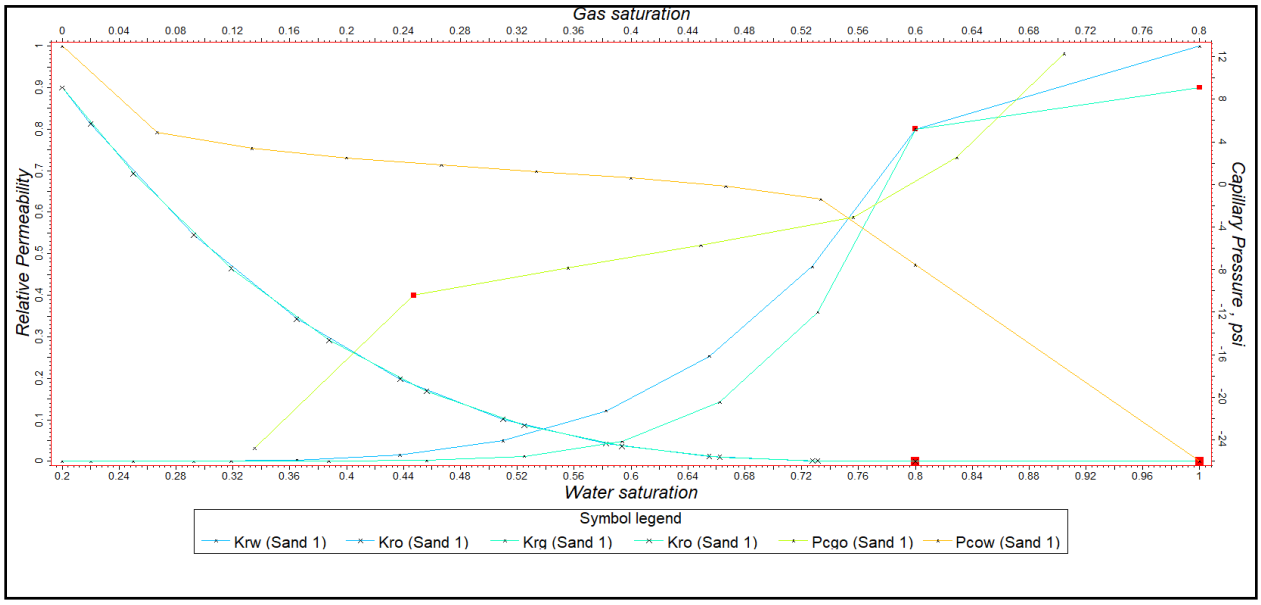

Figure 3.38: Plot for saturation function of sand formation

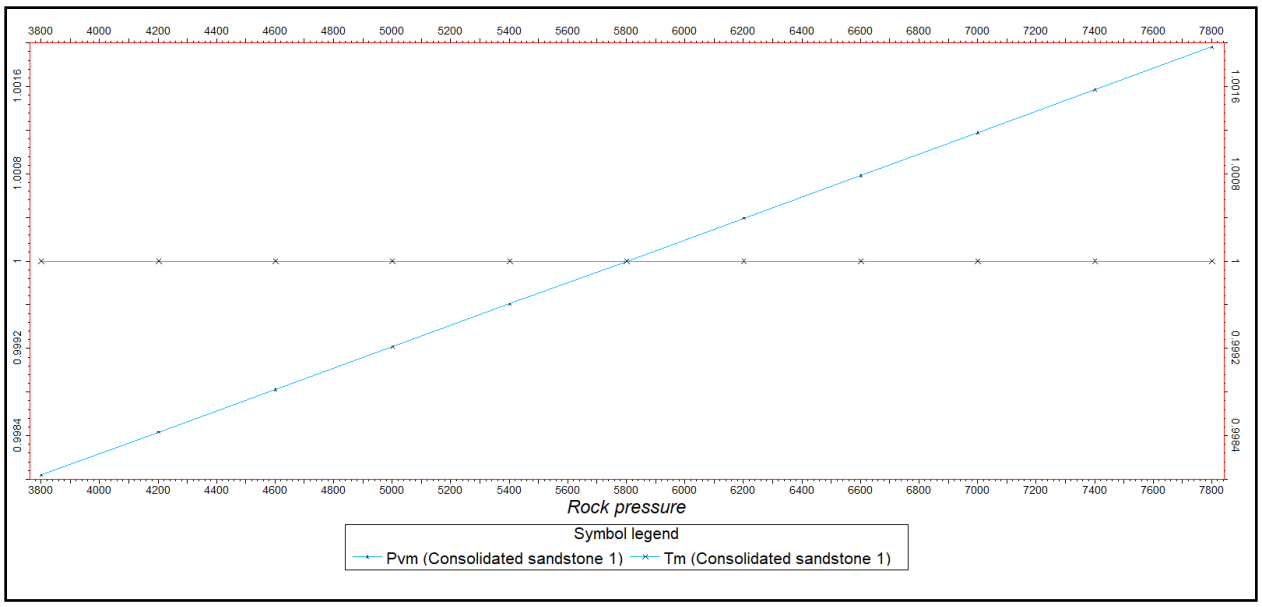

Figure 3.39: Plot for rock compaction of consolidated sands

Table 3.7: Water-Oil capillary pressure data

	Sw	Pcow psi
1	0.2	13
2	0.26667	4.9018
3	0.33333	3.3877
4	0.4	2.5005
5	0.46667	1.8225
6	0.53333	1.2142
7	0.6	0.58678
8	0.66667	-0.17596
9	0.73333	-1.3948
10	0.8	-7.5552
11	1	-26.037

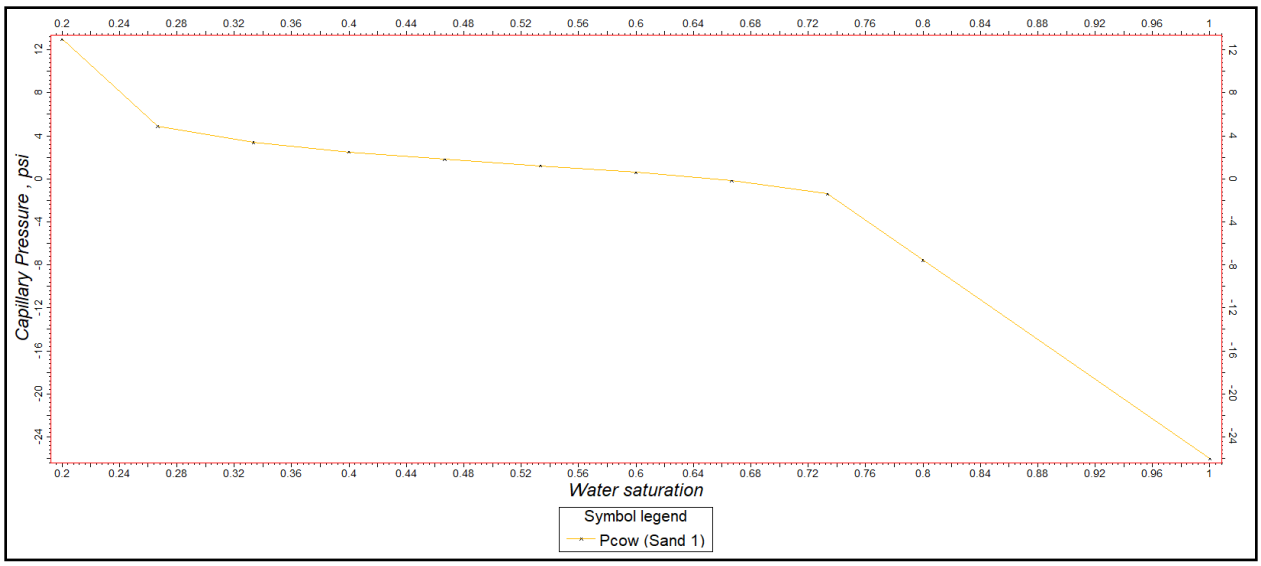

Figure 3.40: Water-Oil capillary pressure curve

Table 3.8: Gas-oil relative permeability

	Sg	Krg	Kro
1	0	0	0.9
2	0.05	0	0.69323
3	0.11875	3.0518E-06	0.46441
4	0.1875	0.00019531	0.29246
5	0.25625	0.0022247	0.16925
6	0.325	0.0125	0.086654
7	0.39375	0.047684	0.036557
8	0.4625	0.14238	0.010832
9	0.53125	0.35904	0.001354
10	0.6	0.8	0
11	0.8	0.9	0

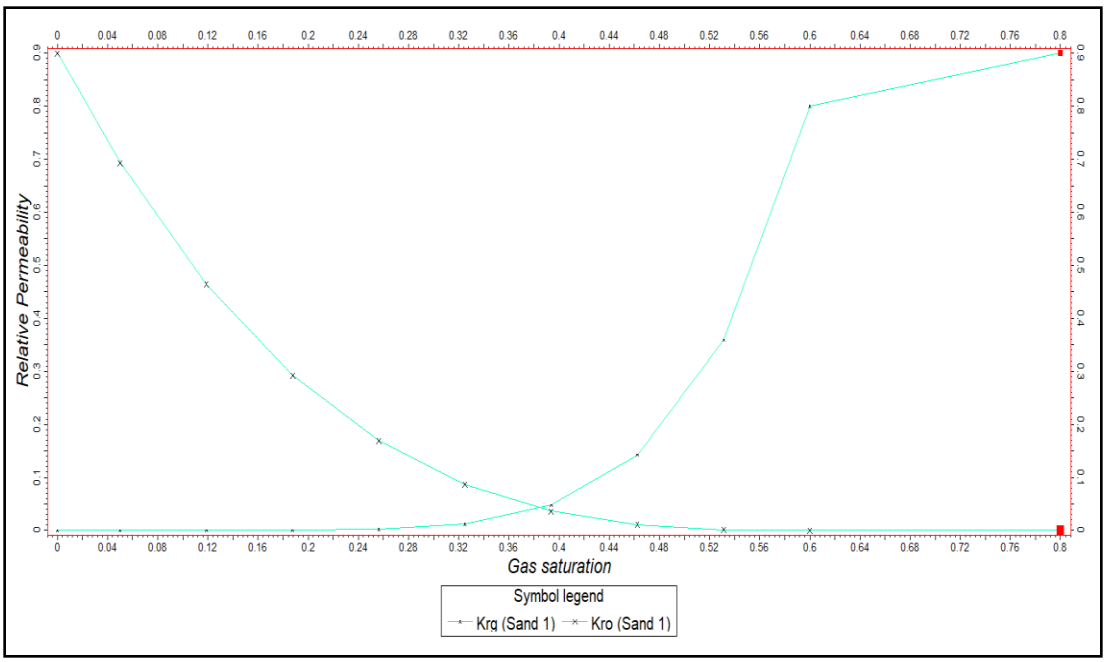

Figure 3.41: Gas-Oil relative permeability curve

Table 3.9: Oil-water relative permeability

	Sw	Krw	Kro
1	0.2	0	0.9
2	0.22	0	0.81297
3	0.2925	0.00019531	0.54462
4	0.365	0.003125	0.34297
5	0.4375	0.01582	0.19848
6	0.51	0.05	0.10162
7	0.5825	0.12207	0.042871
8	0.655	0.25313	0.012703
9	0.7275	0.46895	0.0015878
10	0.8	0.8	0
11	1	1	0

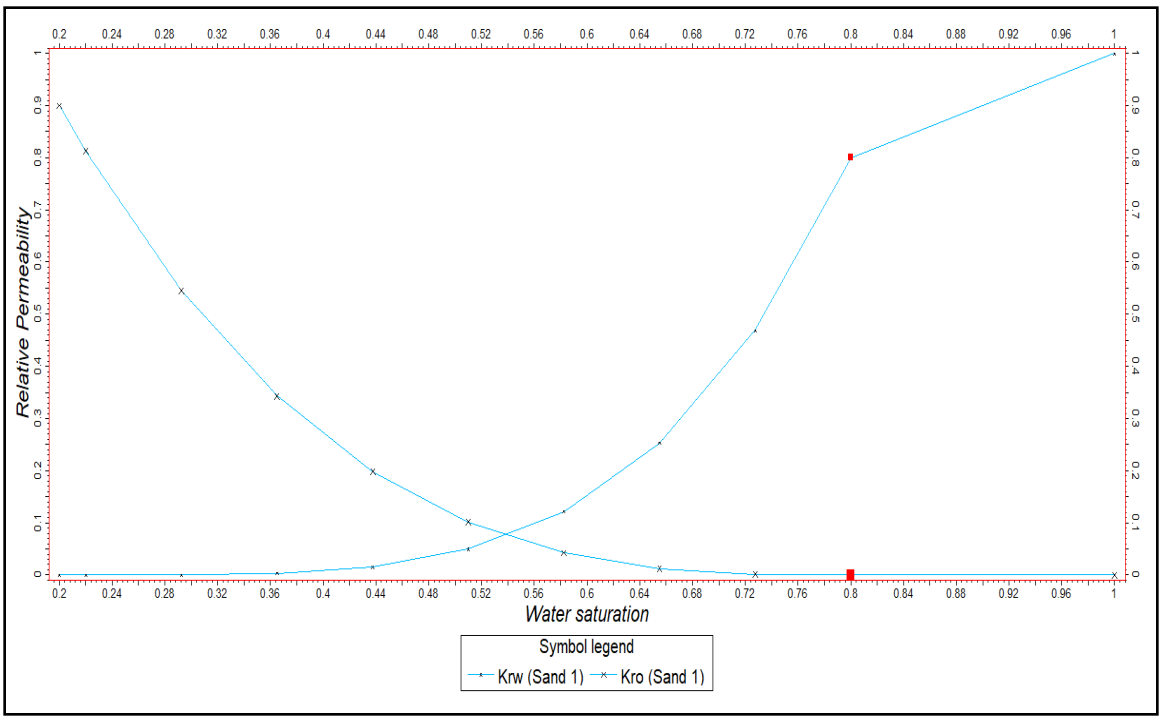

Figure 3.42: Oil -Water relative permeability curve

The simulation model computes the saturation change of three phases (oil, water and gas) and pressure of each phase in each cell at each time step. As a result of declining pressure as in a reservoir depletion study, gas will be liberated from the oil. If pressures increase as a result of water or gas injection, the gas is re-dissolved into the oil phase.

A simulation project of a developed field, usually requires "history matching" where historical field production and pressures are compared to calculated values.The model's parameters are adjusted until a reasonable match is achieved on a field basis and usually for all wells. Commonly, producing water cuts or water-oil ratios and gas-oil ratios are matched.

3.3.2 History Matching and Prediction

Reservoir simulation involves two key phases: history matching and future prediction. Here, we'll delve into understanding these concepts in reservoir modeling.

3.3.2.1 History Matching

History matching focuses on refining reservoir characterization to enhance production estimates in the prediction phase. During history matching, reservoir characteristics are not fully known,

while well rates are established. In prediction, the reservoir is characterized, but future well rates are estimated from simulation results. Typically, a simulation project involves history matching, comparing historical field production and pressures with calculated values. The goal is to ensure that the geological model accurately reproduces observed rates and pressures. This process involves multiple simulations to find the best match, analyzed through tools like Petrel's History Match Analysis. The primary aim of history matching is to improve and verify the reservoir simulation model, considering factors like gas/oil ratios, water/oil ratios, observed pressures, and oil production rates. Although time-consuming, history matching is essential for accurate reservoir predictions, a global history might be matched, but locally, wells are unlikely to match the pressure and production history requiring iterative adjustments and the expertise of reservoir engineers to enhance model sensitivity and predictive capability. Achieving a perfect history match is challenging, often necessitating adjustments to modeling parameters for a more reliable future performance prediction.

3.3.2.2 Prediction

During history matching, the simulator strives to replicate historical reservoir performance. In the prediction phase, the matched simulation case becomes instrumental in forecasting the future performance of a well or reservoir under various operating strategies as shown in (Figure 3.43). The reservoir engineer explores a spectrum of scenarios and chooses a strategy anticipated to yield the most favorable results. This predictive process involves selecting prediction scenarios, preparing input data for these cases, utilizing history matching effectively, evaluating, and analyzing predicted performance, and ultimately presenting a comprehensive report on the anticipated outcomes. Beyond meeting historical performance, this predictive approach allows engineers to illustrate the potential advantages of new ideas and deliver results of significant interest to the company.

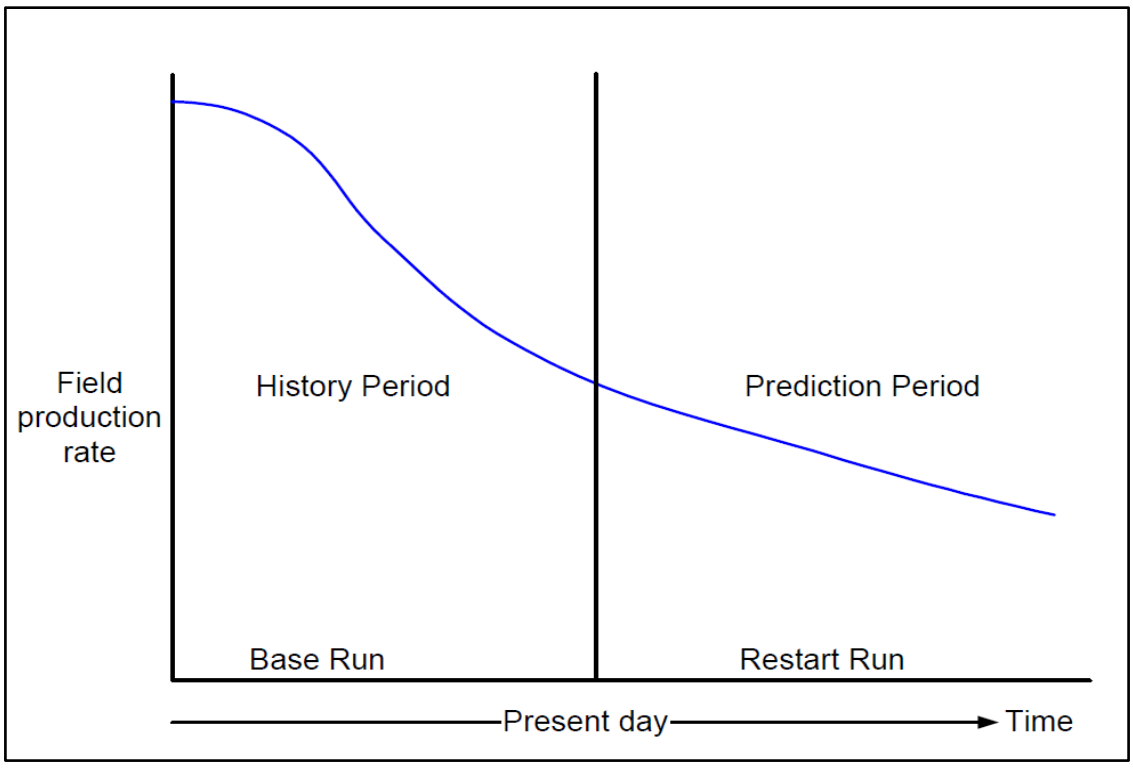

Figure 3.43: Curve scheme illustrate the history & prediction periods

3.3.2.3 Defining a Simulation Case

The Case concept contains a description of cases and how they are used. There are two options for defining a simulation case in petrel:

- Construct a full simulation case inside petrel.
- Import an existing ECLIPSE (an EXLIPSE .DATA file) or convert an imported case to create a partial simulation case within petrel.

To construct a simulation case within petrel you use the Define simulation case process in Simulation folder of the process pane as shown in (Figure 3.44); this will enable us to pull together already defined models, functions and controls into a case defining the model that will run in the simulation.

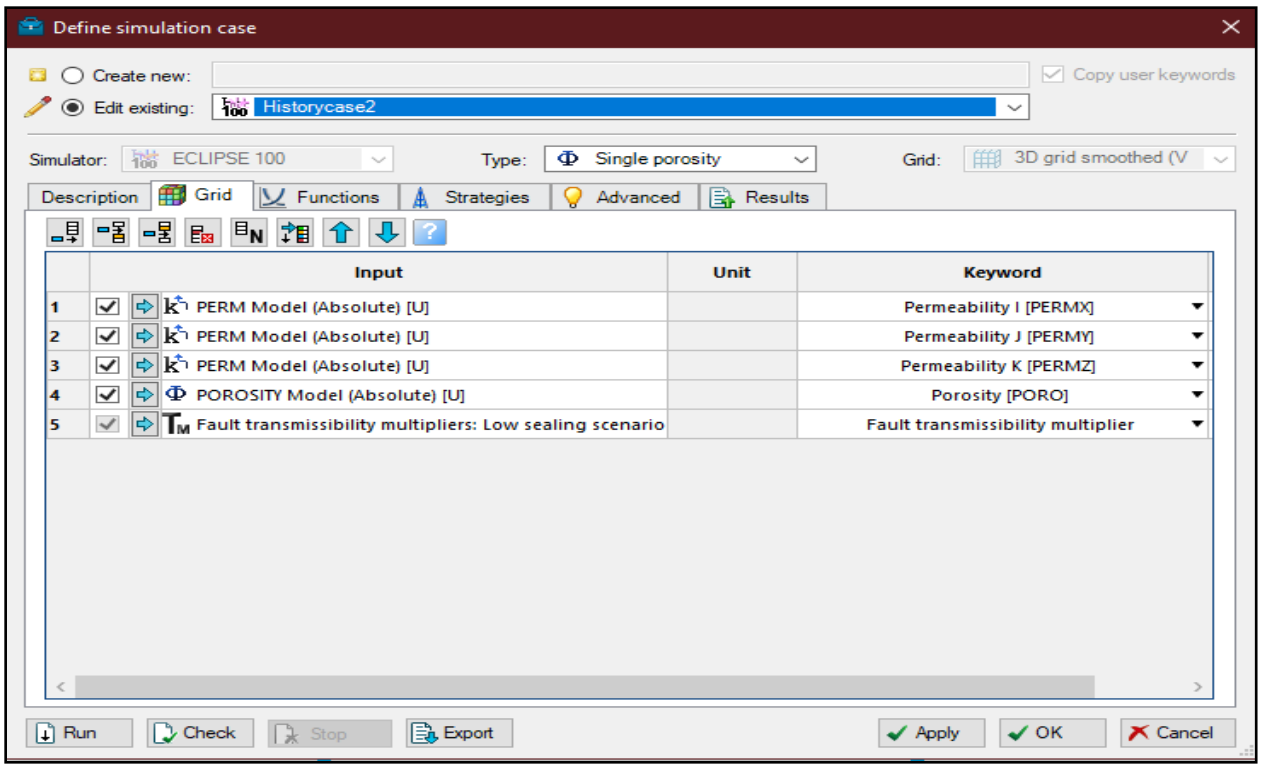

Figure 3.44: Input parameters for defining a simulation case

Defining simulation case consists of specifying the input properties, then selecting predefined initial conditions and fluid models, separators, rock physics functions, and development strategies. You can select the result that the simulation should generate and the type of simulator. The completed simulation case will appear in the Cases pane list (Figure 3.45).

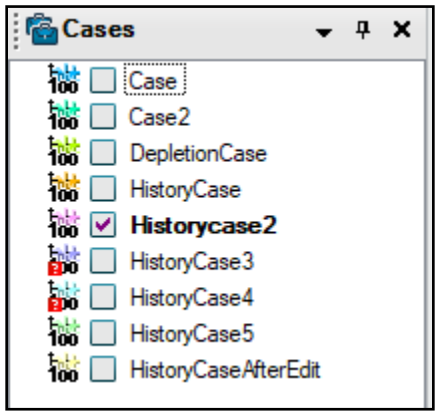

Figure 3.45: Result cases pane in petrel

Once the appropriate simulator is selected, clicking "Run" in the Define Simulation Case dialog initiates the simulation process in the background. Upon completion, a simulation log emerges, presenting the simulation results along with any encountered errors during the run. Dynamic results, encompassing reservoir pressures, production rates, and various other outcomes, manifest in the Results pane under Dynamic Results Data. These results are visually represented in section 4 for a comprehensive understanding of the simulation's dynamic aspects.

3.3.3 Machine Learning

Machine learning is a cutting-edge subfield of artificial intelligence that has revolutionized the way we analyze and interpret data. At its core, machine learning leverages algorithms and statistical models to enable computer systems to learn from and make predictions or decisions based on data, without being explicitly programmed for each task. This technology has found applications in diverse domains, from natural language processing and image recognition to healthcare and finance. Machine learning algorithms adapt and improve their performance over time, making them invaluable for automating tasks, uncovering hidden insights in large datasets, and enhancing decision-making processes. As machine learning continues to evolve, it promises to reshape industries and drive innovation, enabling us to solve complex problems and uncover patterns and predictions that were once beyond our reach.

Machine Learning and Forecasting, particularly utilizing Long Short-Term Memory (LSTM) networks, have emerged as transformative tools in various domains. LSTM is a specialized recurrent neural network architecture capable of capturing intricate patterns within sequential data, making it ideal for time-series forecasting and predictive modeling. With its ability to retain context over extended sequences, LSTM has significantly enhanced our capacity to predict future trends, outcomes, and behaviors, revolutionizing decision-making processes across industries. In this exploration, we delve into the captivating world of LSTM-based forecasting, unraveling its potential and impact on predictive analytics. Below is a flow chart will show the steps that will be taken in the machine learning procedures (Figure 3.46).

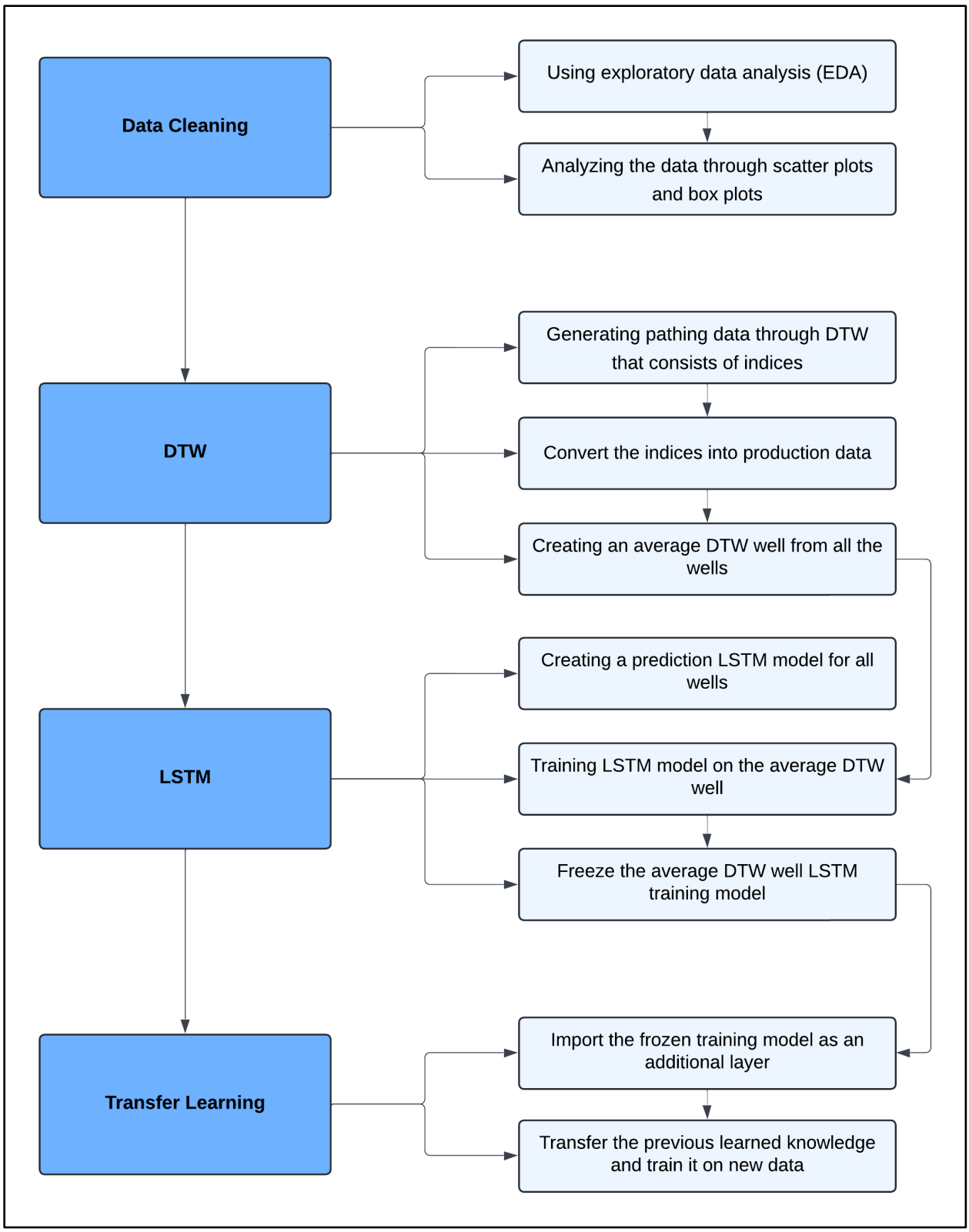

Figure 3.46: Flowchart of Machine learning steps

The implementation of the machine learning models such as DTW, LSTM and transfer learning utilized a range of libraries, including numpy, pandas, keras, tensorflow, and matplotlib. The JupyterLab package in Anaconda Navigator served as the software environment for conducting the experiments and analyzing the results.

3.3.3.1 Data Gathering and Cleaning

Data gathering and cleaning are essential stages in the machine learning process, with Exploratory Data Analysis (EDA) serving as a vital tool for ensuring data quality and suitability. Data gathering involves collecting relevant information from diverse sources, and the data must be representative and comprehensive for the problem at hand. Data cleaning, on the other hand, addresses errors, inconsistencies, and missing values, which can significantly impact model performance. This involves handling missing data, detecting, and addressing outliers, transforming data types, and reducing noise. EDA, as an integral part of data cleaning, aids in understanding data patterns, distributions, and variable relationships. It enables data scientists to visualize data, uncover anomalies, identify trends, and prepare the data for effective machine learning model development, ensuring that the models are accurate and capable of delivering valuable insights.

Using Python and its libraries the EDA is constructed by importing all the Production wells available, below in the (Figures 3.47 & 3.48) and (Tables 3.10 - 3.13) shows the data distribution and provides an idea of what is missing from variables. However, the well C006 and C255 will be used to demonstrate the table of content examples.

Table 3.10: Showing the head of 10 units for the well C006

	Date	BOPD	BWPD	GOR
0	2000-10-01	651.7	0.0	58
1	2000-11-01	660.2	0.0	58
2	2000-12-01	641.3	0.0	58
3	2001-01-01	628.0	0.0	58
4	2001-02-01	693.6	0.0	111
5	2001-03-01	646.7	0.0	113
6	2001-04-01	634.8	0.0	113
7	2001-05-01	701.1	0.0	113
8	2001-06-01	607.0	0.0	113
9	2001-07-01	654.5	0.0	113

Table 3.11: Showing the head of 10 units for the well C255

	Date	BOPD	BWPD	GOR
0	1986-12-01	1044.0	0.0	0
1	1987-01-01	933.1	0.0	0
2	1987-02-01	1236.0	0.0	0
3	1987-03-01	1266.7	0.0	0
4	1987-04-01	1233.5	0.0	0
5	1987-05-01	1127.6	0.0	0
6	1987-06-01	1543.9	15.6	0
7	1987-07-01	1664.2	16.8	0
8	1987-08-01	1894.5	19.1	0
9	1987-09-01	1757.3	17.7	0

The following table will show the shape of each well to better understand how much data each well has X being the rows and Y being the columns.

Table 3.12: Showing the shape of each well

Well Name	Rows X, Columns Y
C006	(220, 4)
C035	(414, 4)
C198	(398, 4)
C213	(370, 4)
C236	(398, 4)
C249	(369, 4)
C253	(386, 4)
C255	(386, 4)

Now that we have a better understanding of the available data, we will go more in detail to describe them using scatter plots and box plots for oil production.

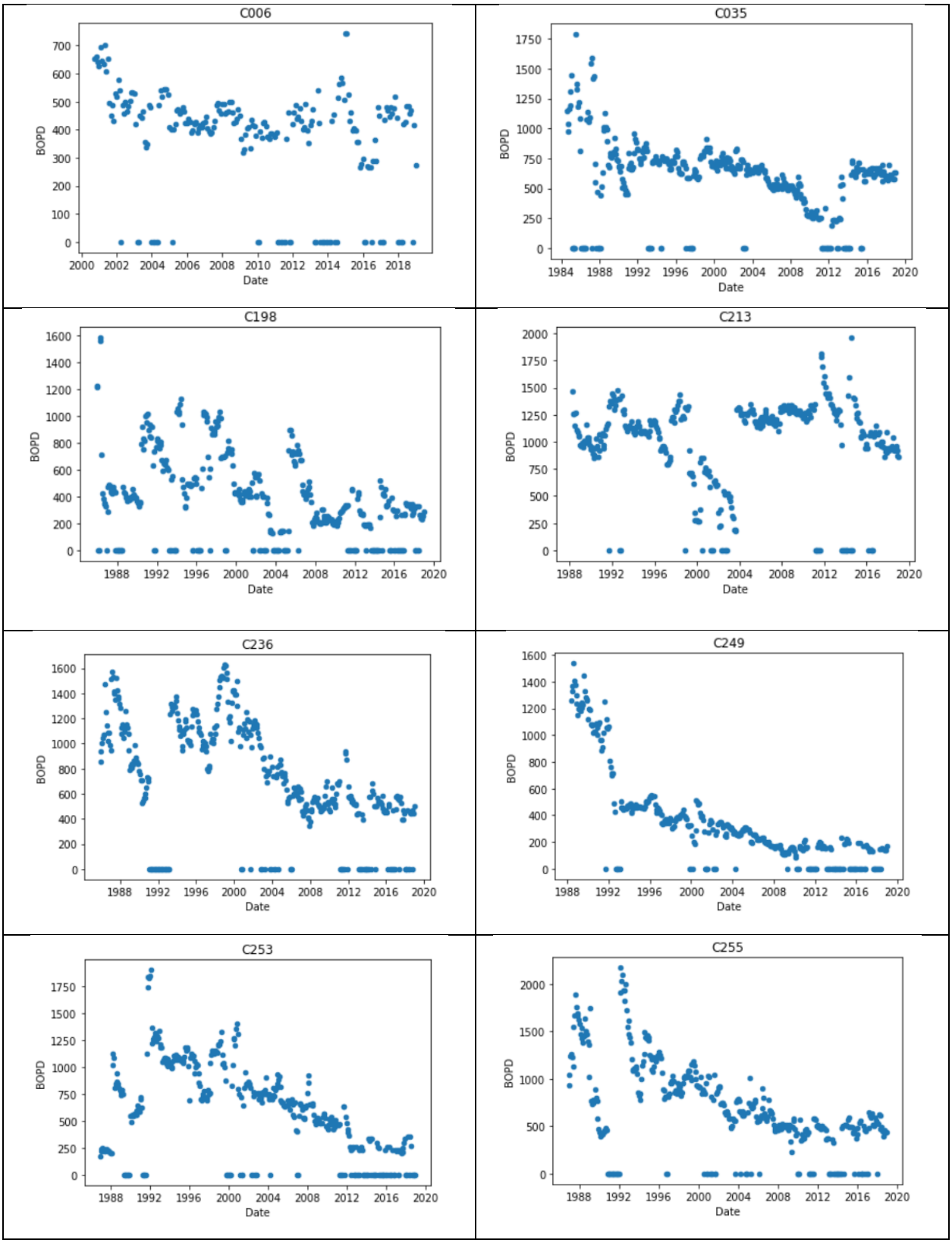

Figure 3.47 : Scatter plot for all the wells

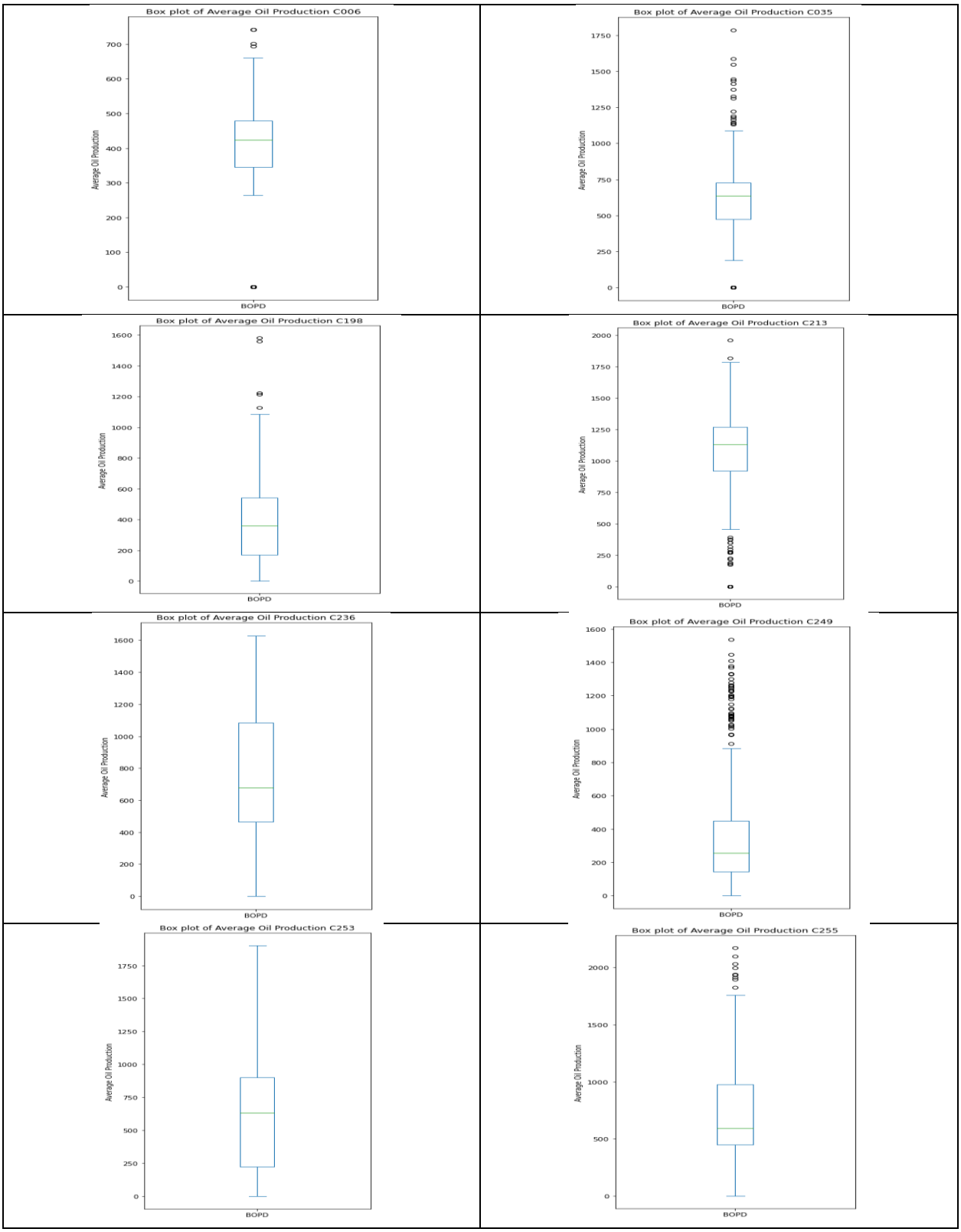

Figure 3.48: Box plot for all the wells

Histogram plots visually represent the data distribution within each column, offering insights into the predominant data values. Upon closer examination, it becomes increasingly evident that a substantial number of zero values are prevalent.

Table 3.13: Histograms showing the predominant data values in all wells

Well	BOPD vs Rows	BWPD vs Rows	GOR vs Rows
C006	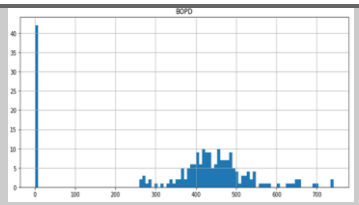	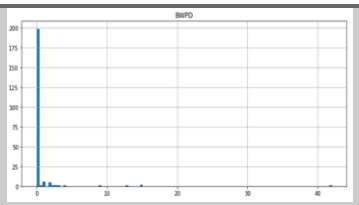	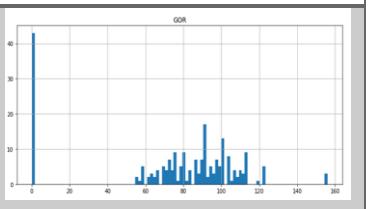
C035	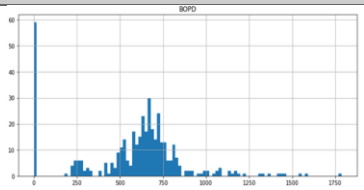	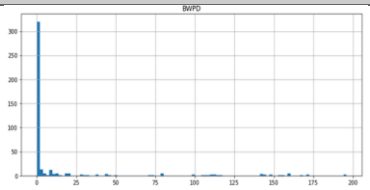	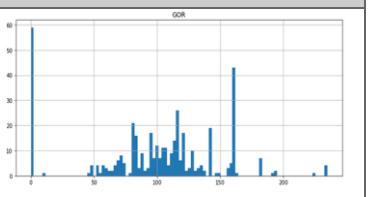
C198	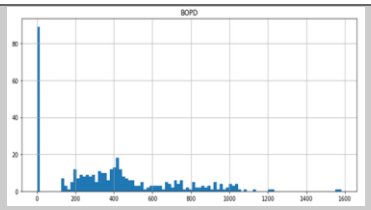	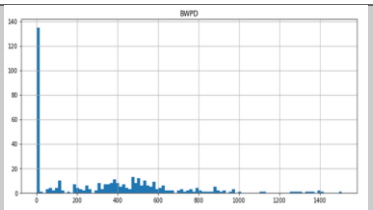	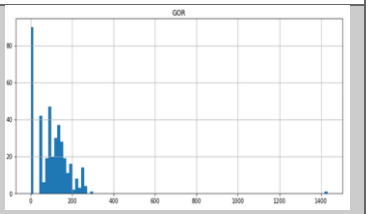
C213	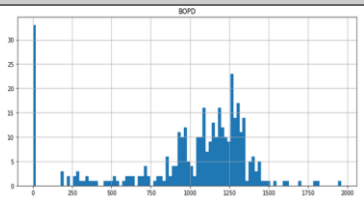	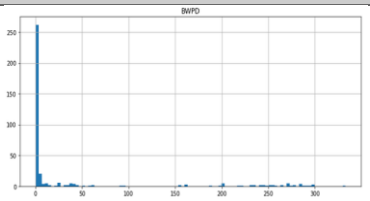	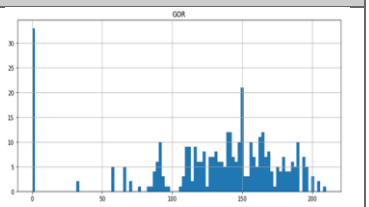
C236	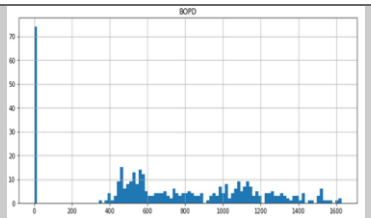	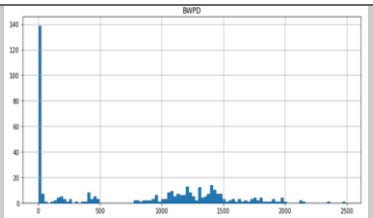	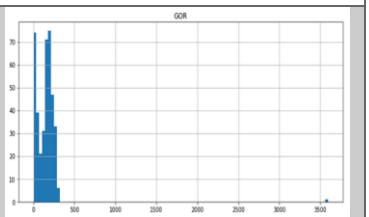
C249	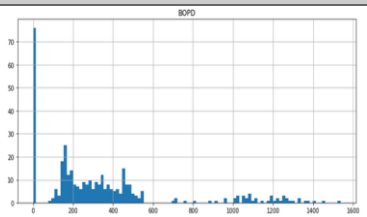	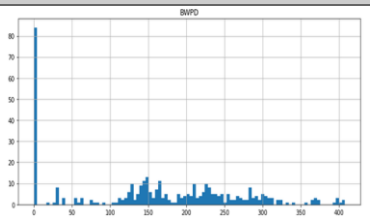	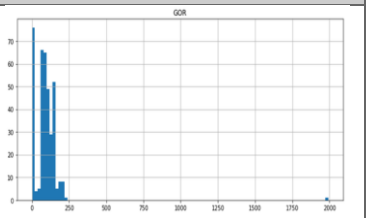

C253	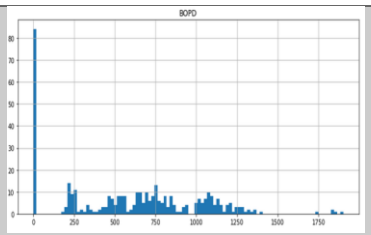	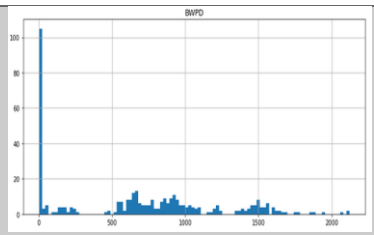	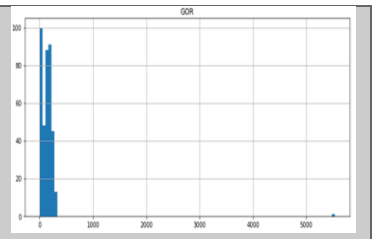
C255	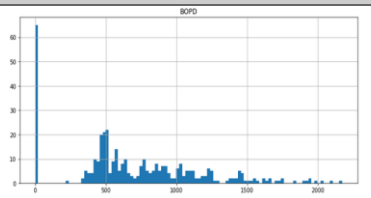	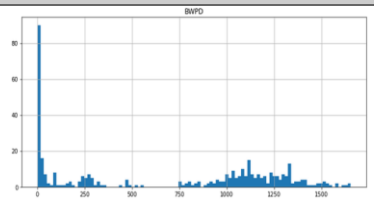	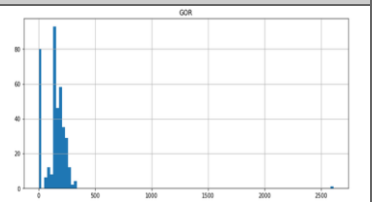

3.3.3.2 Dynamic Time Warping (DTW)

Dynamic Time Warping (DTW) is a powerful technique in time series analysis, renowned for its ability to address the challenges posed by missing data and irregularities in temporal sequences. Unlike traditional methods that assume a fixed and consistent time step between data points, DTW excels in aligning time series with varying time intervals. This flexibility is especially advantageous when dealing with real-world datasets that often contain gaps, irregular sampling, or temporal misalignments. DTW's capacity to find the optimal alignment between time series enables accurate forecasting and analysis, making it an indispensable tool in various fields, including finance, speech recognition, and healthcare. In this context, DTW stands out as a versatile and robust solution for handling missing data, improving prediction accuracy, and enhancing the overall reliability of time series analysis.

During the Exploratory Data Analysis (EDA) phase, it's evident that well C035 offers a robust dataset with 414 rows of data, serving as a reference for Dynamic Time Warping (DTW) to align other wells. The presence of missing data poses challenges, affecting the accuracy of the DTW process, as seen in well C006, which only comprises 220 entries. The extent of missing data directly impacts the efficiency of the DTW alignment, with more missing data correlating with greater challenges and reduced accuracy.

Using the (fastdtw) library the temporal sequences of each well matched with the well C035, the following (Figure 3.49) will compare the temporal sequence for well C006 and C035.

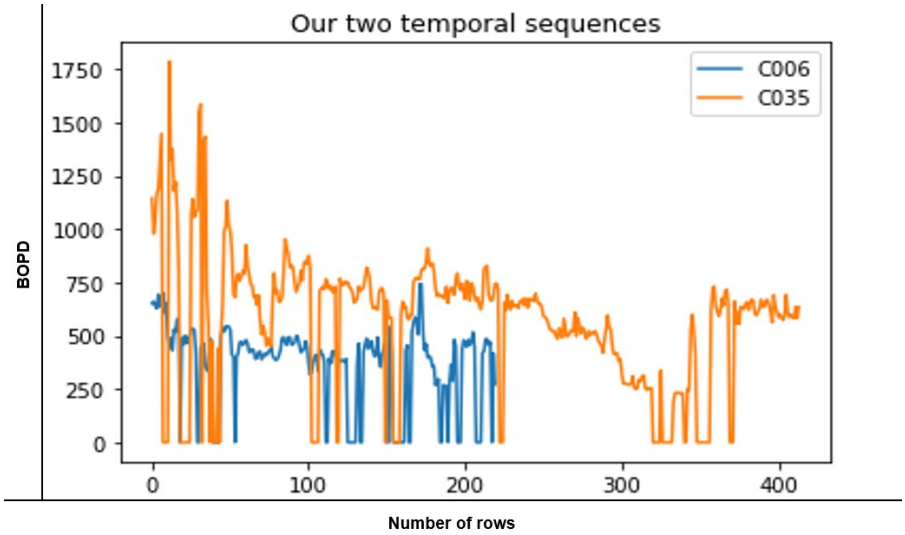

Figure 3.49: Temporal sequence of well C035 and C006

Upon performing Dynamic Time Warping (DTW), pathing data is generated. This pathing data consists of indices representing the alignment of data points relative to the reference well. These indices are subsequently employed to reorganize the test well data accordingly. It is important to note that after the rearrangement process, gaps or missing data may arise if the length of the test well data is shorter than that of the reference well. The pathing result between well C006 and C035 will be shown as an example in (Figure 3.50).

[(0, 0), (1, 1), (1, 2), (1, 3), (1, 4), (1, 5), (1, 6), (1, 7), (1, 8), (1, 9), (1, 10), (1, 11), (1, 12), (1, 13), (1, 14), (1, 15), (1, 16), (1, 17), (1, 18), (1, 19), (1, 20), (1, 21), (1, 22), (1, 23), (1, 24), (1, 25), (1, 26), (1, 27), (1, 28), (1, 29), (1, 30), (1, 31), (1, 32), (1, 33), (1, 34), (1, 35), (2, 36), (3, 37), (3, 38), (3, 39), (3, 40), (3, 41), (3, 42), (3, 43), (3, 44), (3, 45), (4, 46), (4, 47), (4, 48), (4, 49), (4, 50), (4, 51), (4, 52), (4, 53), (4, 54), (4, 55), (4, 56), (4, 57), (4, 58), (4, 59), (4, 60), (4, 61), (4, 62), (4, 63), (4, 64), (4, 65), (4, 66), (4, 67), (4, 68), (4, 69), (4, 70), (4, 71), (4, 72), (4, 73), (4, 74), (4, 75), (4, 76), (4, 77), (4, 78), (4, 79), (4, 80), (4, 81), (4, 82), (4, 83), (4, 84), (4, 85), (4, 86), (4, 87), (4, 88), (4, 89), (4, 90), (4, 91), (4, 92), (4, 93), (4, 94), (4, 95), (4, 96), (4, 97), (4, 98), (4, 99), (4, 100), (4, 101), (4, 102), (4, 103), (4, 104), (4, 105), (4, 106), (4, 107), (4, 108), (4, 109), (4, 110), (4, 111), (4, 112), (4, 113), (4, 114), (4, 115), (4, 116), (4, 117), (4, 118), (4, 119), (4, 120), (4, 121), (4, 122), (4, 123), (4, 124), (4, 125), (4, 126), (4, 127), (4, 128), (4, 129), (4, 130), (4, 131), (4, 132), (4, 133), (4, 134), (4, 135), (4, 136), (4, 137), (4, 138), (4, 139), (4, 140), (5, 141), (5, 142), (5, 143), (5, 144), (5, 145), (5, 146), (5, 147), (5, 148), (5, 149), (5, 150), (6, 151), (6, 152), (6, 153), (6, 154), (6, 155), (6, 156), (6, 157), (6, 158), (6, 159), (6, 160), (6, 161), (6, 162), (6, 163), (6, 164), (6, 165), (6, 166), (7, 167), (7, 168), (7, 169), (7, 170), (7, 171), (7, 172), (7, 173), (7, 174), (7, 175), (7, 176), (7, 177), (7, 178), (7, 179), (7, 180), (7, 181), (7, 182), (7, 183), (7, 184), (7, 185), (7, 186), (7, 187), (7, 188), (7, 189), (7, 190), (7, 191), (7, 192), (7, 193), (7, 194), (7, 195), (7, 196), (7, 197), (7, 198), (7, 199), (7, 200), (7, 201), (7, 202), (7, 203), (7, 204), (7, 205), (7, 206), (7, 207), (7, 208), (7, 209), (7, 210), (7, 211), (7, 212), (7, 213), (7, 214), (7, 215), (7, 216), (7, 217), (7, 218), (7, 219), (7, 220), (7, 221), (8, 222), (8, 223), (8, 224), (9, 225), (9, 226), (9, 227), (9, 228), (9, 229), (9, 230), (9, 231), (9, 232), (9, 233), (9, 234), (9, 235), (9, 236), (9, 237), (9, 238), (9, 239), (9, 240), (9, 241), (9, 242), (9, 243), (9, 244), (9, 245), (9, 246), (9, 247), (9, 248), (9, 249), (9, 250), (9, 251), (9, 252), (10, 253), (10, 254), (10, 255), (10, 256), (10, 257), (10, 258), (11, 259), (12, 259), (13, 259), (14, 260), (15, 261), (15, 262), (15, 263), (15, 264), (15, 265), (15, 266), (15, 267), (15, 268), (15, 269), (15, 270), (15, 271), (15, 272), (15, 273), (15, 274), (15, 275), (15, 276), (15, 277), (15, 278), (15, 279), (15, 280), (15, 281), (15, 282), (16, 283), (17, 284), (18, 285), (19, 285), (20, 286), (20, 287), (20, 288), (21, 289), (22, 289), (23, 289), (24, 289), (25, 290), (26, 291), (26, 292), (27, 293), (28, 294), (29, 294), (30, 294), (31, 294), (32, 294), (33, 294), (34, 294), (35, 294), (36, 294), (37, 294), (38, 294), (39, 294), (40, 294), (41, 294), (42, 294), (43, 294), (44, 294), (45, 294), (46, 294), (47, 294), (48, 294), (49, 294), (50, 294), (51, 294), (52, 294), (53, 294), (54, 294), (55, 294), (56, 294), (57, 294), (58, 294), (59, 294), (60, 294), (61, 294), (62, 295), (63, 295), (64, 295), (65, 295), (66, 295), (67, 295), (68, 295), (69, 295), (70, 295), (71, 295), (72, 295), (73, 295), (74, 295), (75, 295), (76, 295), (77, 295), (78, 295), (79, 295), (80, 295), (81, 296), (82, 297), (83, 297), (84, 297), (85, 297), (86, 297), (87, 297), (88, 297), (89, 297), (90, 297), (91, 297), (92, 297), (93, 297), (94, 297), (95, 297), (96, 297), (97, 297), (98, 297), (99, 297), (100, 298), (101, 298), (102, 298), (103, 298), (104, 299), (105, 299), (106, 299), (107, 299), (108, 299), (109, 299), (110, 299), (111, 299), (112, 299), (113, 299), (114, 299), (115, 299), (116, 299), (117, 299), (118, 299), (119, 299), (120, 299), (121, 299), (122, 299), (123, 299), (124, 300), (125, 301), (126, 302), (127, 303), (128, 304), (129, 305), (130, 306), (131, 307), (132, 308), (133, 309), (134, 310), (135, 311), (136, 312), (137, 313), (138, 314), (139, 314), (140, 314), (141, 314), (142, 314), (143, 314), (144, 314), (145, 315), (146, 316), (147, 317), (148, 318), (149, 319), (150, 320), (150, 321), (150, 322), (150, 323), (150, 324), (151, 324), (152, 325), (153, 325), (154, 326), (154, 327), (154, 328), (154, 329), (154, 330), (154, 331), (154, 332), (154, 333), (154, 334), (154, 335), (154, 336), (154, 337), (154, 338), (154, 339), (154, 340), (154, 341), (155, 341), (156, 341), (157, 341), (158, 341), (159, 341), (160, 341), (161, 341), (162, 342), (162, 343), (163, 344), (163, 345), (163, 346), (163, 347), (164, 348), (164, 349), (164, 350), (164, 351), (164, 352), (164, 353), (164, 354), (164, 355), (164, 356), (165, 356), (166, 357), (167, 357), (168, 357), (169, 357), (170, 357), (171, 358), (172, 359), (172, 360), (173, 361), (173, 362), (173, 363), (174, 364), (175, 365), (176, 366), (177, 367), (178, 368), (179, 368), (180, 368), (181, 369), (182, 370), (183, 371), (184, 371), (185, 371), (186, 371), (187, 371), (188, 371), (189, 371), (190, 371), (191, 371), (192, 371), (193, 371), (194, 371), (195, 371), (196, 371), (197, 371), (198, 372), (199, 373), (200, 374), (201, 375), (202, 376), (203, 377), (204, 378), (205, 379), (205, 380), (205, 381), (205, 382), (205, 383), (205, 384), (205, 385), (205, 386), (205, 387), (205, 388), (205, 389), (205, 390), (205, 391), (205, 392), (205, 393), (205, 394), (205, 395), (205, 396), (205, 397), (205, 398), (205, 399), (206, 400), (207, 401), (208, 402), (209, 403), (210, 404), (211, 405), (212, 406), (213, 407), (214, 408), (215, 409), (216, 410), (217, 411), (218, 412), (219, 413)]

Figure 3.50: Pathing between well C006 and C035

Dynamic Time Warping (DTW) was similarly employed on the water and gas-oil ratio data. Nevertheless, the impact was minimal due to the substantial number of missing values in the dataset.

3.3.3.3 Long Short-Term Memory (LSTM)

Long Short-Term Memory, commonly referred to as LSTM, is a specialized type of recurrent neural network (RNN) within the domain of deep learning. LSTM networks have gained immense popularity and recognition for their remarkable ability to model and predict sequences of data. Unlike traditional RNNs, LSTM units are equipped with a unique architecture that enables them to capture and retain information over extended sequences. This design feature makes LSTMs exceptionally well-suited for a wide range of sequential data applications, such as time series forecasting, natural language processing, speech recognition, and more. Their capacity to understand long-range dependencies and effectively manage both short and long-term information has positioned LSTMs as a fundamental tool in solving complex sequential data challenges. In this section, we'll explore the key principles, architecture, and applications of LSTMs, shedding light on how they have revolutionized the field of deep learning (Figure 3.51).

In addition, Multivariate Long Short-Term Memory (LSTM) is an advanced extension of the LSTM architecture designed to handle and make sense of multiple interrelated time series data streams. Unlike univariate LSTMs, which operate on a single time series, multivariate LSTMs can simultaneously model and forecast data from various sources or variables. This capacity to work with multiple input features makes them particularly well-suited for applications where several factors influence a complex system. By processing and capturing dependencies across multiple variables, such as oil production, water production, and gas oil ratio multivariate LSTMs provide a holistic understanding of intricate temporal relationships. This technology has found wide-ranging applications, from financial forecasting and environmental monitoring to healthcare analytics and more, offering a versatile and powerful approach for solving real-world problems involving multivariate time series data.

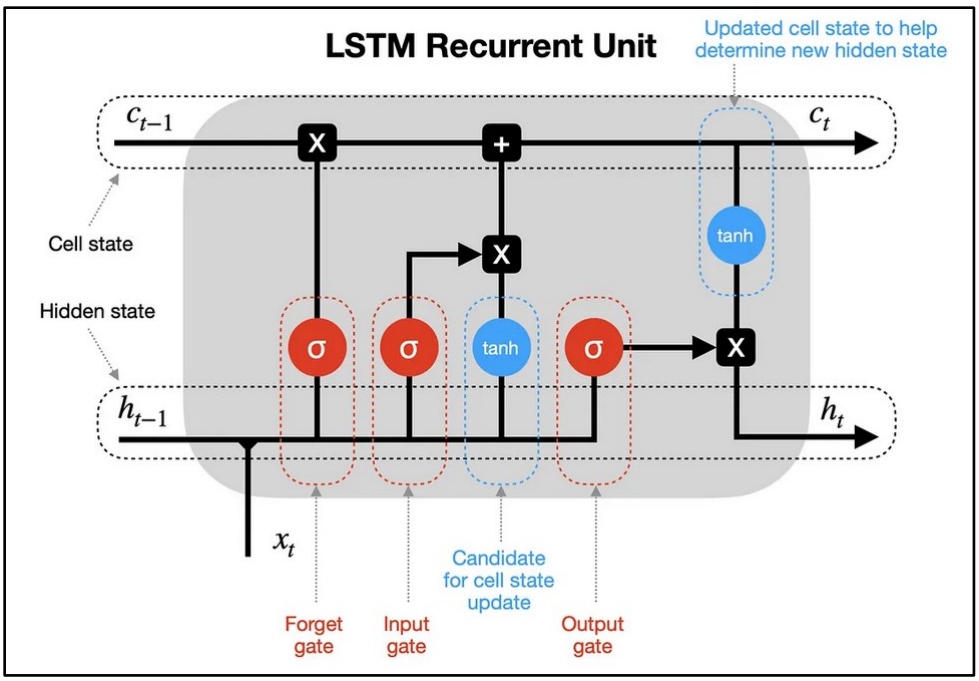

Figure 3.51: Long Short-Term Memory (LSTM) Neural Networks, (Saul Dobilas, 2022)

The equations (3.1 – 3.6) for the forget gate, input gate, candidate cell state, update cell state, output gate, and hidden state are derived from the LSTM model introduced by (Hochreiter & Schmidhuber, 1997).

Forget Gate (f_t): It determines what information to discard from the cell state.

- $f_t = \sigma(W_f[h_{t-1}, x_t] + b_f)$ (3.1)
- Where W_f and b_f are the weight matrix and bias for the forget gate, $[h_{t-1}, x_t]$ represents the concatenation of the previous hidden state and current input, and σ is the sigmoid activation function.

Input Gate (i_t): It decides which values to update and store in the cell state.

- $i_t = \sigma(W_i[h_{t-1}, x_t] + b_i)$ (3.2)
- Where W_i and b_i are the weight matrix and bias for the input gate.

Candidate Cell State ($\tilde{c}_t$): It calculates a new candidate value to be added to the cell state.

- $\tilde{c}_t = \tanh(W_c[h_{t-1}, x_t] + b_c)$ (3.3)
- Where W_c and b_c are the weight matrix and bias for the candidate cell state.

Update Cell State (c_t): It combines the forget gate, input gate, and candidate cell state to update the current cell state.

- $c_t = f_t * c_{t-1} + i_t * \tilde{c}_t$ (3.4)
- Where * denotes element-wise multiplication.

Output Gate (o_t): It determines which values from the cell state should be output as the hidden state.

- $o_t = \sigma(W_o[h_{t-1}, x_t] + b_o)$ (3.5)
- Where W_o and b_o are the weight matrix and bias for the output gate.

Hidden State (h_t): It calculates the updated hidden state based on the output gate and the cell state.

- $h_t = o_t * \tanh(c_t)$ (3.6)

The methodology employed centers on prioritizing oil production as the primary focus for prediction within the context of a multivariate LSTM approach. Water and gas-oil ratio productions serve as crucial features in this predictive model. The data preprocessing involves the application of MinMaxScaler, ensuring that all data values are transformed into a standardized range between 0 and 1. This normalization not only reduces error margins but also enhances prediction accuracy. The dataset is structured by training the model on the preceding 36 timestamp values, generating 12 outputs. Subsequently, these 12 values are utilized for forecasting the next 36 timestamps, thus repeating this contributes to the construction and refinement of the model.
The parameters that were used in the LSTM model will be in the following (Table 3.14).

Table 3.14: Parameters of the LSTM model

Hidden units	150
Dropout rate	0.2
Number of layers	Single layer
Output layer	Dense, units=1
Activation function	Linear
Optimizer	Adam
Learning rate	0.01
Batch size	32
Number of epochs	50

Various parameter combinations were tested to improve the performance of the model, including the number of LSTM units, batch size, and epochs. After thorough experimentation, the parameters mentioned above yielded the most optimal results.

3.3.3.4 Transfer Learning

Transfer learning stands as a pivotal template in the realm of machine learning, revolutionizing the way models acquire and apply knowledge. At its core, transfer learning leverages pre-trained models on one task to boost the performance and efficiency of another related task. Rather than starting with a blank slate, these models, having already learned intricate patterns and features from vast datasets, are fine-tuned to adapt their acquired knowledge to new domains. This approach is particularly advantageous when confronted with limited labeled data for a specific task, as it capitalizes on the wealth of information obtained from other related tasks. By facilitating the transfer of learned representations, transfer learning accelerates model training, enhances generalization, and significantly contributes to the versatility and effectiveness of machine learning applications across diverse domains.

Transfer learning encompasses a wide range of techniques that serve various purposes. Among these techniques, learning rate adjustment is frequently employed in transfer learning to enhance the fine-tuning process. It plays a crucial role in balancing the preservation of pre-trained knowledge with the adaptation to new tasks or domains. During the fine-tuning of a pre-trained model, it is common to initialize the learning rate to a lower value compared to training from scratch. This approach is justified by the fact that the pre-trained model already possesses effective learned representations. By applying smaller updates during fine-tuning, significant changes that could potentially erase valuable knowledge are mitigated. This cautious adjustment of the learning rate facilitates a smoother transition and ensures the model's ability to leverage its prior knowledge effectively.

The pre-trained robust model is built upon a foundation of utilizing a multivariate LSTM. It was trained using identical parameters, except for the output layer (Dense, units=10), which was customized to handle a consolidated well. This consolidation involved averaging production rates across all wells after employing Dynamic Time Warping (DTW) to address missing values.

Following the consolidation step, the model was frozen as the (base_model) and then transferred to incorporate new information (Figure 3.52). Specifically, the model was imported for transfer learning training on the same wells, utilizing the same parameters of the multivariate LSTM. The only difference lies in the addition of an extra output layer (Dense, units=10) and a learning rate of (0.001).

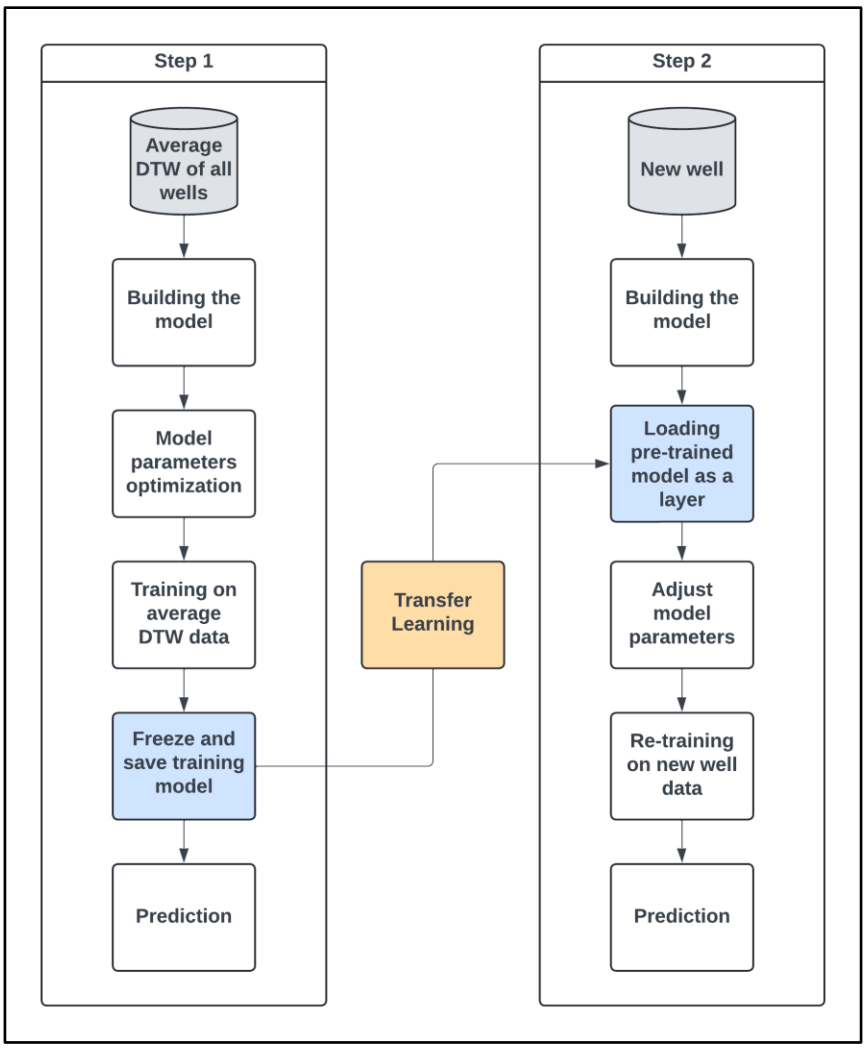

Figure 3.52: Flowchart that demonstrate the steps of building the transfer learning model

This transfer learning process enables an assessment of the model's performance and error margin before it is applied to new data, such as new wells or wells with missing data. By undergoing this evaluation, the model can be better prepared for future applications and ensure its effectiveness in handling diverse datasets.

4. Results and Discussion

4.1 Simulation Results with Petrel

A preliminary test of the model will be conducted through a basic case run, without any editing or additional development parameters. This initial run aims to assess the model's performance and identify potential errors. Subsequently, the following production scenarios will be thoroughly examined, with the outcomes presented in this chapter:

- Basic depletion strategy run.
- History matching scenario.
- Simulation run incorporating well completion alongside history matching.
- History match case in conjunction with prediction.

All simulation runs have been executed within the specified simulation period, spanning from November 1, 1966, to January 1, 2019.

4.1.1 Depletion Strategy

The simulation case has been executed within the abovementioned time period, operating under the following scenarios:

- Each well's production rate has been fixed at 1000 bbl/d.
- The bottom-hole pressure (BHP) for each well is established at 2000 psia.

The outcomes of these simulations are illustrated in (Figures 4.1 - 4.3).

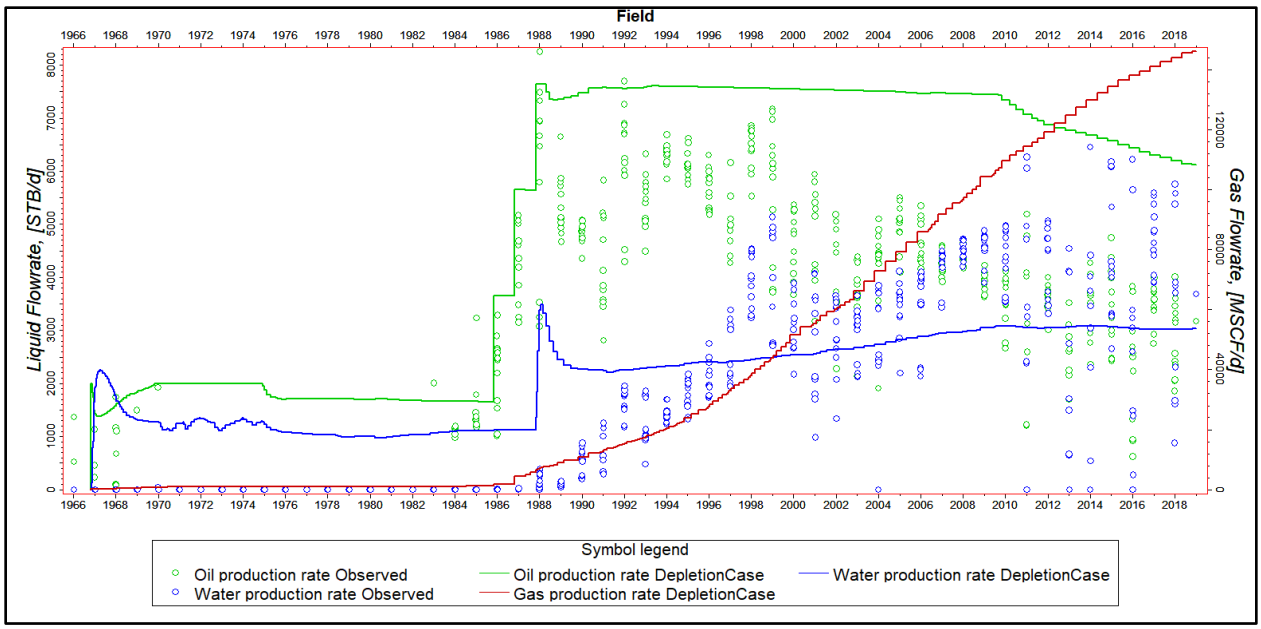

Figure 4.1: Depletion case vs observed data for the study field

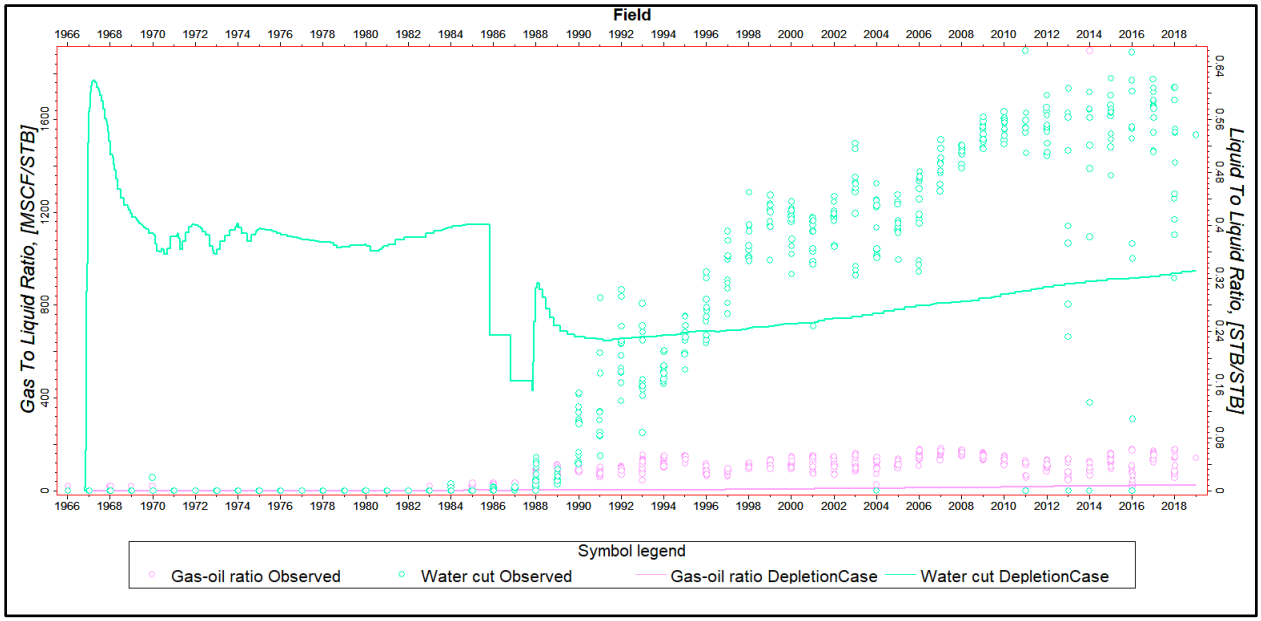

Figure 4.2: Gas oil ratio with water cut in the depletion case vs observed data for the study field

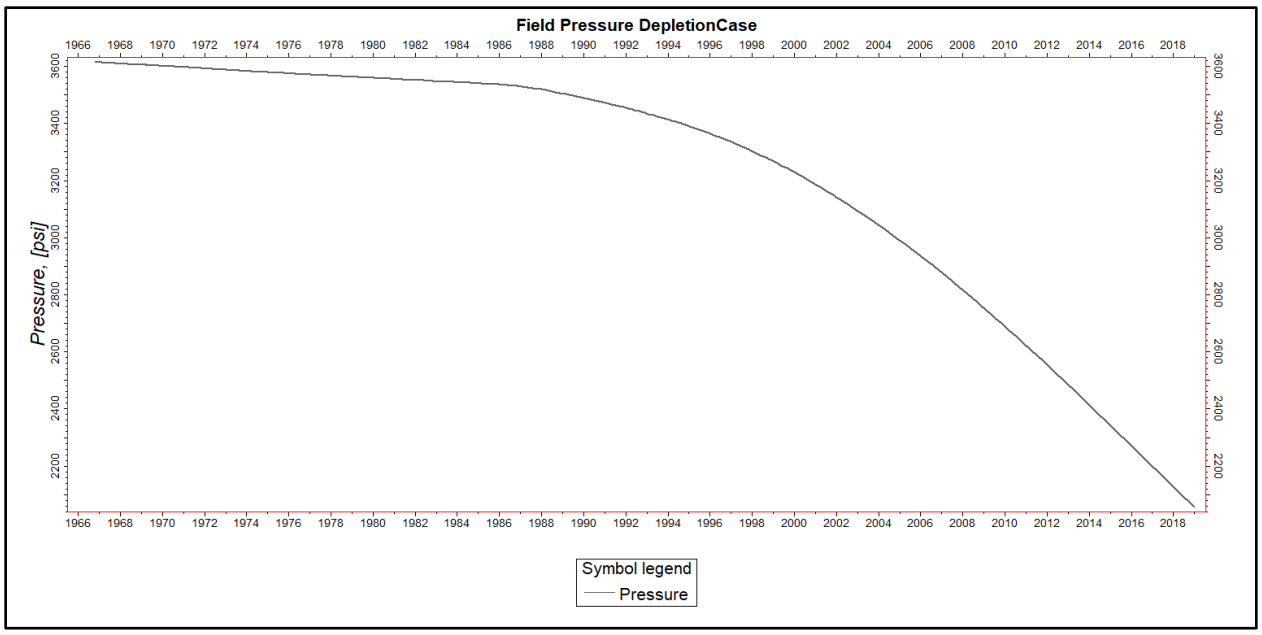

Figure 4.3: Pressure in the depletion case vs date for the study field

In general, the figures indicate that both the static and dynamic models were effectively simulated, yielding satisfactory predictions based on the depletion strategy. However, it is worth noting that the gas production exhibited a noticeable increase, which could potentially be attributed to the prediction scenario involving the open hole concept.

4.1.2 History Matching Case

The simulation has been conducted based on an open-hole concept without any completion, and the production data has been imported without filtering. Consequently, there are gaps and unaccounted values, as previously highlighted. The results are shown below in the (Figures 4.4 - 4.6).

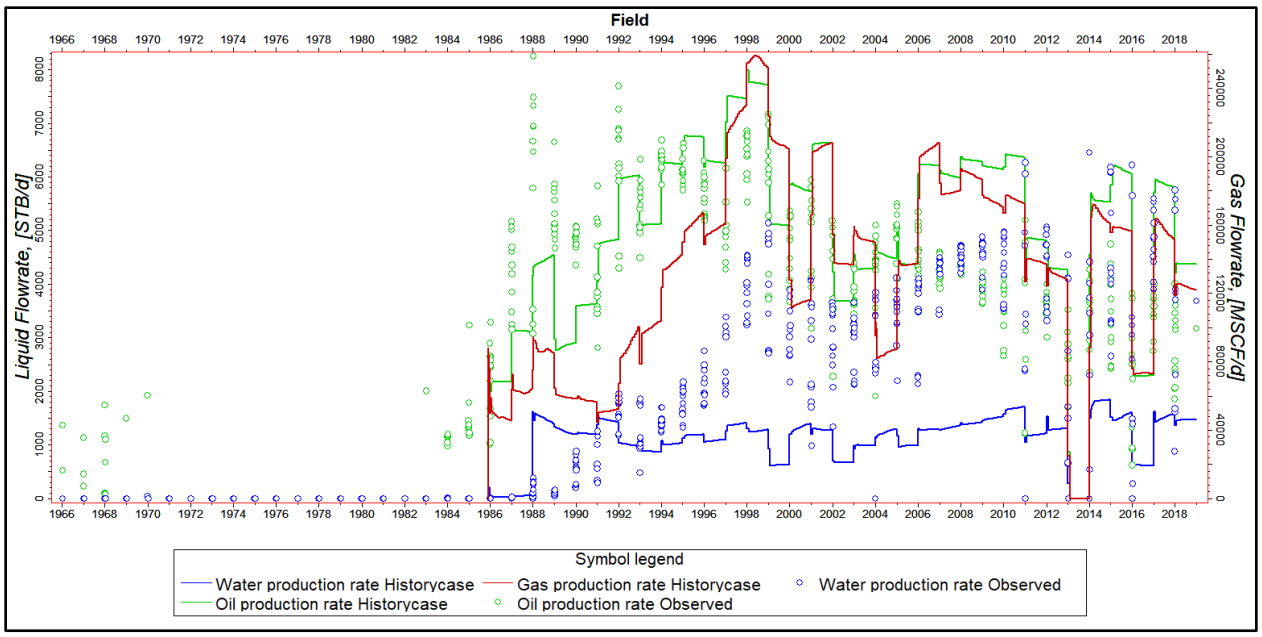

Figure 4.4: History matching case vs observed data for the study field

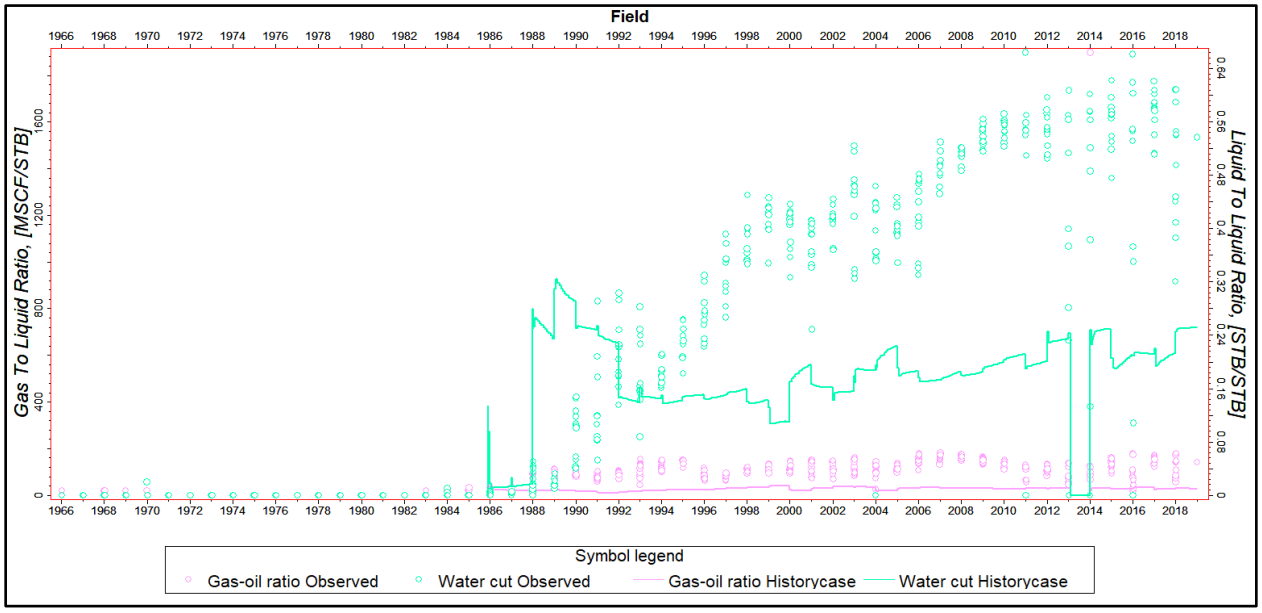

Figure 4.5: Gas oil ratio with water cut in the history matching case vs observed data for the study field

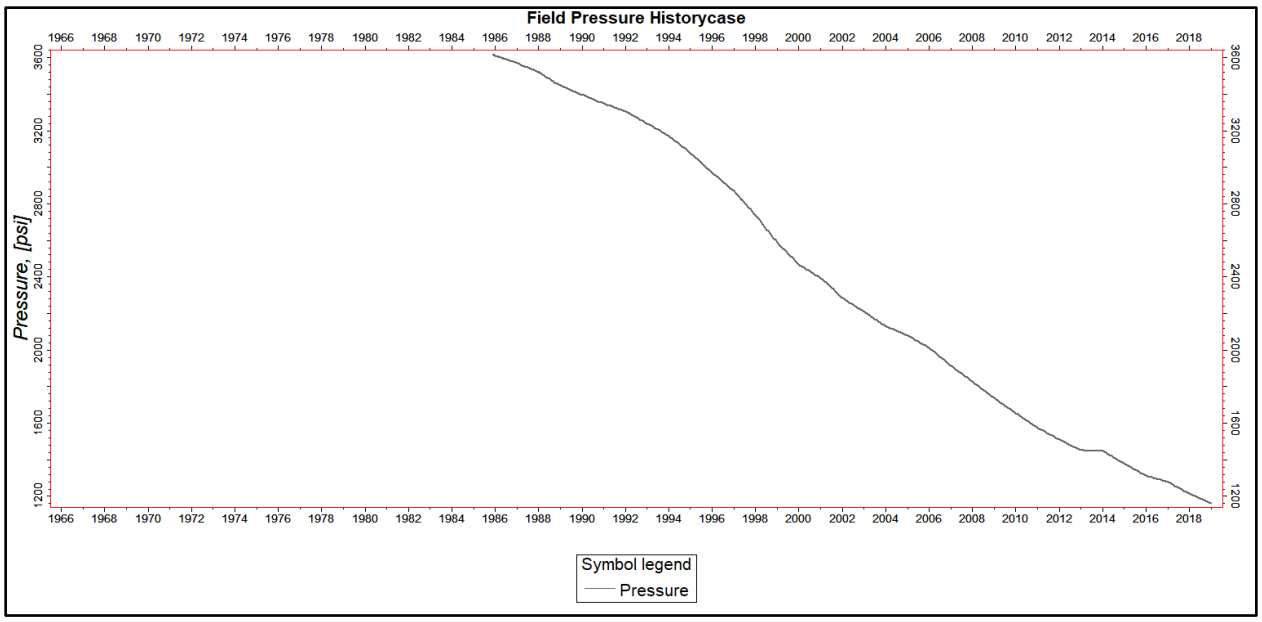

Figure 4.6: Pressure in the history matching case vs date for the study field

Upon analyzing the figures, it is evident that gas production remains significantly high when considering the open hole concept. Conversely, the prediction of oil production aligns exceptionally well with the observed data. However, the matching of water production exhibits some discrepancies, primarily due to the presence of substantial missing data at the well level. It is important to note that history matching primarily emphasizes field-level predictions rather than achieving specific matching at the individual well level.

4.1.3 History Matching with Completion

Following the simulation on the open-hole concept, it became evident that the pressure readings and production results did not align closely with the observed historical data. Consequently, Well Completion procedures were undertaken on the producing wells (C006, C035, C198, C213, C236, C249, C253, and C255). With the completion process concluded, the simulation results have been modified, as shown in (Figures 4.7 - 4.9).

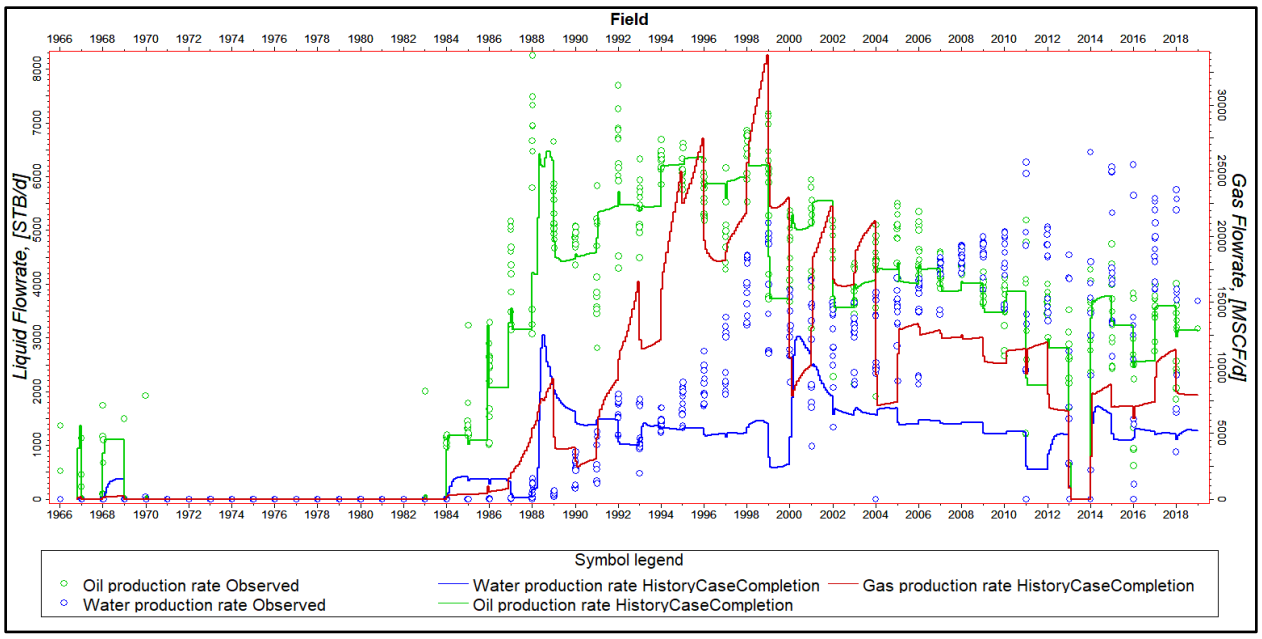

Figure 4.7: History case with well completion vs observed data for the study field

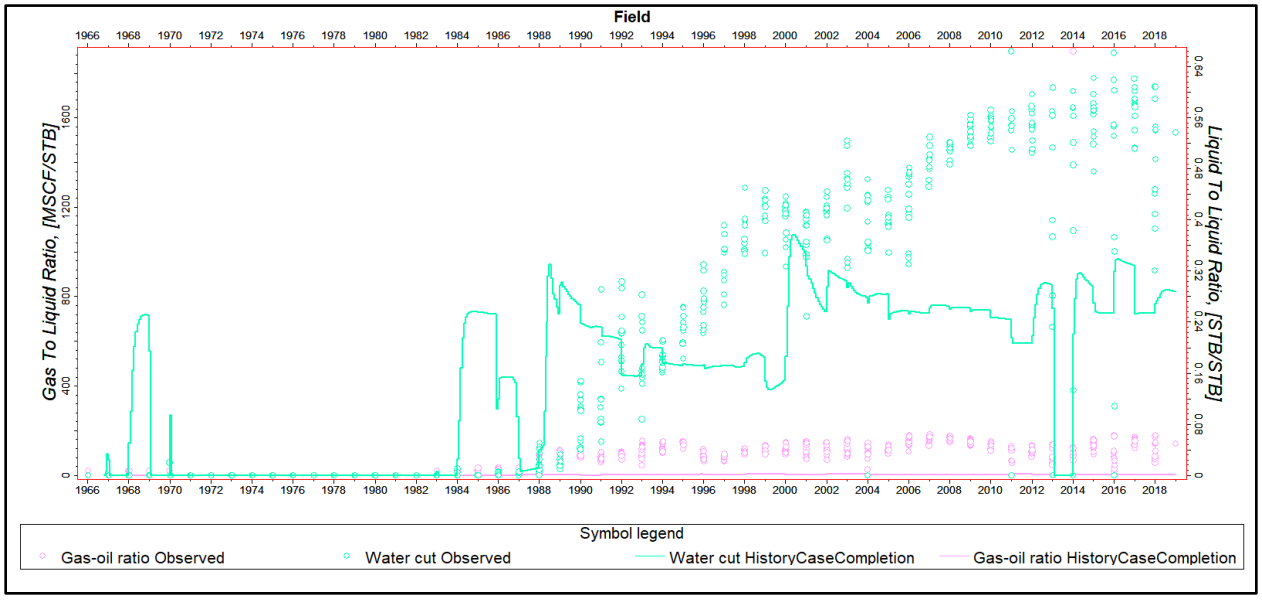

Figure 4.8: Gas oil ratio and water cut in the history case with well completion vs observed data for the study field

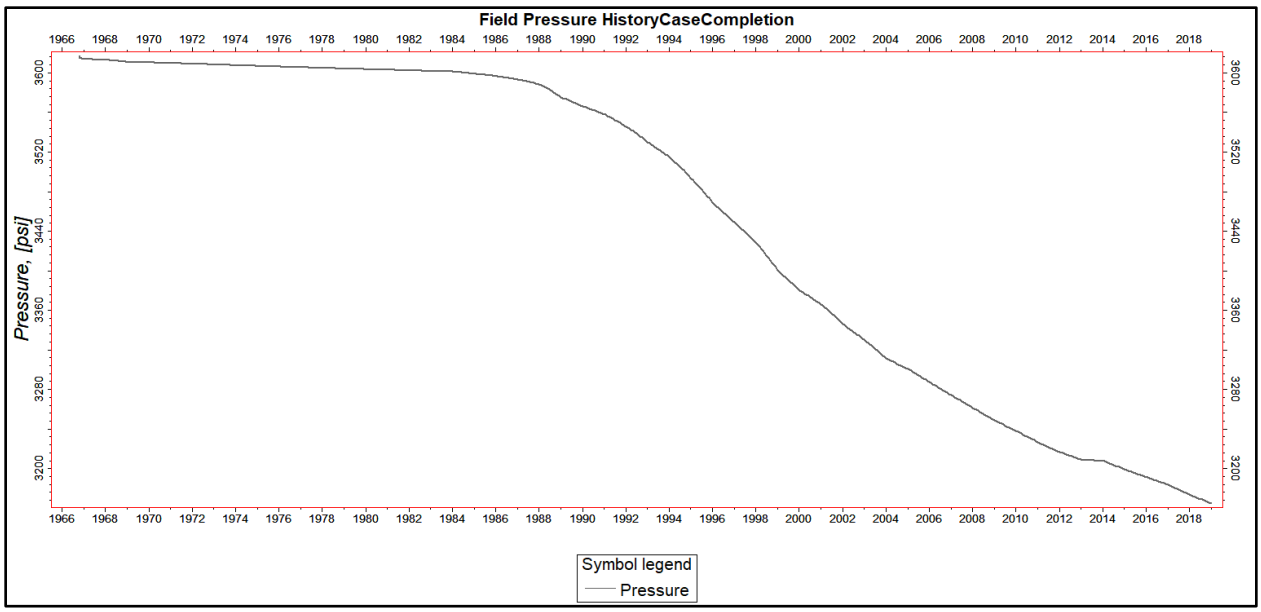

Figure 4.9: Pressure in the history case with well completion vs date for the study field

Upon closer observation, the oil production demonstrates an even more pronounced alignment with the historical data trend, indicating a high level of accuracy in prediction. In contrast, gas production exhibits improvement as it shows a decline compared to the open hole concept. However, due to the presence of missing data, there is limited visibility regarding noticeable changes in water production. Lastly, the pressure data provides a more realistic representation of pressure drop, suggesting a reliable simulation outcome.

4.1.4 History Matching and Prediction with Depletion Strategy

Utilizing the predictive depletion strategy, we have designated a prediction period extending from January 1, 2019, to January 1, 2020. Within this timeframe, a group rate production control has been implemented for the field, specifying an oil rate production target of 3500 STB/d. Additionally, constraints have been imposed on water and gas rate production, limiting them to 1250 STB/d and 10500 MSCF/d, respectively. These production target and limits are derived from the average rates observed in the preceding years, the following (Figures 4.10 & 4.11) will show the results of the one-year prediction with history match.

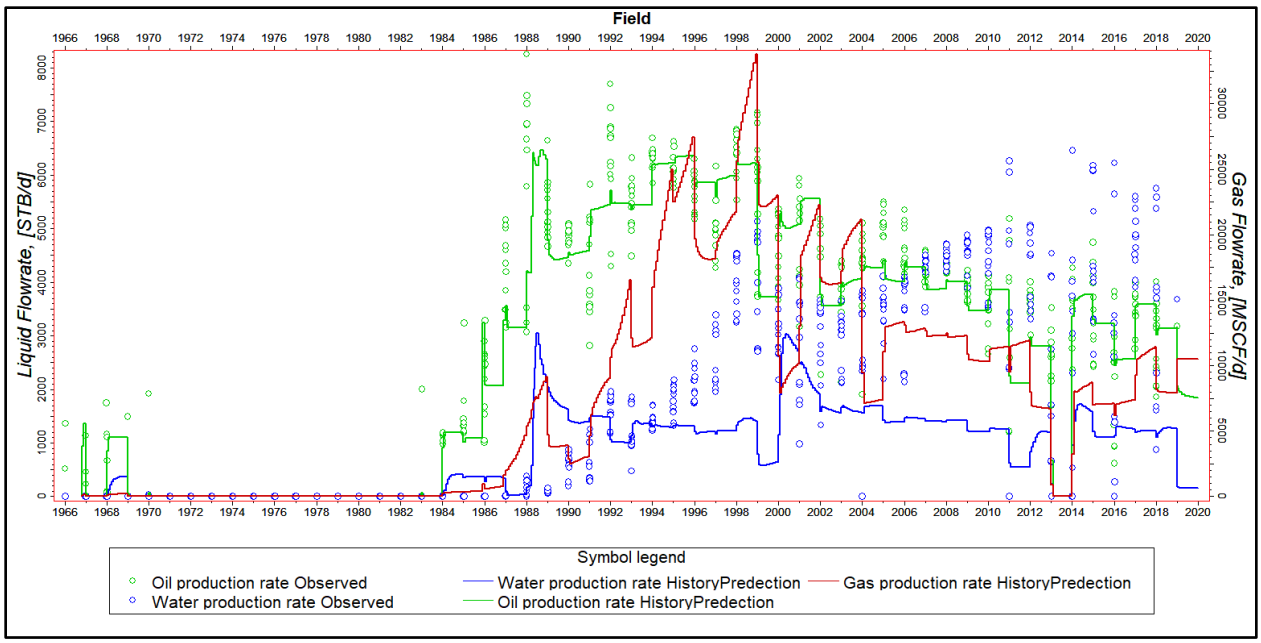

Figure 4.10: History case with Prediction vs observed data for the study field

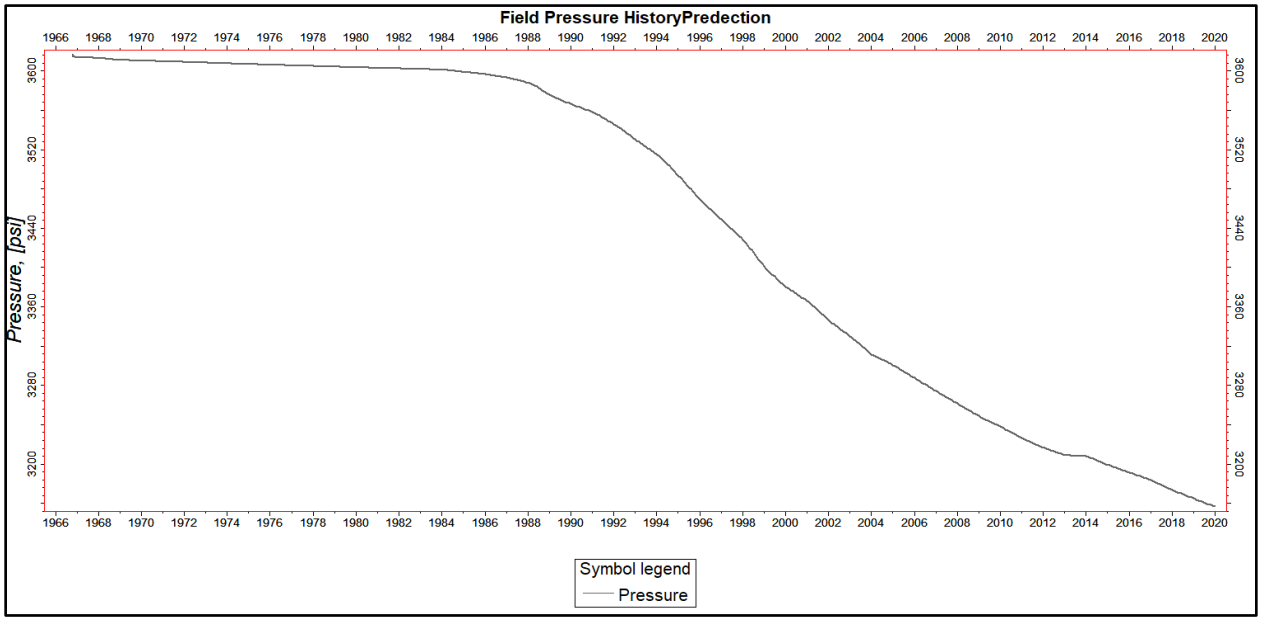

Figure 4.11: Pressure in the history case with Prediction vs date for the study field

The final year of predictions reveals a consistent downward trend in oil, gas, and water production, indicating that the field still has a significant production potential. This observation suggests that there is sufficient remaining reservoir life. However, to gain a more comprehensive understanding of the model's performance, a longer prediction period would be beneficial. Extending the

prediction horizon would provide greater insights into the model's accuracy and its ability to capture long-term production patterns.

4.2 Machine Learning Results

4.2.1 Dynamic Time Warping (DTW) Results

After conducting the DTW it will produce pathing data, this pathing data are the indices of the data points with respect to the reference well. These indices were used to rearrange the test well data. After rearranging there would be some gaps or missing data in case the length of the test well data is smaller than the reference well. A visual representation in (Figures 4.12 - 4.17) will showcase the oil production trends for each well both before and after the application of DTW.

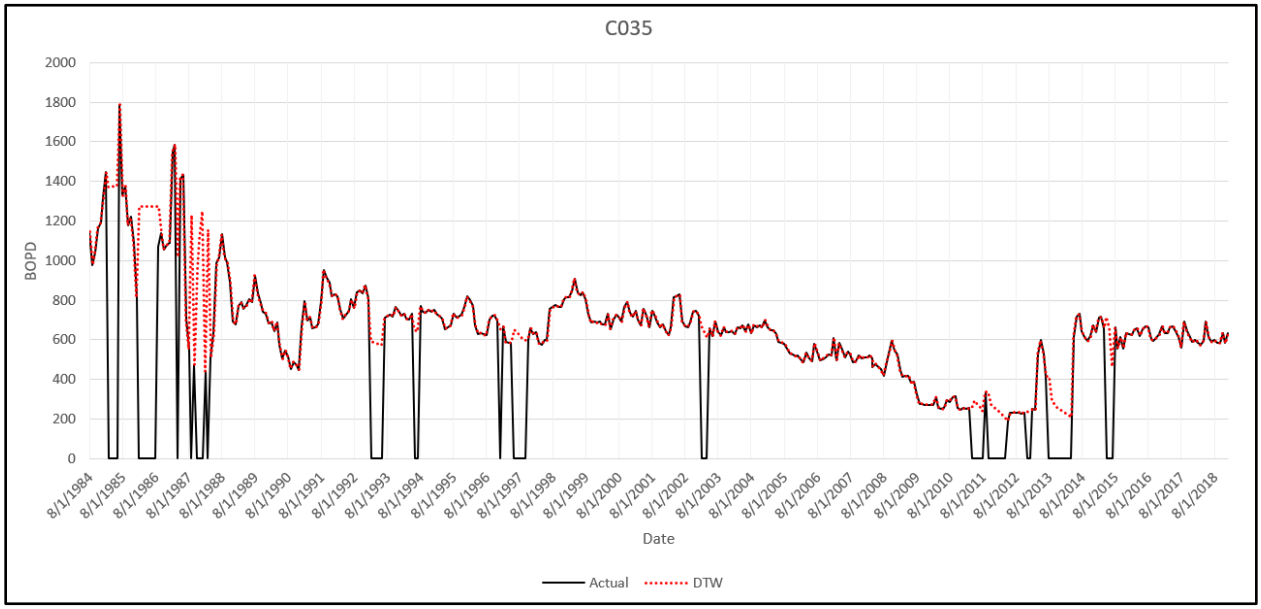

Figure 4.12: Oil production before and after DTW for well C035

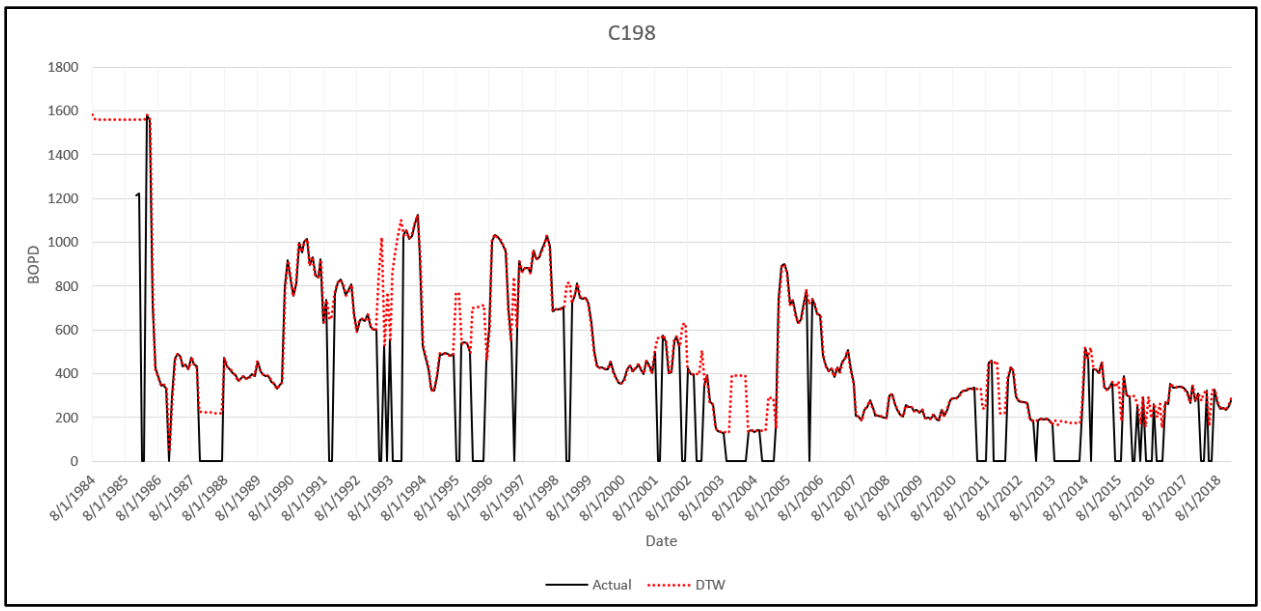

Figure 4.13: Oil production before and after DTW for well C198

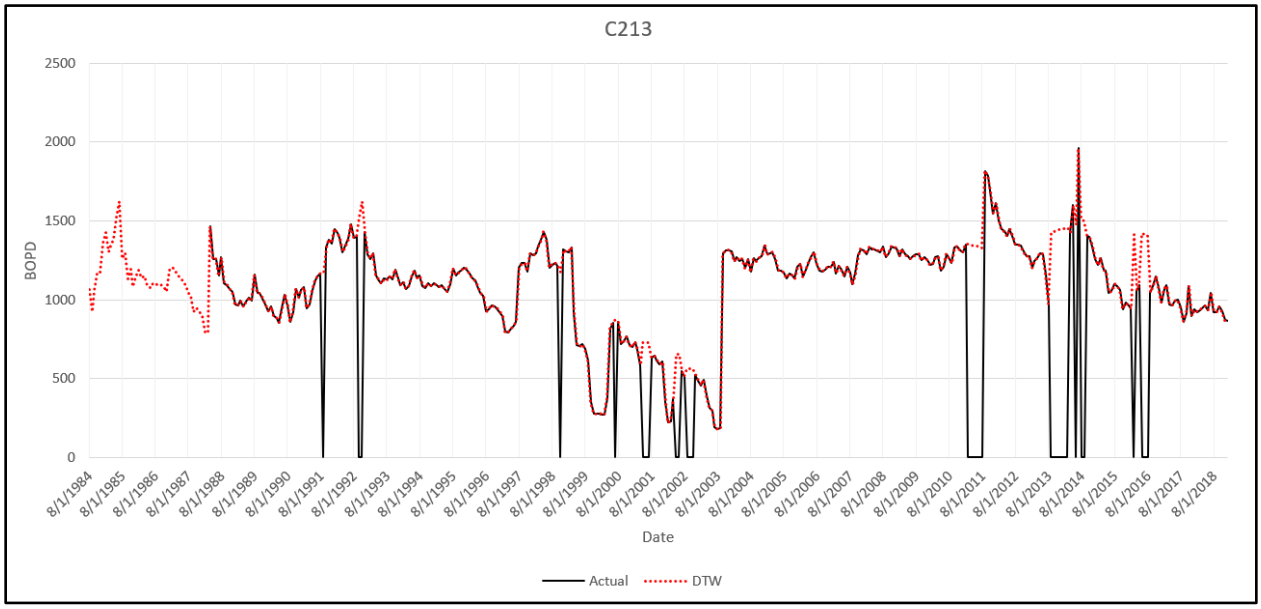

Figure 4.14: Oil production before and after DTW for well C213

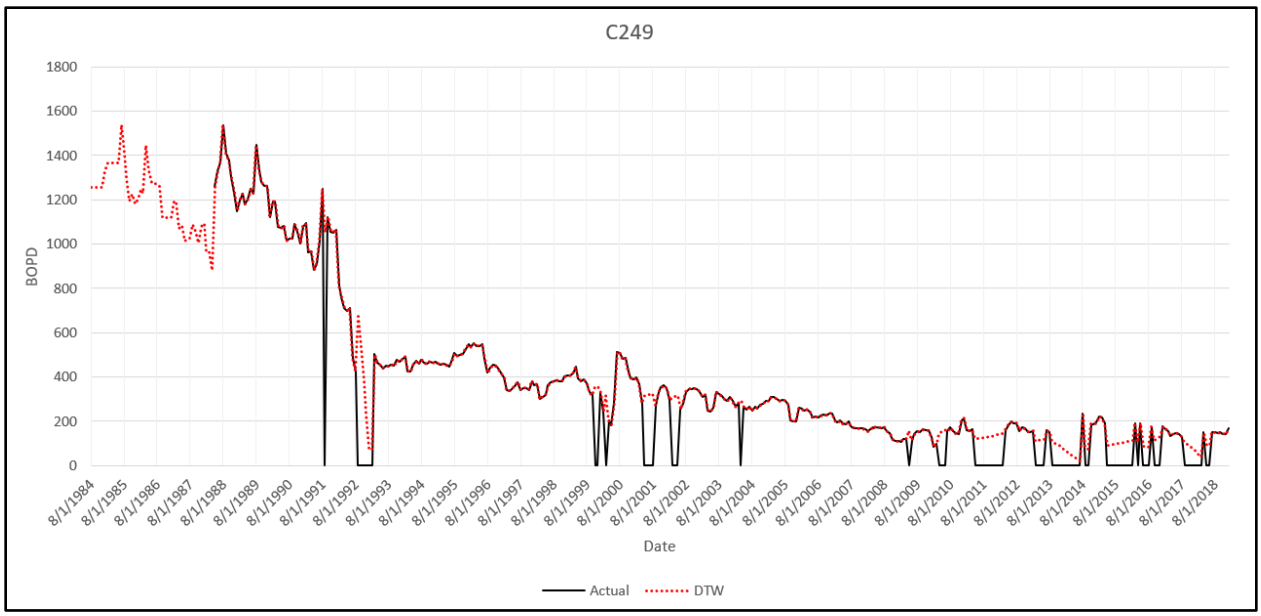

Figure 4.15: Oil production before and after DTW for well C249

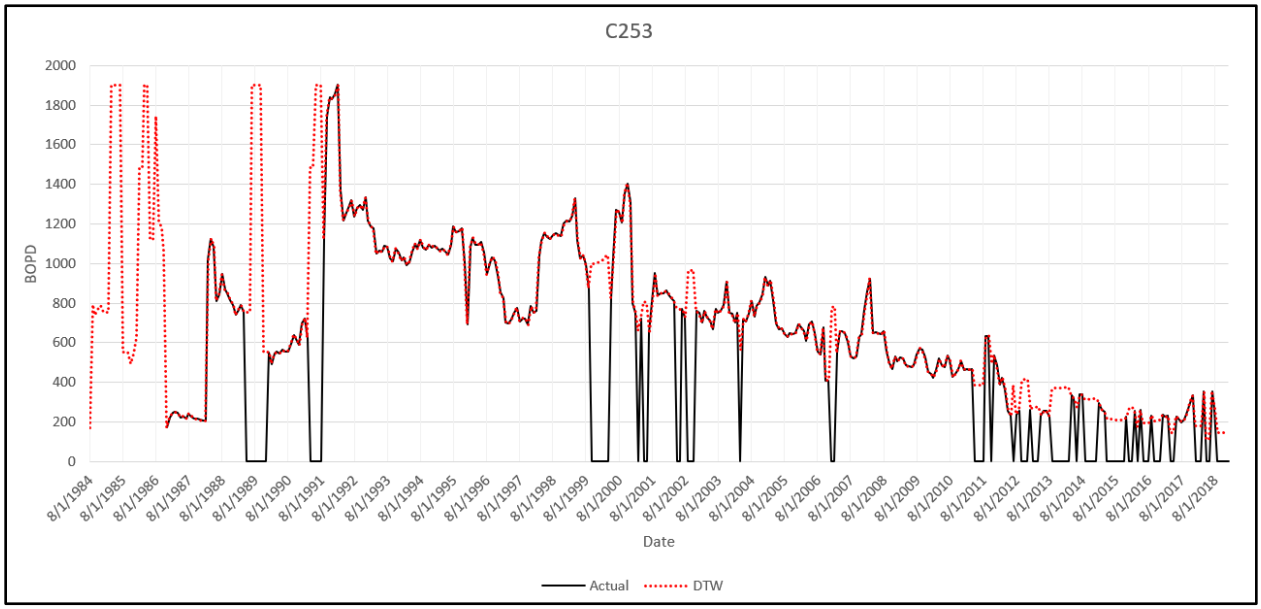

Figure 4.16: Oil production before and after DTW for well C253

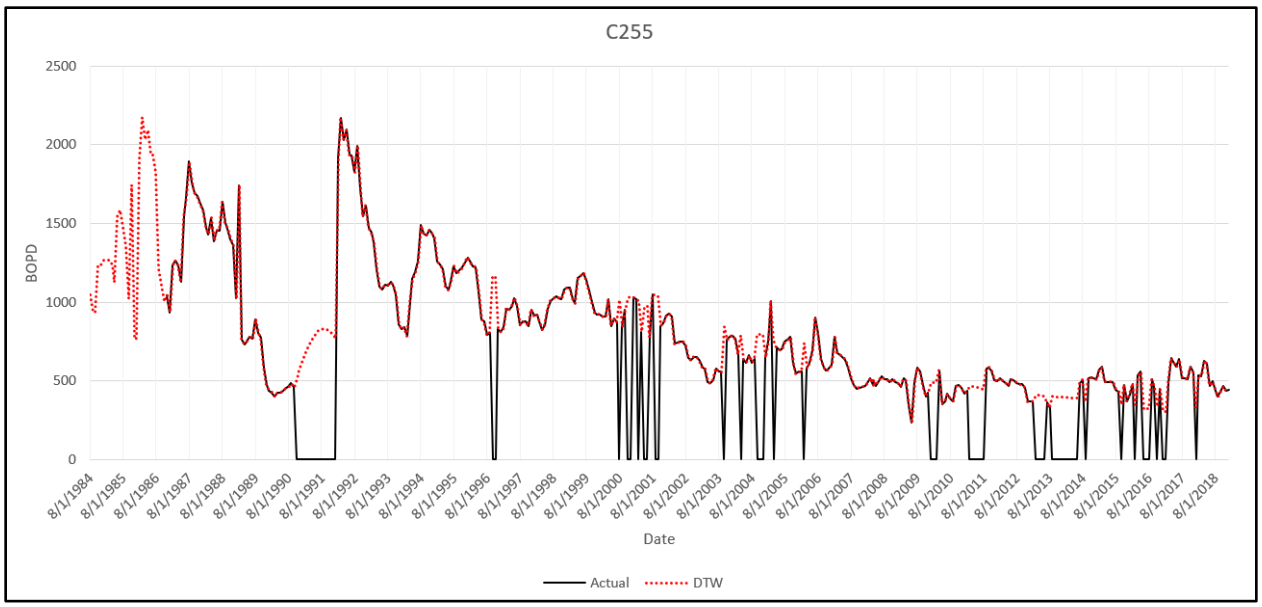

Figure 4.17: Oil production before and after DTW for well C255

The figures clearly exhibit a remarkable alignment and stretch of the data, highlighting the effectiveness of Dynamic Time Warping (DTW) as one of the most suitable methods for filling in missing data. By leveraging DTW, the prediction capabilities of the LSTM model can be significantly enhanced, leading to improved accuracy and reliability.

4.2.2 Long Short-Term Memory (LSTM) Results

The Long Short-Term Memory (LSTM) results offer valuable insights into the model's capacity to capture and comprehend temporal dependencies within sequential data. The results showcase the model's proficiency in learning and retaining information over extended periods, contributing to enhanced prediction accuracy. The discussion involves an exploration of the impact of hyperparameters, such as the number of LSTM layers, hidden units, and sequence lengths, on the model's performance. After applying DTW and filling up the gaps in the data, the (Figures 4.18 - 4.23) below we will display the LSTM results for all the wells.

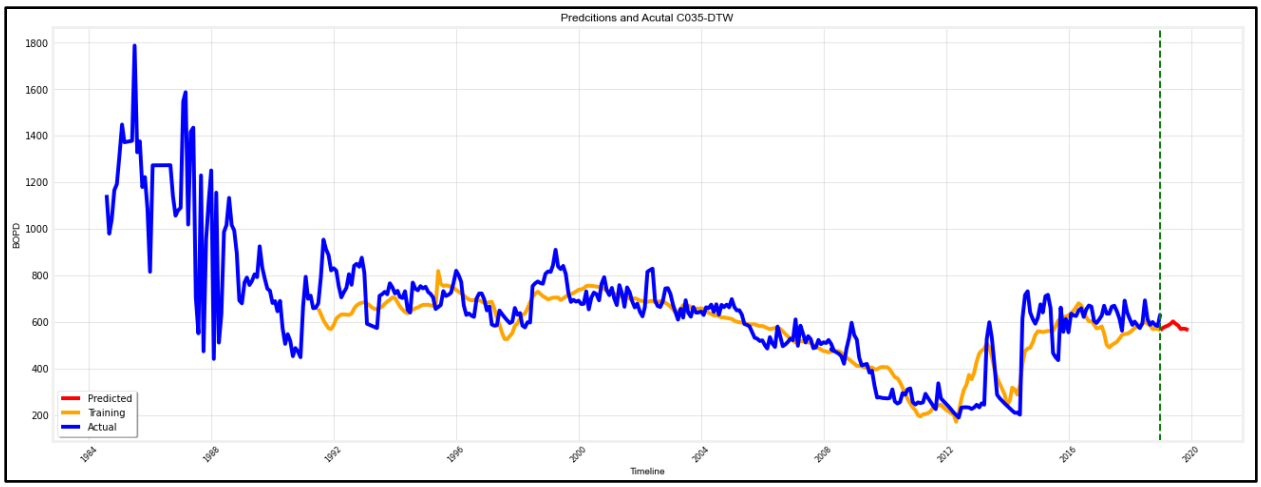

Figure 4.18: LSTM result for well C035 after DTW

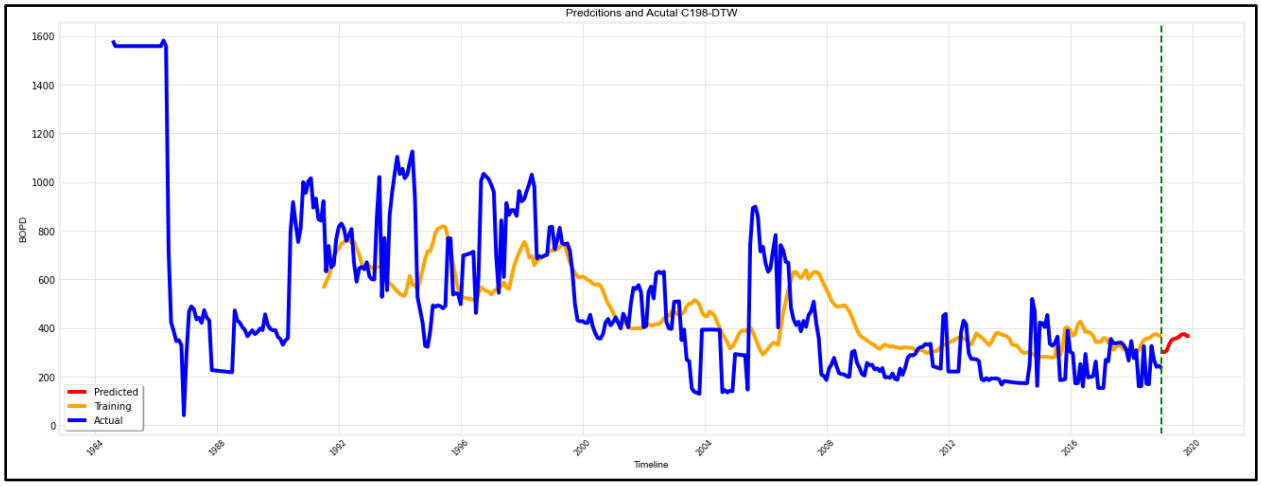

Figure 4.19: LSTM result for well C198 after DTW

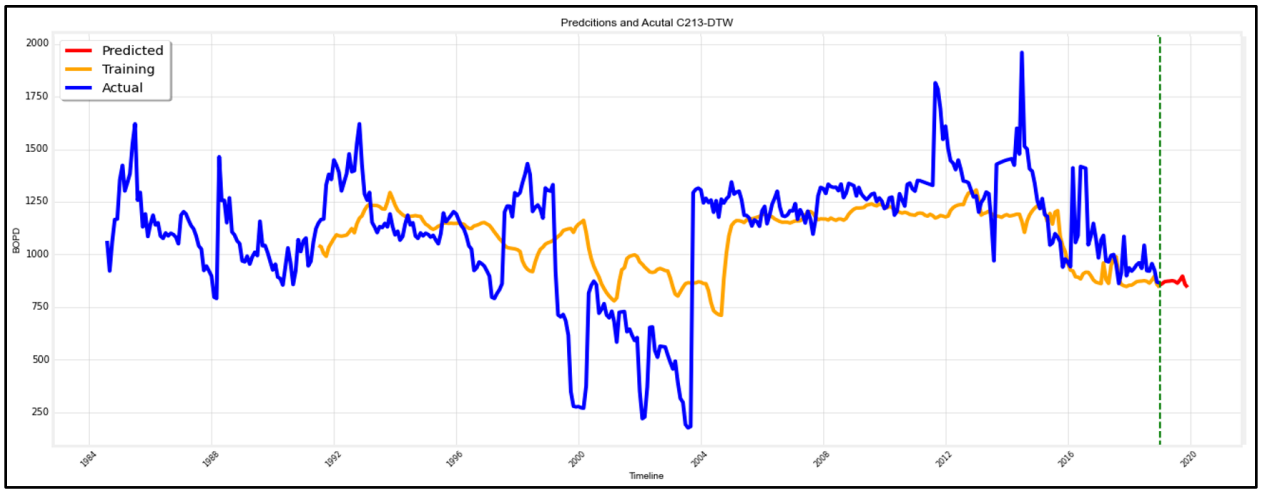

Figure 4.20: LSTM result for well C213 after DTW

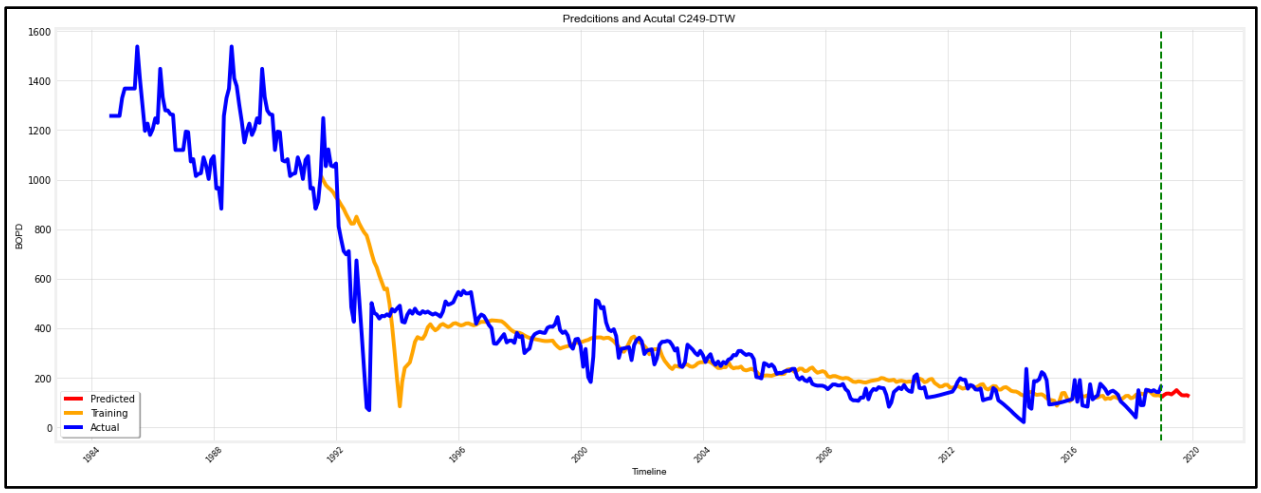

Figure 4.21: LSTM result for well C249 after DTW

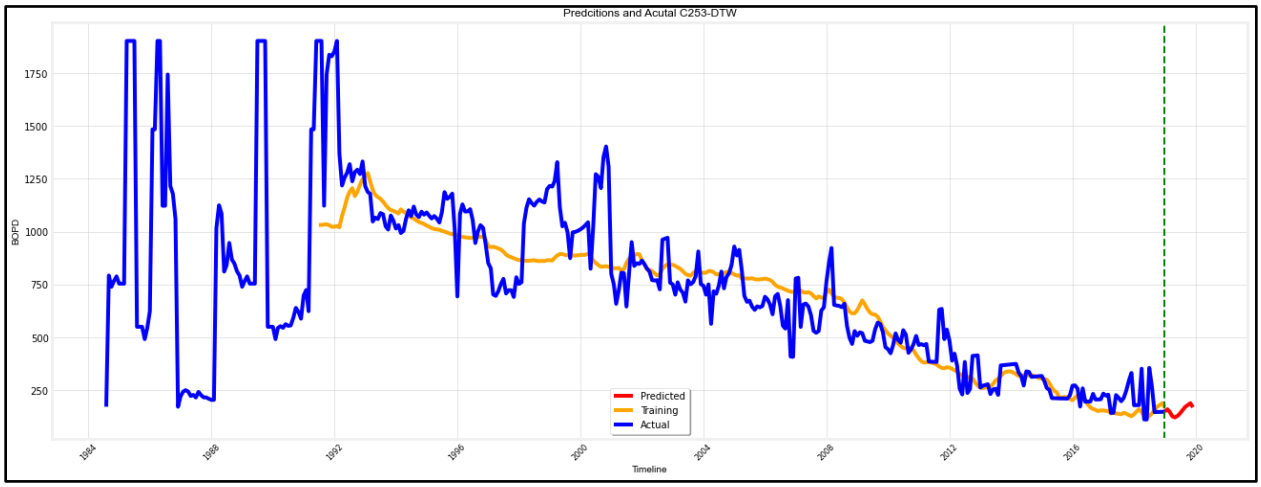

Figure 4.22: LSTM result for well C253 after DTW

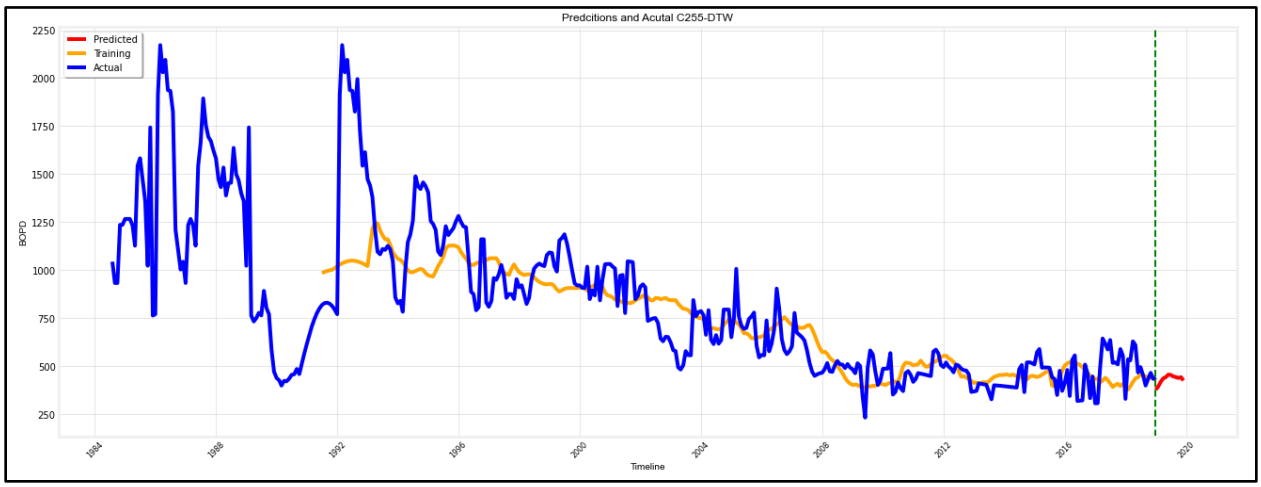

Figure 4.23: LSTM result for well C255 after DTW

Overall, the results of the code appear promising, demonstrating accurate predictions in many instances. However, upon closer examination, it becomes apparent that certain wells exhibit a discernible lag pattern in the predicted training data like in (Figure 4.21). Additionally, in some cases, there is a noticeable shift in the predictions for the last 12 months in (Figure 4.19). Several factors could contribute to these observations. One potential reason for the observed lag pattern and shift is the training methodology employed. The model is trained using a sliding window approach, where 32 months of historical data are utilized to predict the subsequent 12 months. This approach inherently introduces a lag between the input data and the corresponding predictions. Consequently, the model might struggle to capture short-term fluctuations or react promptly to sudden changes in the data. Another factor that could influence the predictions is the size of the dataset. If the available data is limited, it might not encapsulate the full range of variability and complexity present in the underlying phenomenon. As a result, the model may struggle to generalize accurately to unseen data or exhibit limitations in capturing certain patterns or trends.
However, it is crucial to note that the chosen training model serves a specific purpose, explicitly to demonstrate that even with a relatively small training dataset, it is still possible to obtain reasonably accurate predictions. Despite the potential limitations mentioned above, the model manages to produce favorable results, showcasing its ability to extract meaningful information from a limited amount of training data.

4.2.3 Average Dynamic Time Warping Result

This model is formulated by computing the average production rates of all wells post Dynamic Time Warping (DTW). Subsequently, the model is trained using Long Short-Term Memory (LSTM) as shown in (Figure 4.24), and upon completion of training, the model is frozen for deployment within our transfer learning framework.

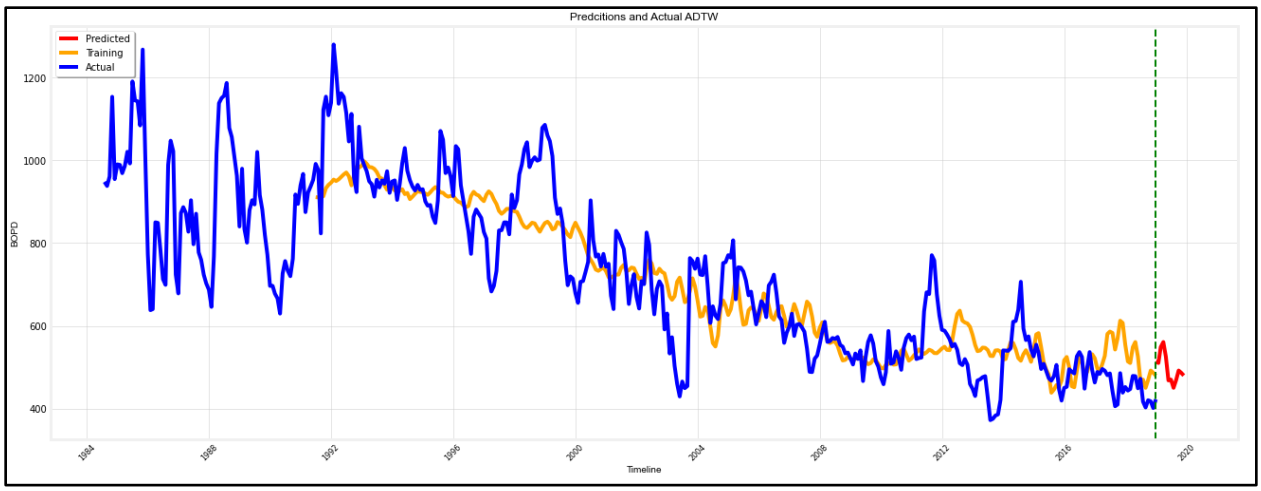

Figure 4.24: LSTM result for average dynamic warping

4.2.4 Transfer Learning Results

Transfer learning involves taking knowledge learned from one task (in this case, the averaged well production rates) and applying it to a related but different task. By utilizing the frozen LSTM model as a starting point, subsequent models can benefit from the previously learned patterns and insights, effectively leveraging the collective knowledge of the wells. The models selected for transfer learning involve well data post Dynamic Time Warping (DTW), aiming to assess whether this approach enhances the results or induces significant changes in the model outcomes (Figures 4.25 - 4.30).

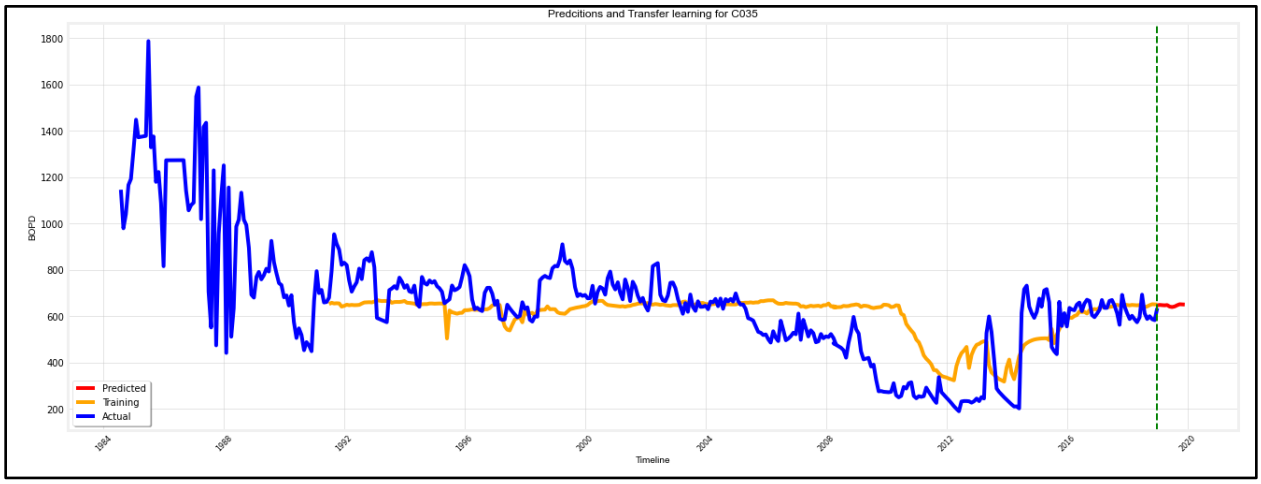

Figure 4.25: Transfer learning result for well C035

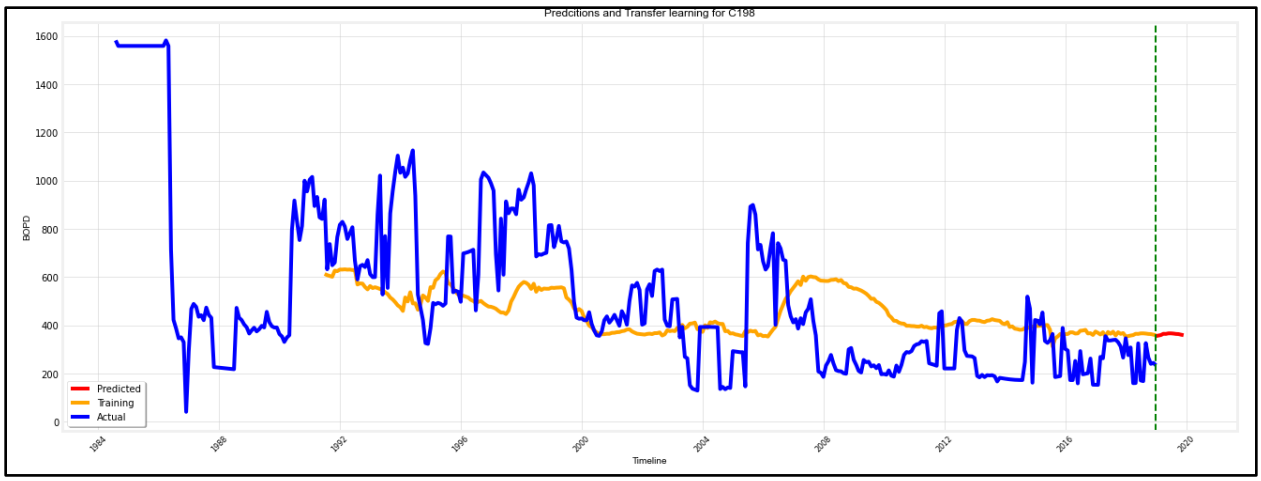

Figure 4.26: Transfer learning result for well C198

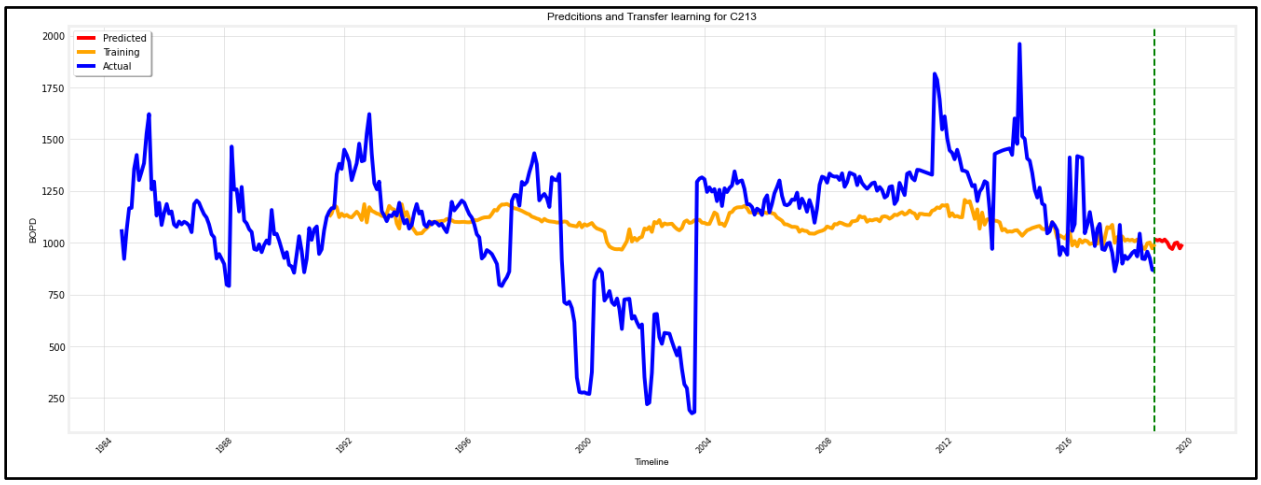

Figure 4.27: Transfer learning result for well C213

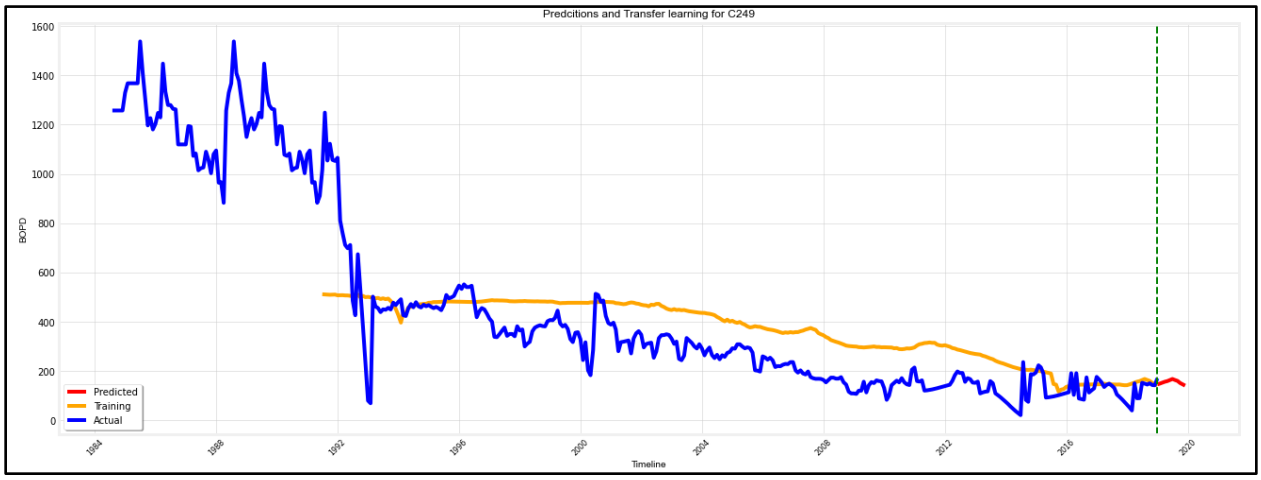

Figure 4.28: Transfer learning result for well C249

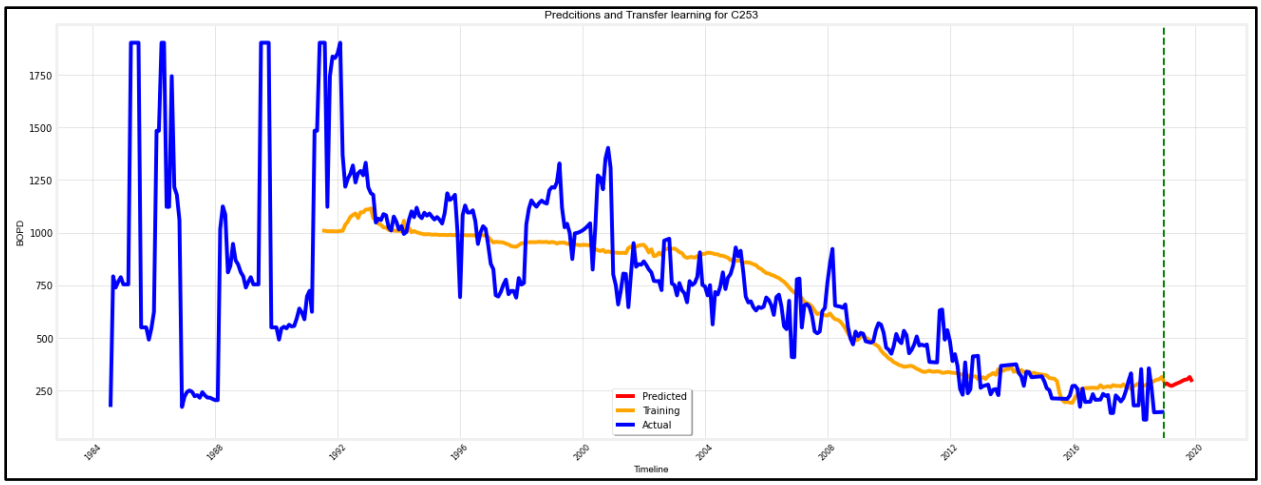

Figure 4.29: Transfer learning result for well C253

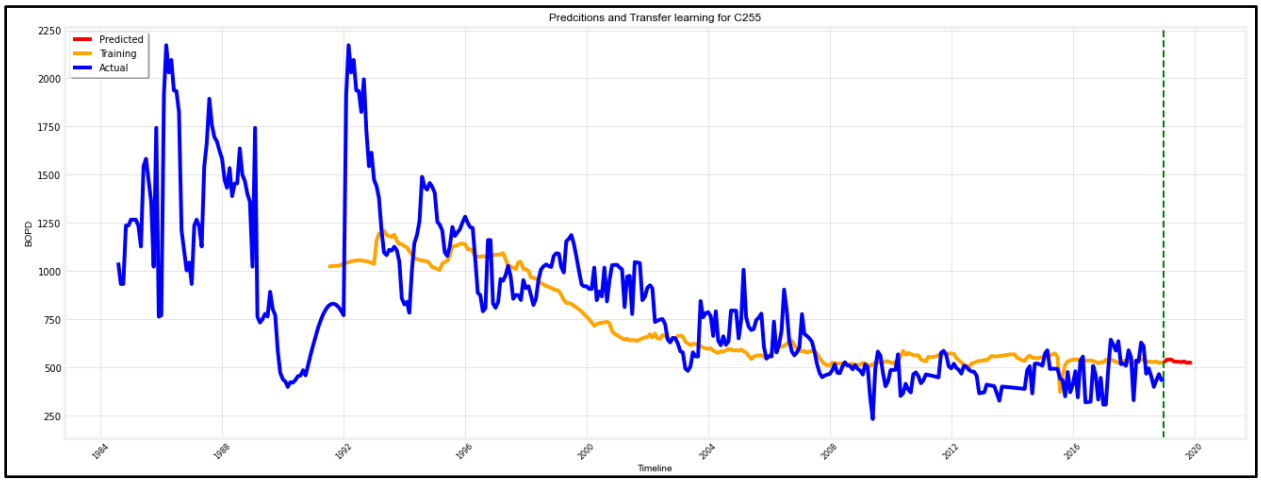

Figure 4.30: Transfer learning result for well C255

Despite efforts to improve the results, there appears to be a limited enhancement observed. However, the predictions exhibit reduced fluctuations and a more stable pattern. As a result, the model still holds potential to provide reliable predictions for various scenarios, such as new wells or wells with limited available data. While further improvements may be desirable, the current model demonstrates its ability to generate decent predictions under these circumstances.

4.3 Final Results Comparison

In this section, a thorough comparison of the final results will be presented through a single chart. The chart will include multiple data sets, allowing for a complete assessment. Specifically, it will showcase the actual well data both before and after applying Dynamic Time Warping (DTW), the

LSTM training data, the history matching data derived from the simulated Petrel model, and, finally, the training data obtained from transfer learning across all wells (Figures 4.31 - 4.36). This visual representation will enable a clear evaluation of the performance and alignment of the different data sets. It will make it easier to identify any disparities or similarities among the various sources. This comparison will also provide insights into the effectiveness of the different approaches and their ability to capture the underlying patterns and dynamics of the predicted data. Additionally, alongside the chart, the root mean square deviation (RMSD) error will be calculated for each individual well (Table 4.1). This metric serves as a quantitative measure of the accuracy of the predictions. By evaluating the RMSD error, it becomes possible to gauge the level of agreement between the predicted values and the actual observed values for each well. Overall, through this comprehensive comparison and the calculation of the RMSD error, a thorough assessment of the model's performance can be obtained, shedding light on its predictive capabilities and highlighting any areas for further improvement or refinement.

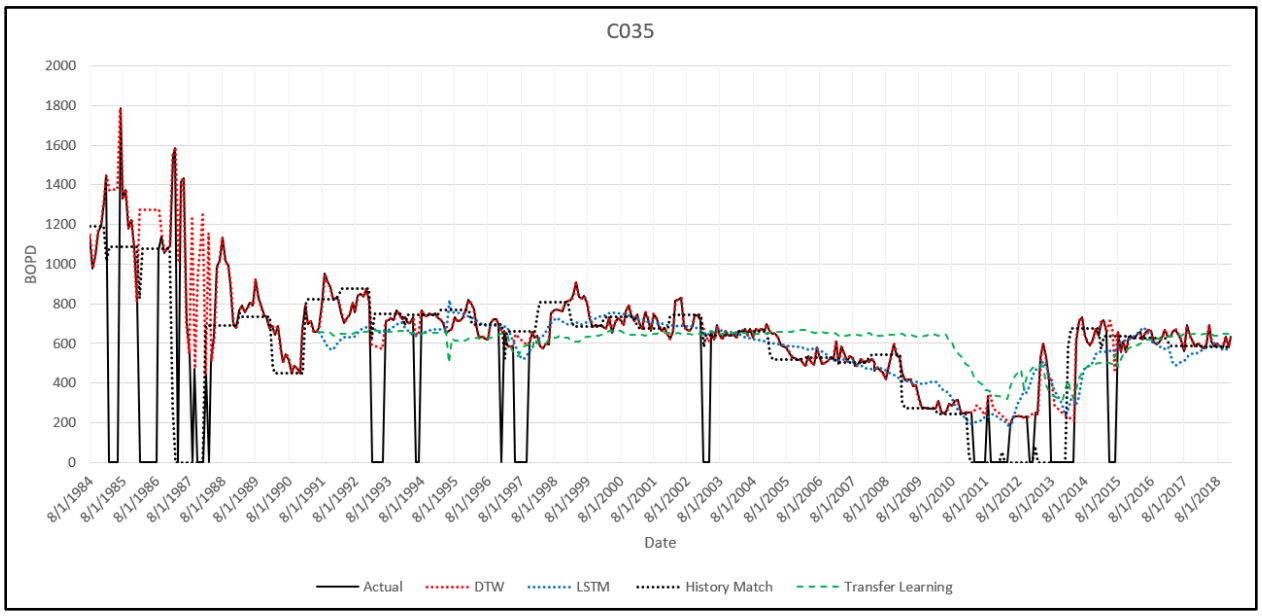

Figure 4.31: Actual oil production data and DTW along with different prediction scenarios for well C035

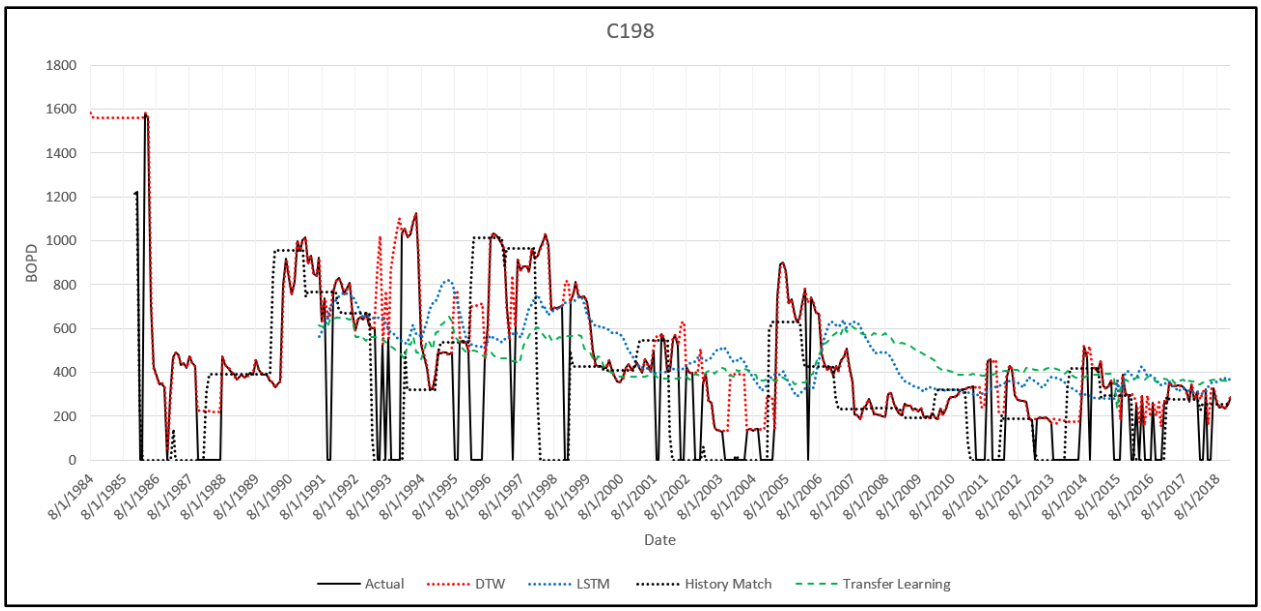

Figure 4.32: Actual oil production data and DTW along with different prediction scenarios for well C198

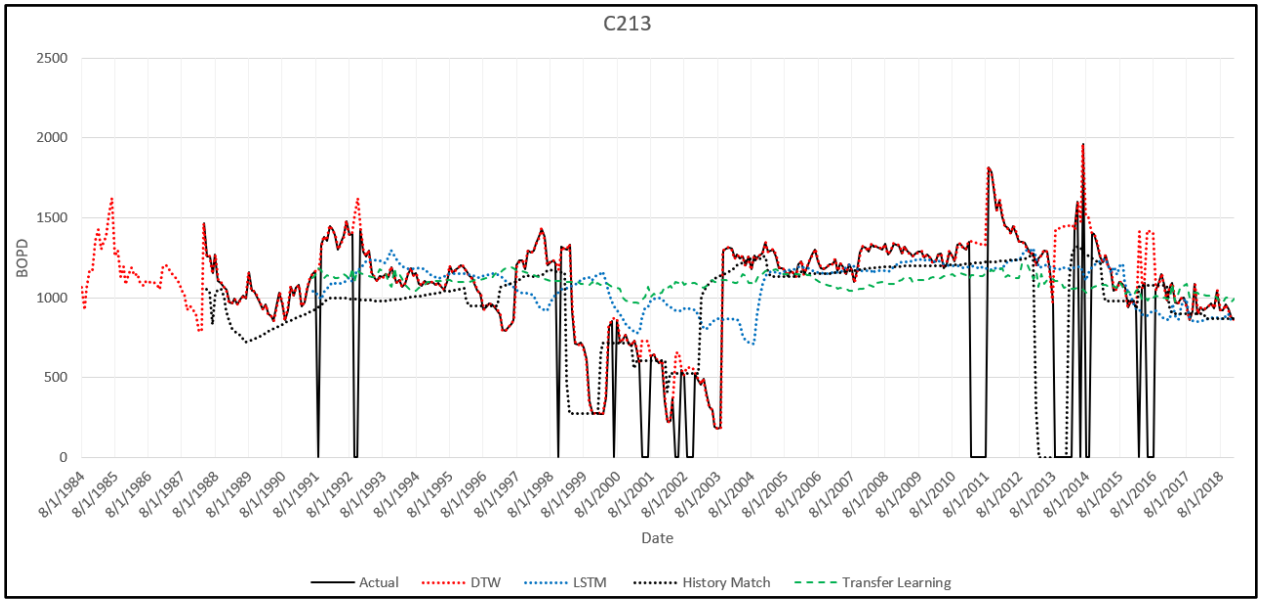

Figure 4.33: Actual oil production data and DTW along with different prediction scenarios for well C213

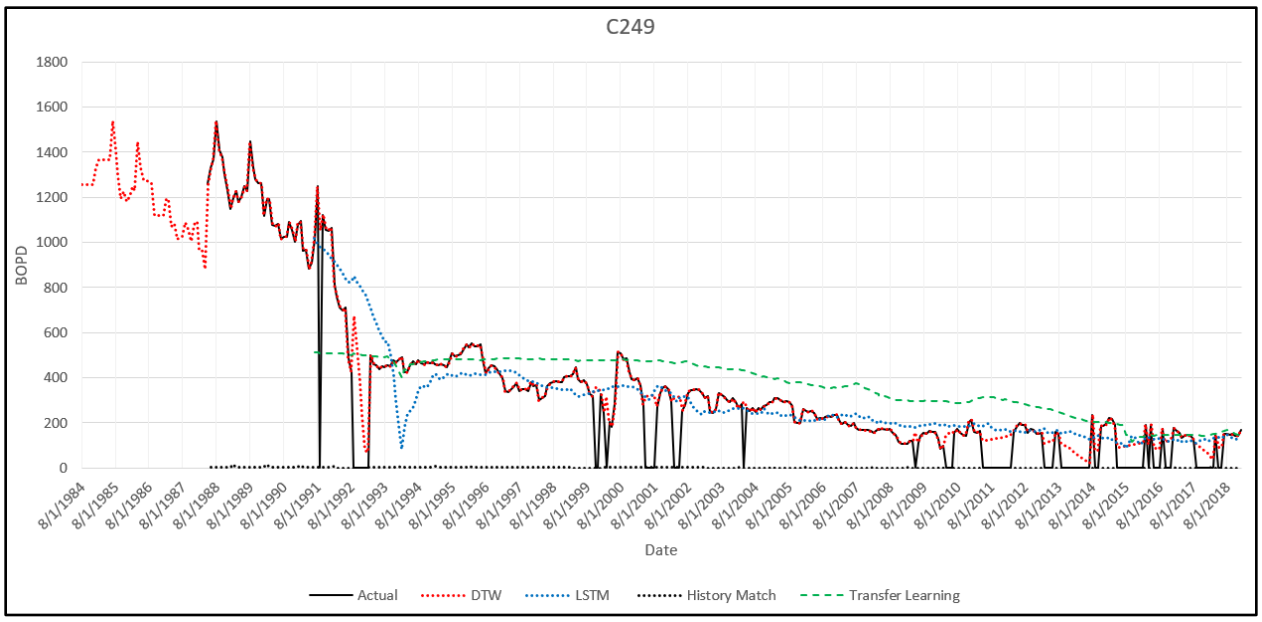

Figure 4.34: Actual oil production data and DTW along with different prediction scenarios for well C249

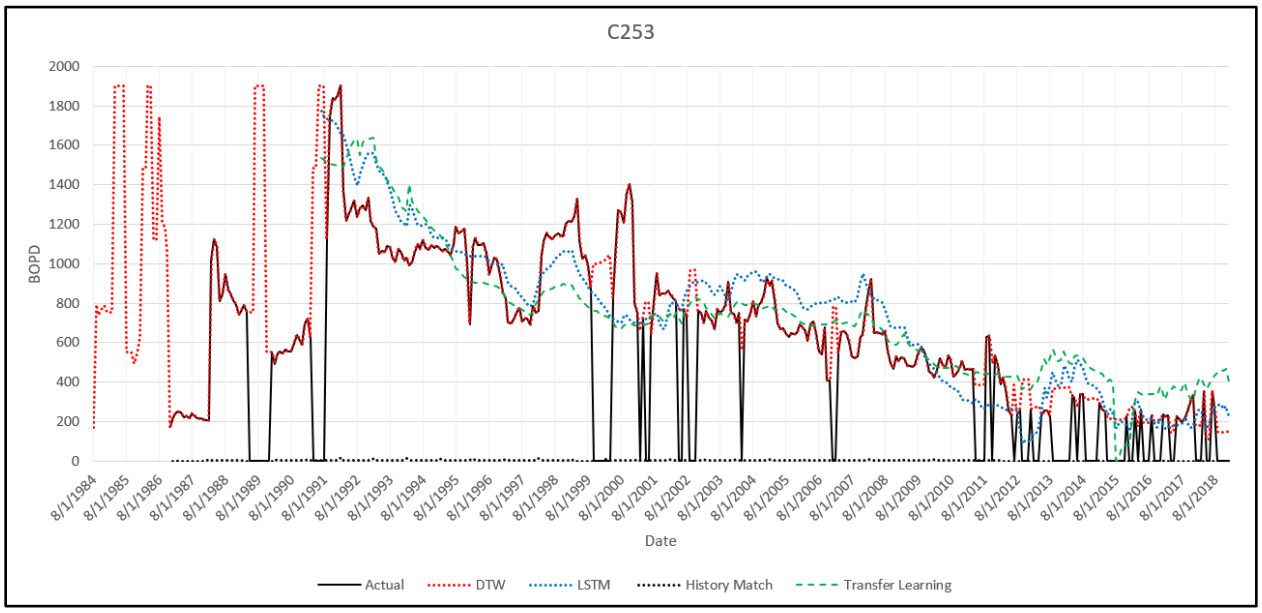

Figure 4.35: Actual oil production data and DTW along with different prediction scenarios for well C253

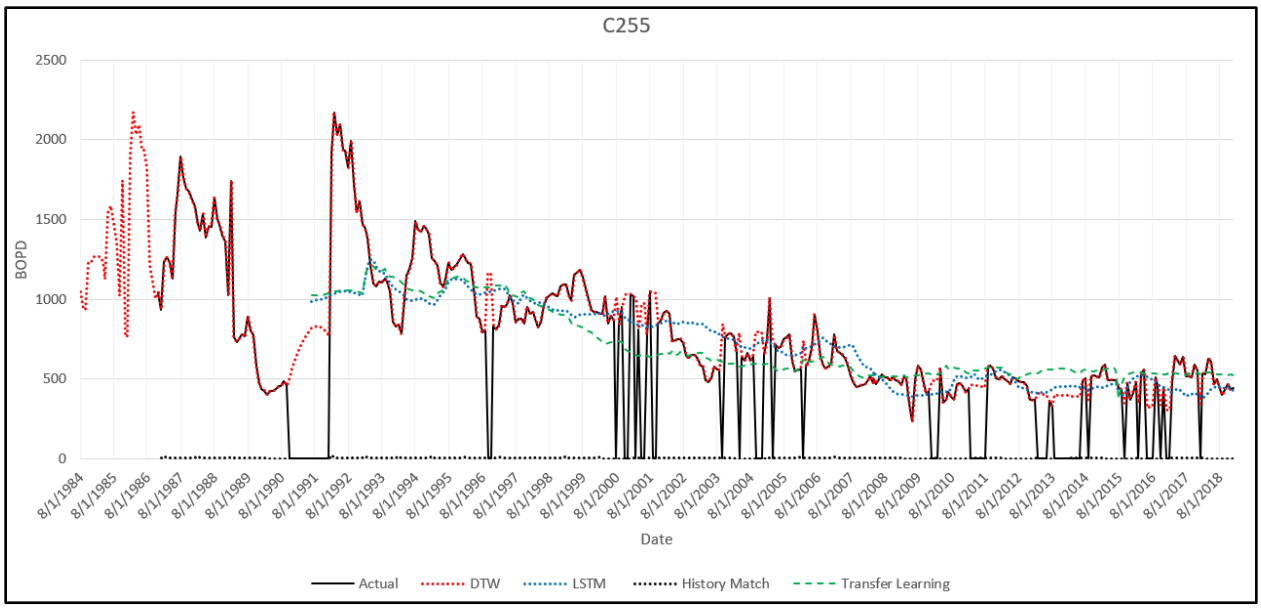

Figure 4.36: Actual oil production data and DTW along with different prediction scenarios for well C255

Table 4.1: RSMD results for all wells between different prediction scenarios

Well	RSMD in between		
	Actual & History matching	**DTW & LSTM**	**DTW & Transfer learning**
C006	212.84	85.19	123.09
C035	299.42	90.18	139.12
C198	322.1	207.37	302.58
C213	394.73	274.28	294.59
C236	324.24	242.45	268.53
C249	487.35	105.5	153.56
C253	726.36	179.89	197.89
C255	833.22	210.61	224.77

Upon analyzing the charts and root mean square deviation error (RSMD), it becomes evident that the LSTM model outperforms the history matching approach, exhibiting lower error rates. However, in the case of transfer learning, there is no significant improvement observed. Nevertheless, the transfer learning predictions still demonstrate decent accuracy. Notably, the last three wells in the history matching results display remarkably low production rates between (0-30) bbl/day and high error values. This outcome can be attributed to the inherent complexity of reservoir simulation, as well history matching tends to focus more on field prediction rather than individual wells. The simulation process relies on numerous inputs and necessitates precise interpretation, making it prone to potential errors and uncertainties. Additionally, reservoir simulation is not only time-consuming but also resource intensive.

5. Conclusion and Future Work

5.1 Conclusion

In this thesis, we have conducted a comprehensive investigation into the application of reservoir simulation and machine learning techniques for enhanced reservoir characterization and production forecasting in the Sarir C-Main field. Outlined below are the key findings and conclusions drawn from this research:

- The study focused on the Sarir C-Main field and utilized various data sources such as seismic cubes, well logs, base maps, check shot data, and production history.
- The methodology involved the development of static and dynamic models, including processes like quality control, log interpretation, seismic interpretation, fault interpretation, gridding, property and petrophysical modeling.
- Well completion, fluid model definition, and rock physics functions were established to capture reservoir behavior accurately.
- History matching and prediction were performed using simulation cases, and machine learning techniques such as dynamic time warping (DTW), long short-term memory (LSTM), and transfer learning were applied.
- The results obtained from the Petrel simulation clearly demonstrate the effectiveness of history matching in reservoir behavior prediction. Furthermore, the incorporation of completion techniques has shown even more improvements in capturing and understanding reservoir behavior.
- DTW exhibit a remarkable alignment and stretch of the data, highlighting the effectiveness of it as one of the most suitable methods for filling in missing data.
- Machine learning techniques, particularly the implementation of LSTM models, have demonstrated exceptionally better results in predicting oil production. These results have surpassed the traditional approach of history matching.
- Transfer learning demonstrates a limited enhancement compared to the LSTM, yet the predictions show reduced fluctuations, increased stability, and potential for reliable predictions in scenarios involving new wells or limited available data.

- The history matching prediction had an average RMSD of 450.03, while the LSTM approach achieved an average of 174.43 and the transfer learning approach averaged 213.01.
- Machine learning approaches provide prominent advantages by significantly reducing the time required for analysis and enabling reliable predictions even when confronted with limited data. Leveraging the power of machine learning facilitates the efficient attainment of accurate predictions, presenting a streamlined and practical alternative to conventional reservoir simulation methods.
- History matching has certain limitations, notably its primary emphasis on field-level predictions while often neglecting individual well analysis. Moreover, history matching is not only time-consuming but also resource-intensive, potentially overlooking crucial details that can impact accurate predictions.
- While LSTM model demonstrates promising results overall, it is important to consider these limitations, including the lag pattern, shift in predictions, training methodology, and dataset size, which impacted the accuracy and responsiveness of the predictions.

5.2 Future Work

To further enhance the accuracy of predictions and address the observed lag and shift, several strategies can be explored. Firstly, alternative training methodologies such as Autoregressive Integrated Moving Average (ARIMA), Prophet, and Gaussian Processes (GP) could be experimented with. Additionally, adjusting the sliding window size, overlapping windows, or implementing a recursive forecasting approach may mitigate the lag pattern and align predictions more closely with actual values. Furthermore, incorporating additional features or engineered variables through the addition of more layers could improve the model's ability to capture complex relationships and enhance prediction accuracy. Modifying the number of LSTM units, adjusting the dropout rate, or exploring different activation functions may also boost the model's performance and address the identified issues. Finally, it is recommended to continuously monitor the model's performance and evaluate its generalizability on unseen data. Employing robust validation techniques such as cross-validation and regularly updating the model with new data can ensure its reliability and effectiveness over time.

6. References

Abadi, A., Van Wees, J., Dijk, P. M., & Cloetingh, S. (2008). Tectonics and subsidence evolution of the Sirt Basin, Libya. *Aapg Bulletin - AAPG BULL*, *92*, 993–1027. https://doi.org/10.1306/03310806070

Cao, J., & Roy, B. (2017). Time-lapse reservoir property change estimation from seismic using machine learning. *The Leading Edge*, *36*(3), 234–238.

Cao, Q., Banerjee, R., Gupta, S., Li, J., Zhou, W., & Jeyachandra, B. (2016). Data driven production forecasting using machine learning. *SPE Argentina Exploration and Production of Unconventional Resources Symposium*, D021S006R001.

Desbordes, J. K., Zhang, K., Xue, X., Ma, X., Luo, Q., Huang, Z., Hai, S., & Jun, Y. (2022). Dynamic production optimization based on transfer learning algorithms. *Journal of Petroleum Science and Engineering*, *208*, 109278.

Dong, Y., Zhang, Y., Liu, F., & Cheng, X. (2021). Reservoir production prediction model based on a stacked LSTM network and transfer learning. *ACS Omega*, *6*(50), 34700–34711.

Foroud, T., Seifi, A., & AminShahidi, B. (2014). Assisted history matching using artificial neural network based global optimization method–Applications to Brugge field and a fractured Iranian reservoir. *Journal of Petroleum Science and Engineering*, *123*, 46–61.

Han, D., & Kwon, S. (2021). Application of machine learning method of data-driven deep learning model to predict well production rate in the shale gas reservoirs. *Energies*, *14*(12), 3629.

Harris, D. G. (1975). The Role of Geology in Reservoir Simulation Studies. *Journal of Petroleum Technology*, *27*(05), 625–632. https://doi.org/10.2118/5022-PA

Heinemann oil technology and engineering (HOT). (1993). *Sarir C-main reservoir geological study*.

Hernandez-Mejia, J. L., Pisel, J., Jo, H., & Pyrcz, M. J. (2023). Dynamic time warping for well injection and production history connectivity characterization. *Computational Geosciences*, *27*(1), 159–178.

Hochreiter, S., & Schmidhuber, J. (1997). Long short-term memory. *Neural Computation*, *9*(8), 1735–1780.

Hossain, M. E. (2010). The Real Challenges in Reservoir Simulation. *2nd Saudi Meeting on Oil and Natural Gas Exploration and Production Technologies (OGEP 2010)*, 18–20.

Hossain, M. E., & Islam, M. R. (2010). Knowledge – Based Reservoir Simulation – A Novel Approach. *International Journal of Engineering*, *3*(6), 622–638.

Hossain, M. E., Mousavizadegan, S. H., & Islam, M. R. (2009). The mystery and uncertainty cloud during reservoir simulation in petroleum industry. *Advances in Sustainable Petroleum Engineering Science*, *2*(3), 283–300.

Islam, M. R., Mousavizadegan, H., Mustafiz, S., & Belhaj, H. (2008). A Handbook of Knowledge-Based Reservoir Simulation. *Houston, TX: Gulf Publishing Co., to Be Published In*.

Larue, D., Jian, F. X., Castellini, A., Toldi, J., & Chawathe, A. (2005). *Geologic Models And Flow Simulation Studies of a Shoreface Reservoir: From Stratigraphic Characterization to History Matching*. *All Days*, SEG-2005-2322.

Maschio, C., & Schiozer, D. J. (2014). Bayesian history matching using artificial neural network and Markov Chain Monte Carlo. *Journal of Petroleum Science and Engineering*, *123*, 62–71.

Mustafiz, S., & Islam, M. R. (2008). State-of-the-art Petroleum Reservoir Simulation. *Petroleum Science and Technology*, *26*(10–11), 1303–1329. https://doi.org/10.1080/10916460701834036

Odeh, A. S. (1969). Reservoir Simulation ...What Is It. *Journal of Petroleum Technology*, *21*(11), 1383–1388. https://doi.org/10.2118/2790-PA

Odeh, A. S. (1982). An Overview of Mathematical Modeling of the Behavior of Hydrocarbon Reservoirs. *SIAM Review*, *24*(3), 263–273. https://doi.org/10.1137/1024062

Oliver, D. S., & Chen, Y. (2011). Recent progress on reservoir history matching: a review. *Computational Geosciences*, *15*(1), 185–221. https://doi.org/10.1007/s10596-010-9194-2

Saul Dobilas. (2022, February 6). *LSTM Recurrent Neural Networks — How to Teach a Network to Remember the Past*. Towards Data Science. https://towardsdatascience.com/lstm-recurrent-neural-networks-how-to-teach-a-network-to-remember-the-past-55e54c2ff22e

Shirangi, M. G. (2012). Applying machine learning algorithms to oil reservoir production optimization. In *Tech. Rep. Machine Learning Course Project Report*. Stanford University Stanford, CA, USA.

Singh, V., Yemez, I., & Sotomayor, J. (2013). Integrated 3D reservoir interpretation and modeling: Lessons learned and proposed solutions. *The Leading Edge*, *32*(11), 1340–1353. https://doi.org/10.1190/tle32111340.1

Stags, H. M., & Herbeck, E. F. (1971). Reservoir Simulation Models An Engineering Overview. *Journal of Petroleum Technology*, *23*(12), 1428–1436. https://doi.org/10.2118/3304-PA

Vyas, A., Datta-Gupta, A., & Mishra, S. (2017). Modeling early time rate decline in unconventional reservoirs using machine learning techniques. *Abu Dhabi International Petroleum Exhibition and Conference*, D041S113R002.